SDRD

SITE-DIRECTED RESEARCH & DEVELOPMENT

SITE-DIRECTED RESEARCH & DEVELOPMENT

ANNUAL REPORT OVERVIEW FY 2024

Export Controlled Information
Export Classification: EAR99
Reviewed for Classification
Paul P. Guss, MSTS, EU12
March 28, 2025

NEVADA NATIONAL NNSS SECURITY SITES

SITE-DIRECTED RESEARCH & DEVELOPMENT

NEVADA NATIONAL NNSS SECURITY SITES

SITE-DIRECTED RESEARCH & DEVELOPMENT

ANNUAL REPORT OVERVIEW FY 2024

How to Read this Report

The SDRD program's annual report for fiscal year (FY) 2024 consists of two parts: the Overview, which contains the three major sections of Program Description, Program Accomplishments, and Program Value; and individual project report summaries. Public summaries are included at the end of this report and published electronically on the Nevada National Security Site's website, https://nnss.gov/mission/sdrd. Controlled project summaries are available in the CUI document. Complete technical reports for concluding projects are available internally on iCon or from the principal investigator. Contact the SDRD Program Office at SDRDAdmin@nv.doe.gov for more information.

On the Cover

Front cover: *Static image of shocked antimony experiment in "Thermal Transport Detection of Phase Boundaries," G. Stevens (24-022).*

Staff

SDRD Program Manager	Michael Reed
SDRD Deputy Program Manager	Cameron Hawkins
Editors	Madeline Gauthier, Anne Totten, Kristen Vernon
Design & Layout	Kristen Vernon
Web Design & Production	Kirsten Kellogg, Tyler Patterson
Management and Support	Michael Baldonado, Elizabeth Craft, Leslie Esquibel, B. Lisa Garcia, Emma Gurr

www.nnss.gov

This work was done by Mission Support and Test Services, LLC, under Contract No. DE-NA0003624 with the U.S. Department of Energy and the National Nuclear Security Administration's Office of Defense Programs, and supported by the Site-Directed Research and Development Program. DOE/NV/03624--2141.

Table of Contents

Letter from the Chief Scientist

José Sinibaldi
Science and Technology
Director & Chief Scientist
Nevada National Security Sites

As the Nevada National Security Sites (NNSS) celebrates 75 years, I am proud of our rich R&D history and, in that spirit, I am proud to submit the Fiscal Year 2024 (FY24) Site Directed Research and Development (SDRD) Annual Report. Since 1951, the NNSS has served as a cornerstone in advancing our nation's most essential security missions. Established in 2002, SDRD provides a critical platform for high-risk, high-reward innovation; enables the development of a skilled and agile technical workforce; and ensures our researchers can swiftly respond to pressing national security challenges.

SDRD projects drive innovation in stockpile experimentation and global security with technology advances in these areas:

- Accelerator Beam Science and Target Interactions
- Communications and Computing
- Dynamic Experiment Diagnostics
- Enabling Technologies for Autonomous Systems and Sensing
- Neutron Technologies and Measurements
- Radiographic Systems Imaging and Analysis
- User-Centered Remote Testing and Operations

Achievements in FY24 include a low-cost wearable microwave detection system, a transformative platform for high-yield neutron experiments, and a reimagined approach to subcritical experiment data management, underscoring how SDRD-funded efforts continue to shape and strengthen our mission. Concurrently, our collaboration with universities and industry—exemplified by efforts to train the next generation of pulsed-power experts for the Scorpius accelerator—ensures a robust talent pipeline vital to sustaining our legacy of innovation. SDRD also motivates our workforce through the opportunity for prestigious awards, publications, and successful technology transfer endeavors. In FY24, an SDRD-developed Electromagnetic Spectrum Management System earned an R&D 100 award and one of our SDRD investigators won a Presidential Early Career Awards for Scientists and Engineers (PECASE) award, honoring the impact of our research and talented researchers beyond our own mission.

Within this Annual Report, you will find detailed accounts of achievements across our seven Thrust Areas, insights on the program's performance metrics, and an overview of our updated proposal review and selection process. We also include a comprehensive look at the 33 funded projects from FY24.

I am confident SDRD's continued commitment to discovery and collaboration will keep the NNSS at the forefront of national security innovation, effectively meeting the evolving threat environment of today and tomorrow.

March 2025

PROGRAM DESCRIPTION

SDRD Program Mission, Alignment, and Objectives

History and Impact

The Site-Directed Research and Development (SDRD) program was initiated through Public Law (P.L.) 107-66, "Energy and Water Development Appropriations Act, 2002," Section 310, which grants the NNSA authority to allow the NNSS contractor to conduct an R&D program aimed at supporting innovative and high-risk scientific, engineering, and manufacturing concepts and technologies with potentially high payoff for the nuclear security enterprise.

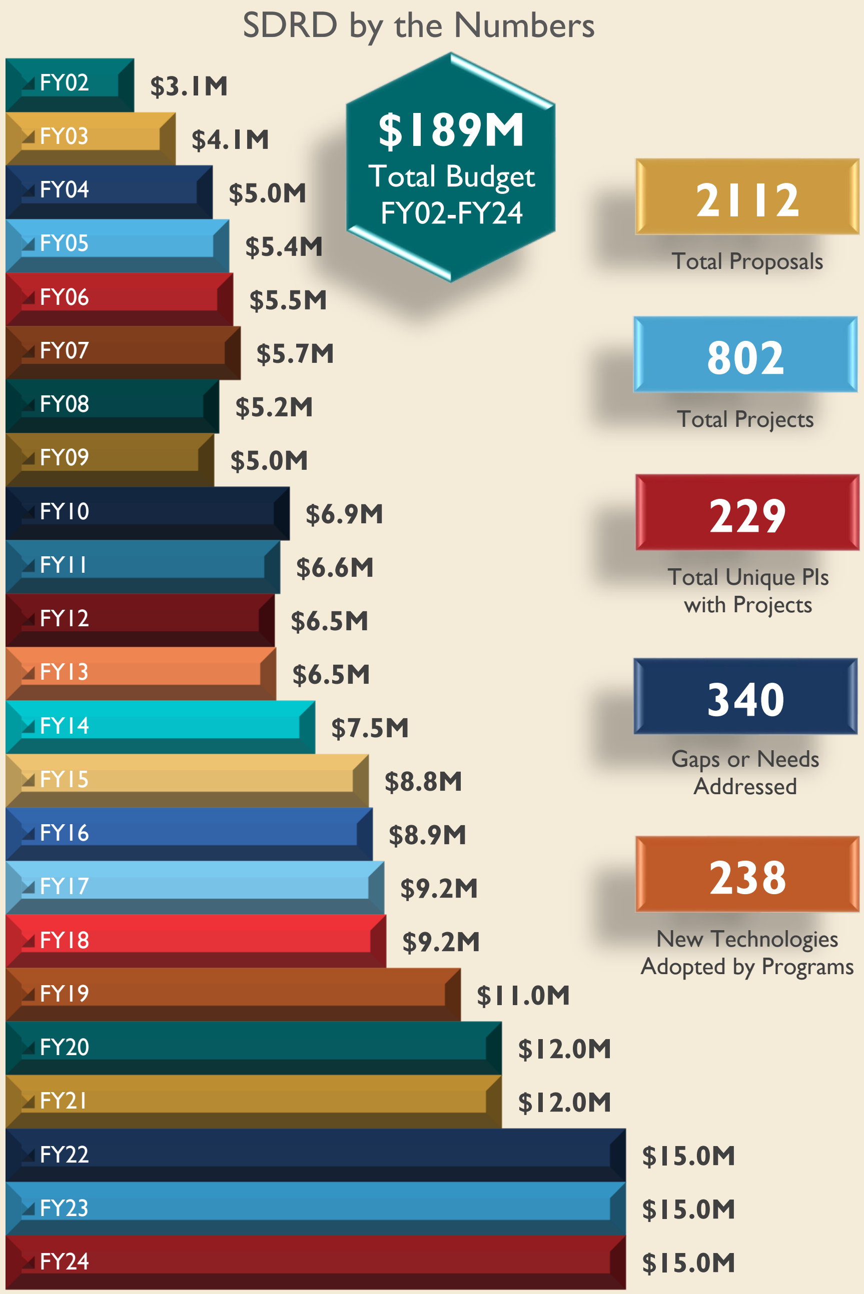

The program is modeled after the Laboratory Directed Research and Development (LDRD) program, which is conducted in accordance with the guidance provided by U.S. DOE Order 413.2C Chg1, "Laboratory Directed Research and Development," and the supplemental augmenting document "Roles, Responsibilities, and Guidelines for Laboratory Directed Research and Development at the Department of Energy/National Nuclear Security Administration Laboratories." We are also committed to the guiding principles as outlined in the 2019 Strategic Framework for the NNSA Laboratory and Site-Directed Research and Development.

P.L. 110-161 (H.R. 2764), "The Consolidated Appropriations Act, 2008," provides that up to 4% of the NNSS site costs may be applied to the SDRD program. In addition, SDRD is an allowable cost within the NNSS management and operating contract and as such is identified in the NNSS contractor accounting system. The program is currently funded at 2.5%. In its first year (2002) the baseline budget was $3.1M, and roughly $15.5M has been allotted for FY 2025 by the senior management team.

As the illustration on the previous page shows, SDRD has made a significant impact in the past 22 years, providing nearly 240 innovative technologies to NNSS programs from 2002 to 2024, a high return on the investment of R&D dollars.

Alignment with the NNSA LDRD/SDRD Strategic Framework

The NNSA laboratories and NNSS R&D programs have five objectives as described in DOE Order 413.2C. They are to:

- maintain the scientific and technical vitality of the laboratories,
- enhance the laboratories' ability to address current and future DOE/NNSA missions,
- foster creativity and stimulate exploration of forefront areas of science and technology,
- serve as a proving ground for new concepts in research and development, and
- support high-risk, potentially high-value research and development.

These objectives underpin the 2019 Strategic Framework for the NNSA Laboratory and Site-Directed Research and Development, a document signed in July 2019 by the three NNSA laboratory directors, Mark Martinez (NNSS President), and Lisa E. Gordon-Hagerty (Under Secretary for Nuclear Security for DOE and NNSA Administrator). This short but key document defines the vision, objectives, and the overarching strategies the R&D programs follow. To quote the Framework, the "NNSA laboratories and NNSS have a shared mission to solve national security challenges by leveraging scientific and engineering excellence." Specifically, the Framework describes how the programs address four important challenges presented in the 2018 Nuclear Posture Review, which are to:

- provide an agile, flexible, and effective nuclear deterrent,
- protect against all weapons of mass destruction threats,
- deter and defend against threats in multiple domains, and
- strengthen our energy and environmental security.

As the Framework also states, "Through their individual strategic planning processes, NNSA laboratories and NNSS use the [R&D] Programs to seed their capability-bases and scientific workforces to prepare for emerging national security challenges, thereby achieving the NNSA mission and supporting the 2018 Nuclear Posture Review."

Mission and Objectives

The SDRD program develops innovative scientific and engineering solutions, replaces obsolete or aging technologies, and rejuvenates the technical base necessary for operations and program readiness at the NNSS. We support high-risk research and potential high-value R&D. Our objectives harmonize with those of the LDRD program, which are:

Mission Agility

Enable agile responses to national security challenges.

Technical Vitality

Advance the frontiers of science technology, and engineering.

Workforce Development

Attract, develop, and retain tomorrow's technical workforce.

Mission Agility

Mission Agility

Enable agile technical responses to current and future DOE and NNSA mission challenges.

Scientific and Technical Vitality

Technical Vitality

Advance the frontiers of science, technology, and engineering by serving as a proving ground for new concepts, exploring revolutionary solutions to emerging security challenges, and reducing the risk of technological surprise.

Workforce Development

Workforce Development

Recruit, retain, and develop tomorrow's technical workforce in essential areas of expertise critical to mission delivery.

The research projects featured on pages 12–18 are keyed to the three objectives, as indicated by these icons.

SDRD Program Leadership

The senior leadership of Mission Support and Test Services, LLC (MSTS), the management and operating contractor for the NNSS, which includes the president, vice president, and senior directors, is committed to advancing the contract's R&D goals. Working closely with senior management and the SDRD program manager, the chief scientist ensures the quality of science and technology across the company's multiple programs and missions; advocates translation of research products through technology readiness levels; and plans and directs new scientific concepts and technologies to provide solutions to identified issues to fulfill the NNSS mission to the nuclear security enterprise.

The SDRD program manager and deputy program manager are the points of contact for SDRD and are responsible for all practical aspects of the program. The program manager and deputy manager are assisted by the NNSS Science and Technology Thrust Area (STTA) leads and SDRD technology representatives (see below) to coordinate technical activities undertaken by principal investigators (PIs). PIs are responsible for all aspects of technical activities on their projects. They deliver monthly updates, present quarterly reviews, submit final annual reports, and report technical outcomes post-project closure. The SDRD program relies on an external advisory board of distinguished individuals from academia, government, and industry to help guide and direct our investments toward the most important areas of national security science and technology. This board has been instrumental in the success of the program since it was instituted in the mid-2000s.

Science and Technology Thrust Areas

The NNSS STTAs are a focused long-term technical investment to prepare the NNSS technology capabilities for future NNSA missions and to enhance our ability to respond to future global threats.

The NNSS STTAs consist of seven areas, and each STTA encompasses a specific segment of science and technology conducted at the NNSS. The Radiographic Systems Imaging and Analysis (RSIA), User-Centered Remote Testing and Operations (UCRTO), Accelerator Beam Science and Target Interactions (ABSTI), and Enabling Technologies for Autonomous Systems and Sensing (ETASS) STTAs were activated in FY 2021 followed by the Neutron Technologies and Measurements (NTM), Dynamic Experiment Diagnostics (DED), and Communications and Computing (C&C) STTAs. STTA leads are assigned to lead and support the STTAs. The goals and objectives for the STTAs are to strengthen our technical capabilities in the near term, enhance the readiness of our core competencies in the long term, and make us more agile and adaptable to new global threats.

The STTAs directly align their efforts to support our NNSA and Strategic Partnership Projects missions and are an integral component of the SDRD program. The STTA leads are involved in shaping the program as well as integrating STTA goals with defined strategic initiatives directed to SDRD proposers.

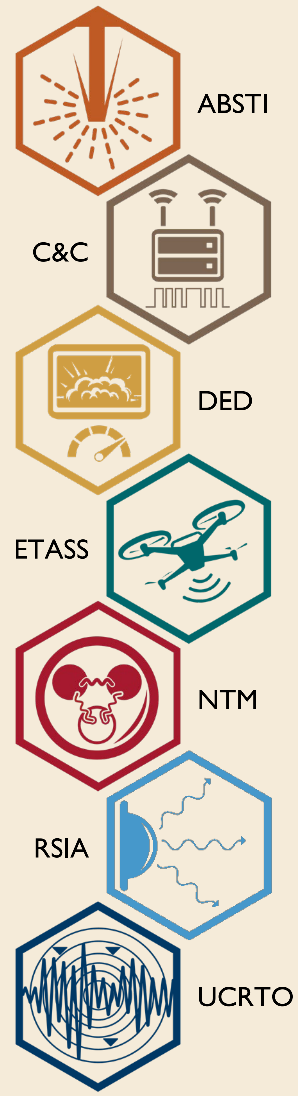

Proposal Cycle and Project Selection

The research undertaken by the SDRD program is inherently staff driven—ideas are submitted annually by staff in response to a call for proposals and these ideas are vetted through a rigorous two-stage review and evaluation process. Proposers are guided by mission needs and other strategic guidance to provide unique solutions to existing and emerging problems. Furthermore, proposers are encouraged to accept higher levels of R&D risk that could nonetheless result in high-reward technological advances that are of immediate benefit to naturally risk-averse programmatic projects.

Call for Proposals

We utilize a two-phase proposal process consisting of a pre-proposal (concept phase) followed by an invited proposal. In the pre-proposal phase, staff are encouraged to submit ideas in a standardized, succinct format that presents the proposed project's essence and impact. In addition, during the pre-proposal phase, proposers are encouraged to obtain feedback from subject matter experts (SMEs) to refine their ideas. This phase sparks innovation and initiates a feedback loop that extends to the invited proposal phase. Guidance for proposers is provided in two major documents, the Broad Site Announcement (BSA) and the NNSS Technology Needs Assessment for R&D. Updated annually, the assessment helps proposers identify and address technology gaps in existing programmatic areas and in addressing emerging threats. The feedback loop also provides specific, useful guidance.

Project Selection

All submitted pre-proposals are evaluated by Program and Senior Director reviewers. Criteria considered in the evaluation of pre-proposals include their alignment with NNSS's current strategic priorities and focus areas, their potential to drive innovation and promote technological advances needed to meet emerging mission requirements, and their impact on our ability to develop cutting-edge capabilities and to attract and retain top talent for future challenges. Individual pre-proposals are evaluated with a reduced-weighted scoring matrix. The scores are then compiled, and a ranking is determined.

Typically, about 50% of the pre-proposals are promoted to invited proposals. Subject Matter Experts (SMEs) evaluate how well each proposal addresses the core questions based on the Heilmeier approach to R&D. Invited proposals are also evaluated according to well-benchmarked and well-established criteria that consist of (1) technical merit, (2) program benefit, (3) probability of success, (4) critical skills, and (5) leverage. Detailed information about these criteria is available for viewing by anyone who has access to the NNSS network. The information is always available via the SDRD program website. In addition, the SDRD program posts an article about these criteria on the company's intranet announcement page every year before the invited proposal phase begins.

The final selection of SDRD investments for the next fiscal year is made and an annual program plan is submitted to the NNSA for concurrence by mid-August.

Feasibility Studies

Several investigative feasibility studies are funded each fiscal year. In FY 2024, there were a total of three feasibility studies. These brief studies (three to six months, usually under $100K) focus on topics that may potentially warrant further study and full funding. In the past, successful endeavors, such as broadband laser ranging began as feasibility studies.

SDRD Portfolio

Mission Categories

The SDRD portfolio falls into two primary mission categories: stockpile stewardship and global security.

Historically, PIs have submitted a nearly equal number of ideas addressing stockpile stewardship and global security areas. In FY 2024, there were 16 projects for stockpile stewardship at approximately $5.7 million, while global security had 20 projects at approximately $6.3 million in funding. In FY 2024, the total amount of funding requested for SDRD was $15M, of which roughly 38 percent was for the stockpile stewardship mission category and about 42 percent for the global security mission category.

Alignment within Science and Technology Thrust Areas

Beginning FY 2021, each funded project is also aligned with one of the seven NNSS STTAs according to its focus. In FY 2024, there were a total of 36 projects, of which 3 were feasibility studies. The pie chart below shows the number of FY 2024 projects that fall into each of the seven thrust areas.

FY24 SDRD Projects by STTA

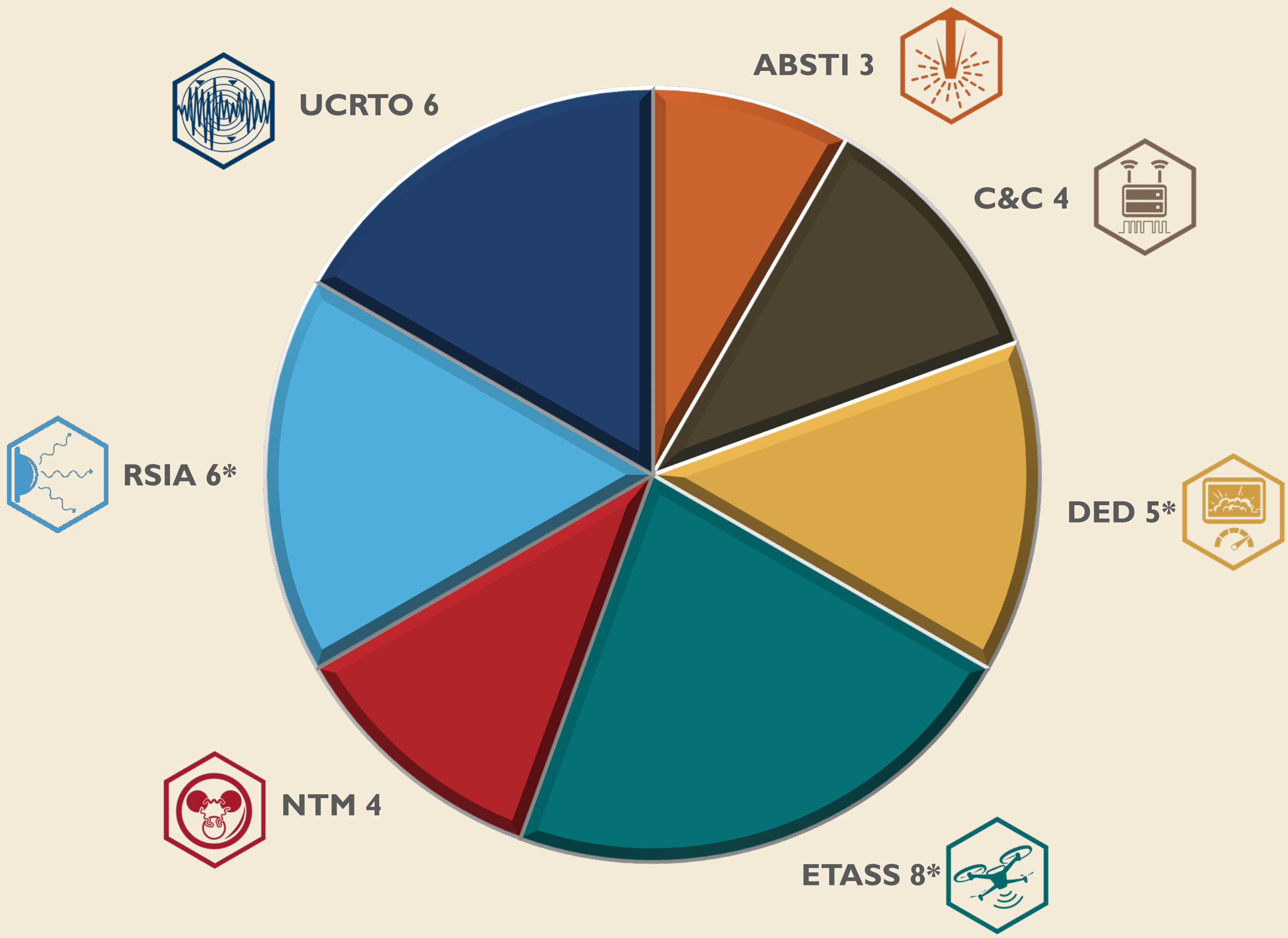

* Indicates a Feasibility Study in that STTA

List of All Projects for FY24

Additive Manufacturing of Structural and Pixelated/Discriminating Scintillators, A. Wolverton (24-019)

AR/VR CBRN Solutions for Emergency Responders, B. Richardson (24-081)

Assessment of Single-Sided Radiographic Imaging Concepts for Future Development of a Compact Manned-Portable Radiographic Device, L. Hovey (24-127)

Cloud-Based Meta-Analysis with Adaptive Learning for Massive Sensor Networks, C. Schuetze (24-117)

Computational Fluid Dynamic Simulations for Critical Infrastructure (CFD-SCI), S. Breckling (24-016)

Cryogenic Deuterium Pellet Injection for Enhanced Neutron Output of a Dense Plasma Focus, D. Lowe (24-011)

Data Fusion: Reconstructing 3D Hydrodynamic Scenes Utilizing Both Radiography and Momentum Diagnostics, J. Pillow (24-052)

Digitized Nanosecond Silicon-Germanium Photomultipliers for Prompt Radiation Detection, J. Mellott (24-069)

Direct Measurement of Metal-Hydride Formation during Ejecta Particle Transport in Reactive Gases Using Ramen Spectroscopy, J. Mance (24-090)

Exploration of an Electron LINAC-Driven Photoneutron Source Based on Scorpius, A. Guckes (24-044)

Feasibility of Reoccupying Historic Testbeds for Future Experiments, I. Bortins (24-120)

Fundamental Experiments for Detonation Signature Modeling, C. Kimblin (24-007)

Incorporation of Geologic Data into Centralized Database, D. Smith (24-062)

Intensity Based Laser Velocimetry Measurements, B. La Lone (24-079)

Low SNR, High Clutter UAS Detection and Tracking, I. McKenna (24-009)

Mass-Selective Photoionization Detector, M. Manard (24-002)

Material Identification in Radiographic Images of Dynamically Formed Metal-Explosive Mixtures by Tuning the X-Ray Sources Spectrum Using Multiple Anodes, B. La Lone (24-070)

Measurements for Combined Gamma-Ray and Video Modalities, C. Burt (24-024)

Microwave Detection through Thin Films, H. Tarvin (24-075)

Modernization and Scalability Enhancements for Sub-Nanosecond Accuracy Diagnostic Cross Timing for Use at Current and Future NNSS Testbeds, D. Champion (24-049)

Multi-modal Remote Vibrometer for Infrastructure Interrogation, S. Koppenjan (24-010)

Needle-Washer Diode for Dynamic X-Ray Diffraction on Actinides at Z, S. Haque (24-107)

Novel Photon-Counting Detector Concept for High-Resolution Radiographic Imaging, S. Miller (24-032)

Optical Comb Techniques for Hyperfine Spectroscopy, R. Trainham (24-014)

Optical Remote Sensing for Facility Monitoring: An Integrated Approach to Modeling, Simulation, and Sensors, C. Burt (24-076)

Spatial Spectral Observations from Near and Far, M. Howard (24-095)

Pulse Optimization with Solid-State Utilization of Modulation, Z. Shaw (24-036)

Selective Isotopologue Capture from Whole Air with Porous Crystalline Solids, M. Morey (24-131)

Solid-State Spectrographic Camera for HED and Pyrometry Applications, A. Lewis (24-064)

Spatially Aware Multi-Modal Directional Radiation Detection Swarms, J. Essex (24-114)

Staged Z-Pinch and Variable-Energy Laser Ablation-Driven New High-Yield Neutron Source, E. Dutra (24-096)

Strategic Initiative: Developing the NNSS Critical Skills in Accelerator Science and Beam Physics, P. Wiewior (24-092)

Surface Gas Sampling Payload for Autonomous Underwater Vehicles, C. Priest (24-034)

Temperature Study of Compressed Porous Materials, B. La Lone (24-144)

Thermal Transport Detection of Phase Boundaries at Elevated Pressures, G. Stevens (24-022)

Ultrafast High-Dynamic-Range Photomultiplier Trials, R. Buckles (24-119)

PROGRAM ACCOMPLISHMENTS

SDRD at a Glance

$15M	**$290K**	**36**	**11**
Total Program Cost	Median Project Size	Total SDRD Projects	New Projects in FY24

Publications	8
Technologies Adopted by Programs	11
Gaps or Needs Addressed	24
Invention Disclosures and Patents	11
Postdocs	1

Featured Research

SDRD projects demonstrate a high level of ingenuity and innovation each year. Selected highlights of the R&D accomplished in FY 2024 by the SDRD program are presented on the following pages. Summaries of all FY 2024 projects can be found on the NNSS website at https://nnss.gov/mission/sdrd. Full reports of all concluding projects and feasibility studies are available upon request from the SDRD Program Management Office or directly from the PI.

NNSS Interns for project 24-062 (D. Smith) (*left to right*) Morgan Aittama, Garrett Datlof, Marc Llanes, and Hali Montano in the NNSS core library.

ABSTI

Exploration of an Electron LINAC-Driven Photoneutron Source Based on Scorpius, A. Guckes (24-044) **Featured**

Pulse Optimization with Solid-State Utilization of Modulation, Z. Shaw (24-036)

Strategic Initiative: Developing the NNSS Critical Skills in Accelerator Science and Beam Physics, P. Wiewior (24-092)

Accelerator Beam Science and Target Interactions

"Exploration of an Electron LINAC-Driven Photoneutron Source Based on Scorpius"

Amber Guckes
24-044

Scorpius, a linear induction accelerator (LIA), will generate a 22.4MeV electron beam upon bombarding a target through Bremsstrahlung to produce energetic X-rays, which capture the late-time dynamics of subcritical hydrodynamic implosions. Scorpius will be the key component of the NNSS's Enhanced Capabilities for Subcritical Experiments (ECSE) when commissioned in the next 5 years. SDRD PI, Amber Guckes, envisions also using Scorpius to push the NNSS's current boundaries in neutron production and diagnostics. In SDRD project 24-044, Guckes explored the feasibility of turning Scorpius into a multi-probe diagnostic LIA that, beyond just generating energetic x-rays, could enable neutron-based measurements (such as neutron radiography and neutron resonance spectroscopy) as well.

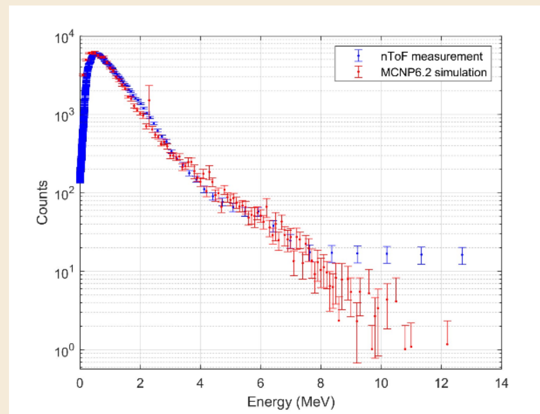

Measured photoneutron energy spectrum created from 20 MeV electrons into a Bremsstrahlung X-ray converter, resultant X-rays impinge on the ¾-inch-thick tungsten photoneutron target; compared to MCNP6.2 simulation normalized to the peak of the measured data.

Guckes and her team performed Monte Carlo N-Particle Code (MCNP) simulations and surrogate experimental measurements at the Idaho State University (ISU) Idaho Accelerator Center (IAC) to inform the photoneutron target design and predict its performance ahead of Scorpius becoming operable. Radiation transport simulations with MCNP provided the basis for the photoneutron target design, and experimental measurements performed at the ISU IAC successfully informed the prediction of a Scorpius photoneutron source performance.


NNSS team at the ISU IAC during the July 2024 photoneutron measurement campaign. Left to right: James Mellott, Amber Guckes, Kevin Yim, Elizabeth Bell, J. Andrew Green, Kaleab Ayalew, and Allan Ortiz.

The team concluded that Scorpius could be used to create useful energies and quantities of neutrons to enable diagnostics such as neutron radiography, fission fragment detection, neutron resonance spectroscopy, and radiation effects studies that produce a far higher neutron yield per pulse than existing short-pulse neutron source capabilities at the NNSS. (For example, the predicted total neutron yield of Scorpius was $9.31\times10^{13} \pm 4.66\times10^{12}$ neutrons/pulse, while the NNSS's dense plasma focus is currently able to yield $1.84 \times10^{12} \pm 0.49\times10^{12}$ neutrons/pulse.)

Looking forward, Guckes hopes to expand on her research through other R&D venues to prove dual x-ray/neutron radiography based on Scorpius and the efforts under this Site-Directed Research and Development project. There is also currently programmatic work to investigate multi-probe radiographic capabilities being headed by LANL. Although their current efforts are focused on laser-driven multi-probe sources, Guckes has emphasized that there remains interest in accelerator-driven multi-probe sources as part of that effort.

Communications and Computing

“*Measurements for Combined Gamma-Ray and Video Modalities*”

Chris Burt
24-024

Previously, the Nevada National Security Sites (NNSS) created a network of spectral gamma-ray sensors in Northern Virginia (aka the NoVArray), supporting the Department of Energy’s Defense Nuclear Nonproliferation (DNN) NA-22. During this SDRD effort, principal investigator Chris Burt and his team upgraded these aging, unused NNSS assets and explored ways to improve detection and identification (ID) of materials of interest through multimodal data analysis. Over the course of this SDRD, the hardware was redesigned then updated, contextual sensors were added, a real-time implementation of the new NoVA data analysis workflow was completed, and the system was evaluated utilizing well-characterized radioactive sources.

C&C

AR/VR CBRN Solutions for Emergency Responders, B. Richardson (24-081)

Cloud-Based Meta-Analysis with Adaptive Learning for Massive Sensor Networks, C. Schuetze (24-117)

Computational Fluid Dynamic Simulations for Critical Infrastructure (CFD-SCI), S. Breckling (24-016)

Measurements for Combined Gamma-Ray and Video Modalities, C. Burt (24-024) **Featured**

The core methodology throughout this work leveraged previous work by the Remote Sensing Laboratory (RSL) and the Special Technologies Laboratory (STL) to develop spectral gamma identification convolutional neural networks (CNNs). The primary output of this SDRD project was the production of 10 upgraded NovArray platforms, ready for deployment, with three additional prototype units in need of minor updates. These platforms provide a ready-to-use solution to many of NNSS’ stakeholder problem sets.

One of the most beneficial outcomes of this project was that it allowed for the development of a coordinated, functional data science team across the NNSS (the “NoVA Constellation of Projects team”). The technical abilities needed to complete this project were not sufficiently covered at one lab. This required coordination between satellite offices and the North Las Vegas facility. This SDRD provided an avenue to develop critical machine learning and embedded systems development skillsets for many NNSS scientists and engineers. These skillsets are now being utilized by other SDRD projects and directly funded projects, including in support of NA-22 work.

NoVA logo featuring ANT.

NoVA sensor in the wild.

This SDRD effort sought to answer three primary questions: Can we extend the applicability space of NNSS’s NoVArray from dataset generation to information generation? Can we leverage and update an unused asset to turn it into a new funding source for NNSS? Can we develop an operational, autonomous, and robust platform for reliable SNM detection?

The results of this research effort demonstrate that the answer to the first two questions is yes. The hardware upgrades and real-time implementation of the software allow for the NoVArray to be a source of information, rather than just unlabeled, uncurated data. The work has been successfully adopted by programmatic efforts. The answer to the third question, however, is less clear. The evaluation of the platform in a relevant environment with real-world targets demonstrated the new NoVArray’s ability to reliably detect industrial sources; however, the system’s real-time performance against objects of primary concern is still unknown.

DED

Digitized Nanosecond Silicon-Germanium Photomultipliers for Prompt Radiation Detection, J. Mellott (24-069)

Direct Measurement of Metal-Hydride Formation during Ejecta Particle Transport in Reactive Gases Using Ramen Spectroscopy, J. Mance (24-090)

Intensity Based Laser Velocimetry Measurements, B. La Lone (24-079)

Temperature Study of Compressed Porous Materials, B. La Lone (24-144)

Thermal Transport Detection of Phase Boundaries at Elevated Pressures, G. Stevens (24-022) **Featured**

Dynamic Experiment Diagnostics

"*Thermal Transport Detection of Phase Boundaries at Elevated Pressures*"

Jerry Stevens
24-022

Principal investigator Gerald (Jerry) Stevens and his team set out to develop a new experimental technique to double-shock-melt a compressible metal and use the resulting hot layer of liquid metal to heat a thin metal coating on a lithium fluoride (LiF) window, driving the material across a phase boundary. This new technique opens new doors to exploring high temperature melt boundaries typically inaccessible on a powder gun.

Old, pure 99.99% Sb - large pits within certain grains

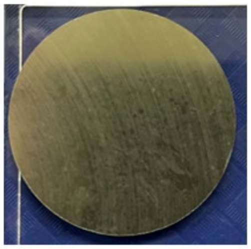

New 99.9% Sb – fine grains, no pits

The process that Stevens and his team used involved shocking, releasing, and then re-shocking a compressible material (such as cerium, tin, or antimony) and using that layer of hot liquid-metal to heat a thin (micron scale) film of metal under investigation against a transparent anvil (such as the LiF window described above) at constant pressure, while thermal diffusion heats the film across phase boundaries in order to investigate phase boundaries at high pressure on single-stage gun experiments. Although Stevens and his team successfully demonstrated that their new technique could indeed reach high temperatures, they encountered a roadblock when they discovered that surface imperfections developed into large features that penetrated the metal film under investigation. Stevens and his team took this obstacle as an opportunity to fine-tune their methodology, and after some trial and error, their final experiments gave temperature histories consistent with one-dimensional thermal diffusion hydrodynamic calculations. They also came up with models that will inform future designs and efforts to find phase boundaries in iron.

Static image from tin experiment.

Now equipped with several ideas to mitigate the issues they encountered with surface imperfections during this project, Stevens and his team plan to leverage the valuable insights they have gained from their research in future projects and collaboration opportunities they have planned with Sandia National Laboratories, and are excited by the insights that their findings will provide to the shock physics community.

Enabling Technologies for Autonomous Systems and Sensing

"*Mass-Selective Photoionization Detector*"

Manuel Manard
24-002

Small, inexpensive, ruggedized, and field-portable systems and instruments capable of providing real-time chemical analysis and detection are of interest to multiple government agencies for both human- and drone-based deployment. Although technology already exists for real-time chemical analysis, these instruments are too large for easy in-field deployment and lack the necessary specificity in the data they collect. To this end, principal investigator Manuel Manard and his team set out to design, build, and test a portable proof-of-concept instrument that couples a photoionization lamp with an array of ion traps to provide mass spectra of chemical species in real time.

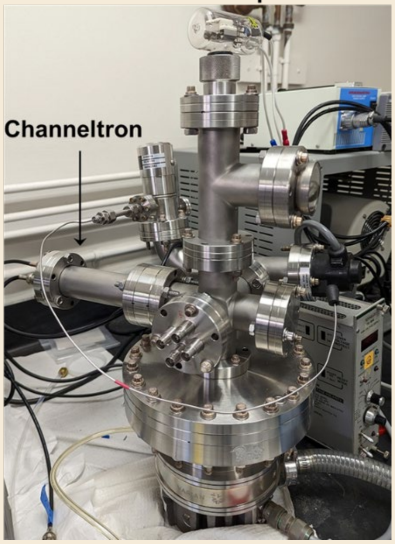

Photoionization detector.

As a result of this SDRD effort, Manard and his team successfully created and tested a device that combines the simplicity of photoionization detectors with the selectivity of mass analyzers in a compact form. A printed circuit board (PCB) containing an array of 25 ion traps, with diameters of 500 μm, was designed and fabricated. The PCB measures 1 inch in diameter and 0.0625 inches thick. This proof-of-concept instrument couples a photoionization lamp with a Paul-type ion trap to provide mass spectra of chemical species. Data was acquired that showed the presence of ions, generated by the photoionization lamp, confined in the trap, and Manard and his team saw a 20x increase in trapped ion signal strength.

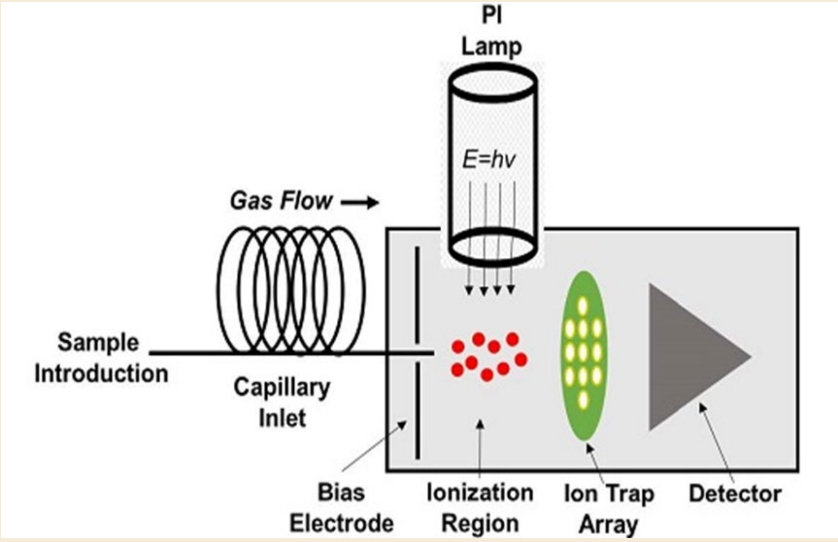

Diagram of device.

ETASS

Low SNR, High Clutter UAS Detection and Tracking, I. McKenna (24-009)

Mass-Selective Photoionization Detector, M. Manard (24-002) **Featured**

Microwave Detection through Thin Films, H. Tarvin (24-075)

Multi-modal Remote Vibrometer for Infrastructure Interrogation, S. Koppenjan (24-010)

Optical Comb Techniques for Hyperfine Spectroscopy, R. Trainham (24-014)

Selective Isotopologue Capture from Whole Air with Porous Crystalline Solids, M. Morey (24-131)

Spatially Aware Multi-Modal Directional Radiation Detection Swarms, J. Essex (24-114)

Surface Gas Sampling Payload for Autonomous Underwater Vehicles, C. Priest (24-034)

NTM

Additive Manufacturing of Structural and Pixelated/Discriminating Scintillators, A. Wolverton (24-019)

Cryogenic Deuterium Pellet Injection for Enhanced Neutron Output of a Dense Plasma Focus, D. Lowe (24-011)

Staged Z-Pinch and Variable-Energy Laser Ablation-Driven New High-Yield Neutron Source, E. Dutra (24-096)

Ultrafast High-Dynamic-Range Photomultiplier Trials, R. Buckles (24-119) **Featured**

Neutron Technologies and Measurements

"*Ultrafast High-Dynamic-Range Photomultiplier Trials*"

Robert Buckles
24-119

Photomultiplier tubes (PMTs) have been the primary photon detection device for many decades and used in many applications for both historic and present-day stockpile stewardship missions. However, as stockpile experimentation methods continue to improve, PMTs and similar, more recent photomultiplier technologies fail to record fast radiation signals at the speed and efficiency that current stockpile needs require.

Dynamic experimentation will continue to need advances in prompt radiation detection and measurement and, given that extremely high dynamic-range (DR) is a unique requirement of the National Security Enterprise complex, principal investigator Robert Buckles determined that the solution to this need is a future-proof photodetector that exceeds the capabilities of legacy prompt detectors.

Zach Wolff works on PMT parts.

This two-year effort built on findings from a prior SDRD project and previous programmatic work to implement a sequence of manufacturing and assembly trials that would produce a wafer-based photomultiplier assembly that would meet current experimentation needs.

Sean Sheehan posses PMT apparatus.

The detector that resulted from Buckles' work is extremely light-weight (approximately the size of a quarter) and is expected to replace and surpass the state of the art in most prompt radiation applications. Buckles and his team were awarded a provisional patent for this technology and are starting to pursue commercial partnerships. As a result of his work, Buckles' project was met with high praise and enthusiasm from the NNSS during the SDRD Annual Program Review in September 2024 and he was named 2024's Most Valuable Principal Investigator.

Congratulations to Rob and his team!

Radiographic Systems Imaging and Analysis

"Material Identification in Radiographic Images of Dynamically Formed Metal-Explosive Mixtures by Tuning the X-Ray Sources Spectrum Using Multiple Anodes"

Brandon La Lone
24-070

The goal of this project was to identify and quantify the amount of a particular atomic element, in a mixture of elements, on a dynamic experiment. Principal investigator Brandon La Lone and his team used two-angle flash radiography for the material identification where the radiographic sources had different anodes that altered their x-ray spectrum.

The ability to correctly identify and quantify materials in x-ray radiographs has several applications within the weapons complex. It could be used for part inspection and for dynamic experiments. The main interest of this work was using x-rays to identify materials in mixed ejecta fields. When an explosively driven shock wave reflects from the free surface of a metal, the metal surface can particulate into ejecta particles. In some instances, it may be possible for the explosive products, or other materials, to breech the metal and mix with the ejecta. These mixed ejecta fields were of interest to the team's work.

La Lone and his team approached the task by comparing x-ray transmission through an object at two different, closely spaced, monochromatic energies. The team found that if the energies were chosen carefully, they could straddle either side of the absorption k-edge of a particular element. For that element, the higher energy x-ray source was more strongly absorbed than the lower energy source (because of the k-edge). By comparing the transmission values through the scene from both x-ray sources, La Lone's team could identify and quantify the element.

RSIA

Assessment of Single-Sided Radiographic Imaging Concepts for Future Development of a Compact Manned-Portable Radiographic Device, L. Hovey (24-127)

Data Fusion: Reconstructing 3D Hydrodynamic Scenes Utilizing Both Radiography and Momentum Diagnostics, J. Pillow (24-052)

Material Identification in Radiographic Images of Dynamically Formed Metal-Explosive Mixtures by Tuning the X-Ray Sources Spectrum Using Multiple Anodes, B. La Lone (24-070)
Featured

Needle-Washer Diode for Dynamic X-Ray Diffraction on Actinides at Z, S. Haque (24-107)

Novel Photon-Counting Detector Concept for High-Resolution Radiographic Imaging, S. Miller (24-032)

Solid-State Spectrographic Camera for HED and Pyrometry Applications, A. Lewis (24-064)

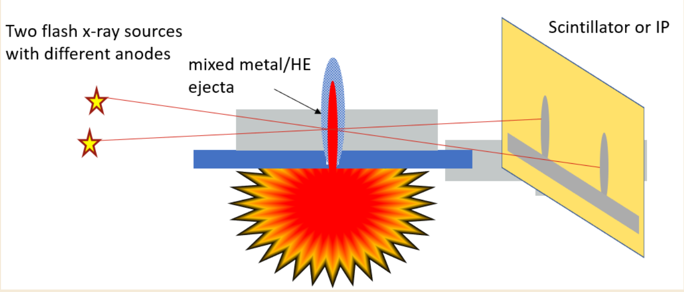

Modelling the dual anode concept.

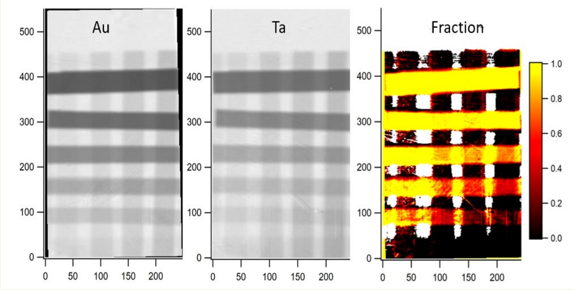

Zinc and zinc mixtures correctly identified in the image.

Using the dual anode approach, La Lone and his team were able to correctly identify the presence of zinc with a mixed element target. The methods also did a reasonably good job of quantifying the amount of zinc in the mixed zinc/plastic target. The plastic areal densities were also quantified, though with greater uncertainty.

UCRTO

Feasibility of Reoccupying Historic Testbeds for Future Experiments, I. Bortins (24-120)

Fundamental Experiments for Detonation Signature Modeling, C. Kimblin (24-007)

Incorporation of Geologic Data into Centralized Database, D. Smith (24-062) **Featured**

Modernization and Scalability Enhancements for Sub-Nanosecond Accuracy Diagnostic Cross Timing for Use at Current and Future NNSS Testbeds, D. Champion (24-049)

Optical Remote Sensing for Facility Monitoring: An Integrated Approach to Modeling, Simulation, and Sensors, C. Burt (24-076)

Spatial Spectral Observations from Near and Far, M. Howard (24-095)

User-Centered Remote Testing and Operations

"*Incorporation of Geologic Data into Centralized Database*"

Devon Smith
24-062

Since its inception in 1950, the Nevada Nuclear Security Site, established as the Nevada Proving Grounds and later renamed the Nevada Test Site, has been a wealth of data for the scientific community beyond the eminent atomic and nuclear data. Geologic data gathered from various tests over the history of the Site have become essential to NNSS geologists and the greater geologic community. As these data sets grow in volume and complexity over time, thoughtful storage and ease of access become paramount considerations for current and future needs.

Since the start of this project in 2023, principal investigator Devon Smith took on the monumental task of consolidating and curating the known geologic data sets over the life of the NNSS. Devon worked with fellow scientists Jacob Gochenour, Matthew Dietel, Andrew Miller, Maggie Townsend, Jennifer Larotonda, Carson Schuetze, and Justin Reppart, as well as engineer Yvonne Diaz and many of the 2024 Science & Technology summer interns.

Drillhole data is currently organized in spreadsheets by project. Some of the desirable data being curated includes location data, drilling data, and geology data (e.g., lithology, rock quality, physical properties, geophysics, etc.). Access to some of this data has been stilted by the retirement of a single user, one of several roadblocks encountered by the team. To add to the complications of the project scope, additional data sets were recently discovered, resulting in a need for data reconciliation to determine differences in the various data sets and properly vet the data prior to import.

Core library samples.

During the February Science & Technology Work-in-Progress Seminar, Cleat Zeiler highlighted the importance of Devon and her team's work on the legacy data: "if we never test again, [that data] is what we have." With over 60 years of drilling operations at the NNSS, the volume of subsurface geologic data is exceptional and needs to be preserved and organized. The goal of this project is to compile the data into a centralized database, preserving the data and making it accessible to our scientists and stakeholders.

To that end, the team has implemented several servers to house and catalog the data. Using the commercial software Datamine Fusion X, Devon and her team have already made significant progress. The project is in the second and final planned year in SDRD and looks to move into programmatic space at the end of the fiscal year.

SDRD MVPI

With many exceptional projects being conducted across the NNSS, the S&T Directorate is proud to honor SDRD's Most Valuable Principal Investigator (MVPI) in FY 2024. Nominations were submitted directly from peers and objectively reviewed by the Chief Scientist and SDRD Leadership. Nominees came from nearly every STTA and reflect our mission to support innovative and high-risk concepts and technologies for the nuclear security enterprise. The MVPI winner and other nominated PIs are highlighted with their projects below.

Winner

Robert Buckles
"Ultrafast High-Dynamic-Range Photomultiplier Trials"
24-119

Congratulations to this year's MVPI winner, Robert Buckles! His work on innovative cesium-activated semiconductor photomultiplier trials and assembly of a brand-new clean room, plus his outreach and mentoring of interns earned him the win. Showera Haque recognized him for his "great mentoring" while Zach Wolff put his assessment of Robert's work plainly: "Dope innovation."

One of the several interns mentored by Robert Buckles this year.

MVPI winner Robert Buckles shows off his clean room created as part of his SDRD project (24-119).

According to Adam Wolverton, "The work Robert has put into GaN photomultipliers is novel and ground-breaking to the development of replacement technologies in radiation detection. This will impact the entire nuclear enterprise for the better." Advanced PMTs like the Hamamatsu mesh dynode have already been discontinued, with the final model in final production. NNSS detectors use this sensor due to its large linear signal output. This mesh style of dynode is the main inspiration for a PMT replacement. Peers recognized the importance of this work and nominated him "[f]or ingenious innovation and for paving the way for PMT alternatives for fast and linear current mode measurements. This is critical for detectors used in stockpile stewardship as PMTs are phased out."

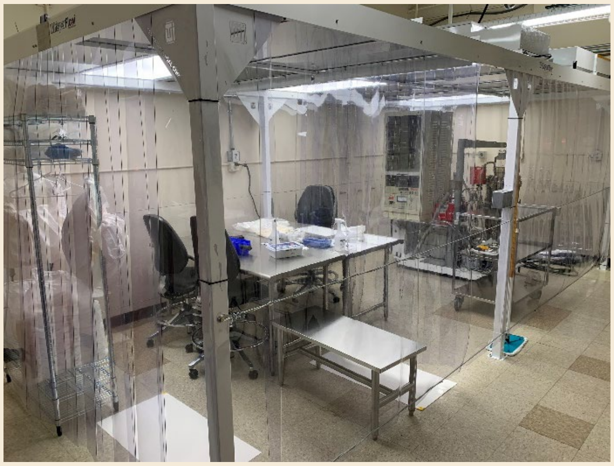

Clean room- completed and ready to go!

Overall, nominators thought Robert should be honored for bringing together good work, good mentoring, and a good presentation: "Nice project, nice presentation, well explained, great work." "Very good presentation. Great examples of SDRD moving into Programmatic space" (Eric Dutra).

Please join SDRD in congratulating our FY24 MVPI, Robert Buckles!

Runners Up

Dan Champion

"Modernization and Scalability Enhancements for Sub-Nanosecond Accuracy Diagnostic Cross Timing for Use at Current and Future NNSS Testbeds"
24-049

Dan Champion was nominated for his work on modernization efforts for testbed diagnostic information. Because NNSS experiments are amongst the highest complexity scientific experiments conducted within the NNSA, we need a scalable and modern approach to diagnostic configuration management that can be deployed at any NNSS testbed (and beyond). The innovation goal of this project is to develop a semi-automated electronic diagnostic timing configuration management capability that can be deployed at a variety of NNSS testbeds (current and future).

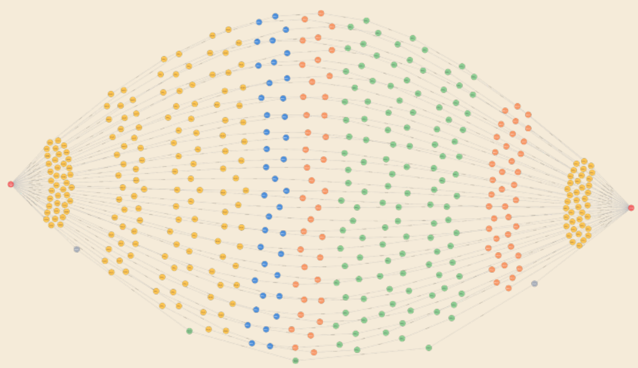

Timing graph from Dan Champion's project presentation (24-049).

External Advisory Board member Gerry Yonas recognized that this is "important work done well." Cleat Zeiler remarked that "innovation is the groundwork for lasting change. The work presented is a game changer that we will see implemented well into the future." Last year's MVPI winner, Hilary Tarvin, wanted Dan heralded for "the amazing wider impact his project had on improving subcrit diagnostics and reducing troubleshooting times."

James Essex

"Spatially Aware Multi-Modal Directional Radiation Detection Swarms"
24-114

Existing radiation detection systems utilize temporal alarming algorithms and lack the ability to perform localization in real-time. Ultimately, we need solutions to aggregate data from multiple passes and multiple detectors to enable automatic search and localize – a "swarm"-type operation. The solution, according to PI James Essex, is SWARMS - Spatially Wise Acquisition Radiation Measurement Sharing. The platform built as part of this SDRD will allow for more complex and math-based methods of data exploitation not previously possible in the realm of radiological search.

Peers were quick to congratulate James on "bridge[ing] the SDRD chasm of death! Tech being actively tested at the 2025 POTUS inauguration. Good use of interns. Great presentation." Jian Ma noted that this was "a very successful project with very promising future applications like environmental protection and bring[s] new generation student[s] to our company. Has a collaboration with a local university." Stuart Baker was sold on the idea and the acronym: "SWARMS. This has the most visible impact to public global security surveillance that can provide transformational visualization with reduced men and man-hours of time for an area."

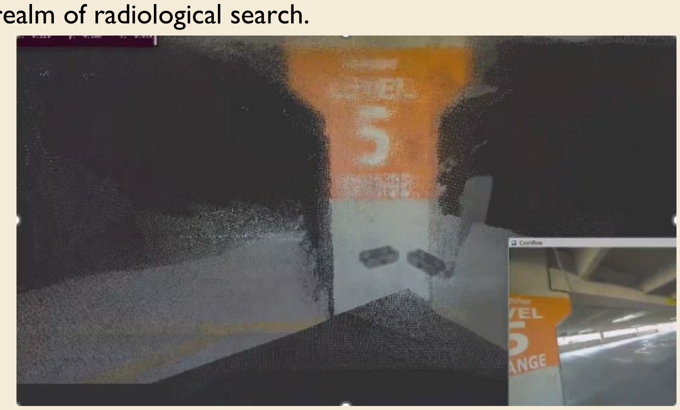

SWARMS output vs. traditional video in real time from James Essex's project (24-114).

Piotr Wiewior

"Strategic Initiative: Developing the NNSS Critical Skills in Accelerator Science and Beam Physics"
24-092

Piotr Wiewior is the PI for one of SDRD's Strategic Initiative (SI) projects designed to address critical skills gaps in accelerator science, engineering, and capabilities at NNSS, while also advaning fundamental research and mitigating beam-target interactions.

The SI established collaborations with leading institutions in accelerator science and in academia.

The SI's ultimate goal is to develop:

- Skills critical for the NNSS to operate and maintain the Scorpius accelerator.
- Beam-target interaction mitigation techniques for single- and multi-pulse LIAs
- Simulations, ML capabilities to support operation and maintenance of LIAs

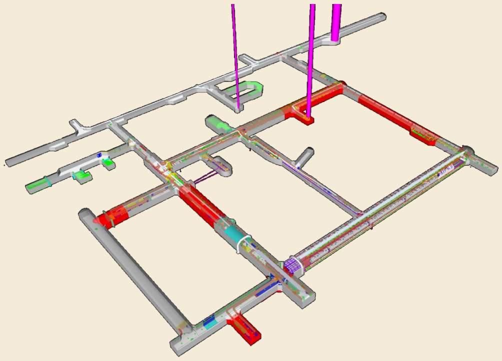

Accelerator rendering from Piotr Wiewior's project presentation (24-092).

Piotr was nominated by his peers who noted the following: "Piotr took over an SDRD SI that was struggling. The external collaboration was not carefully planned, and Piotr re-planned the SI to recover the project." "[Piotr] took over a large and difficult project at the last minute and provided a clear path forward for the next years." "The project is very important for the success of all Scorpius-related activities. It will certainly contribute to the progress of other projects. Piotr is the right man who has the required skills and abilities" (Andrey Esaulov).

Honorable Mentions

Showera Haque, "Needle-Washer Diode for Dynamic X-Ray Diffraction on Actinides at Z" (24-107).

Jerry Stevens, "Thermal Transport Detection of Phase Boundaries at Elevated Pressures" (24-022).

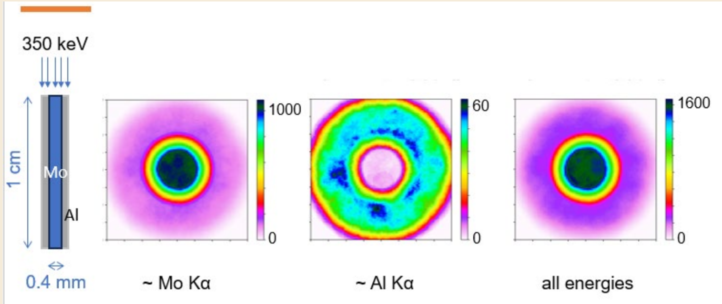

Pinhole images from Showera Haque's project presentation (24-107).

Thin iron coating on a LiF window from Jerry Stevens' project presentation (24-022).

PROGRAM VALUE

SDRD Program Performance Metrics

	FY20	FY21	FY22	FY23	FY24
Number of Projects	29	39	54	47	36
Records of Invention	4	3	0	6	6
Patent Applications	0	1	2	1	5
Technology Adopted by Programs	9	13	9	11	11
Gap or Needs Addressed	12	18	27	29	24
Emerging Area or Special Opportunity	6	18	11	9	9
Journal Publications	24	21	16	5	8
Number of Postdocs	2	12	4	4	1

Records of Invention and Patent Applications

When new and novel research, science, or technologies are achieved in SDRD projects, PIs are invited to submit a Record of Invention detailing their work and protecting their intellectual property. Patents are pursued, when appropriate. In FY 2024, a total of six Records of Invention were filed. Subsequently, five patents were also filed.

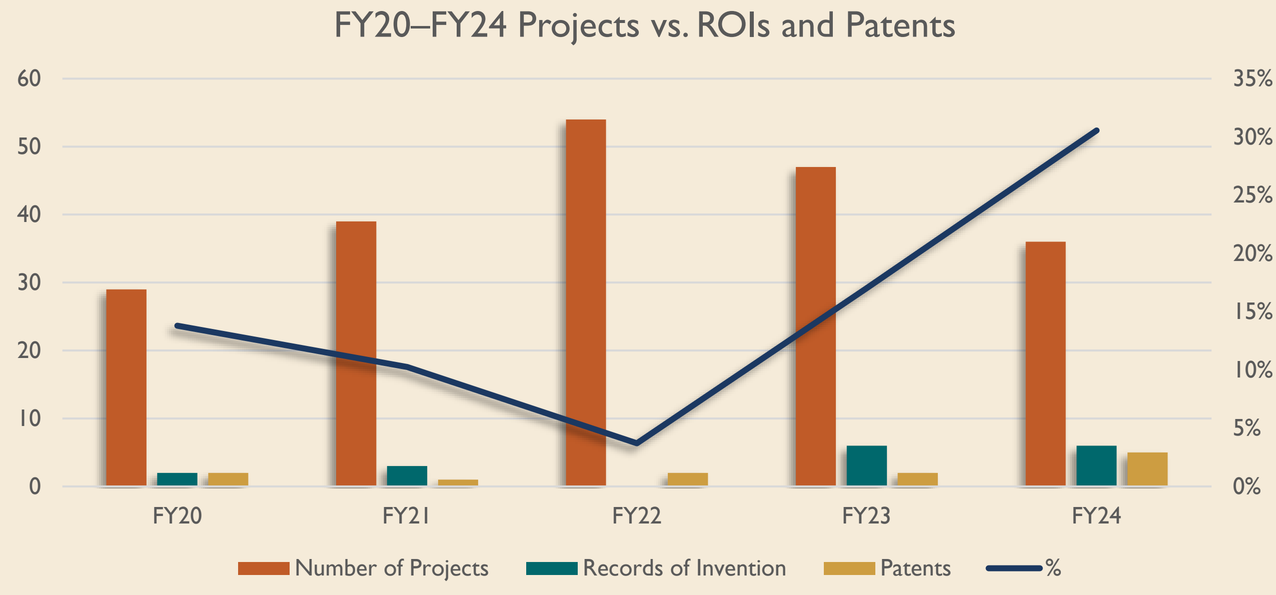

Technology Adopted by Programs

Anticipating needs and providing technology solutions are the cornerstones of the SDRD program, and migrating SDRD-developed technology into programs is a key metric for SDRD program success. In FY 2024, 11 SDRD technologies were adopted by Programs, a rate of nearly 31%.

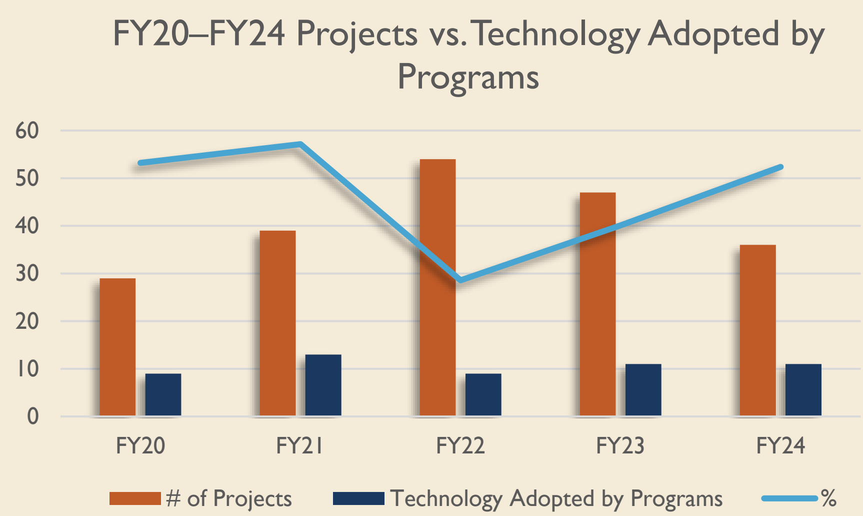

Technology Needs Addressed

Each year, the NNSS creates a Needs Assessment document to guide potential PIs in what mission needs are known and anticipated. The SDRD proposal process evaluates how closely the pre-proposals align with these mission needs. For FY 2024, 67% of the projects funded were directly addressing one of these identified needs. Emerging Areas and Special Opportunities are those that, while not historically under SDRD, fulfill a nationally identified priority. In FY 2024, SDRD had 9 such projects representing 25% of the portfolio.

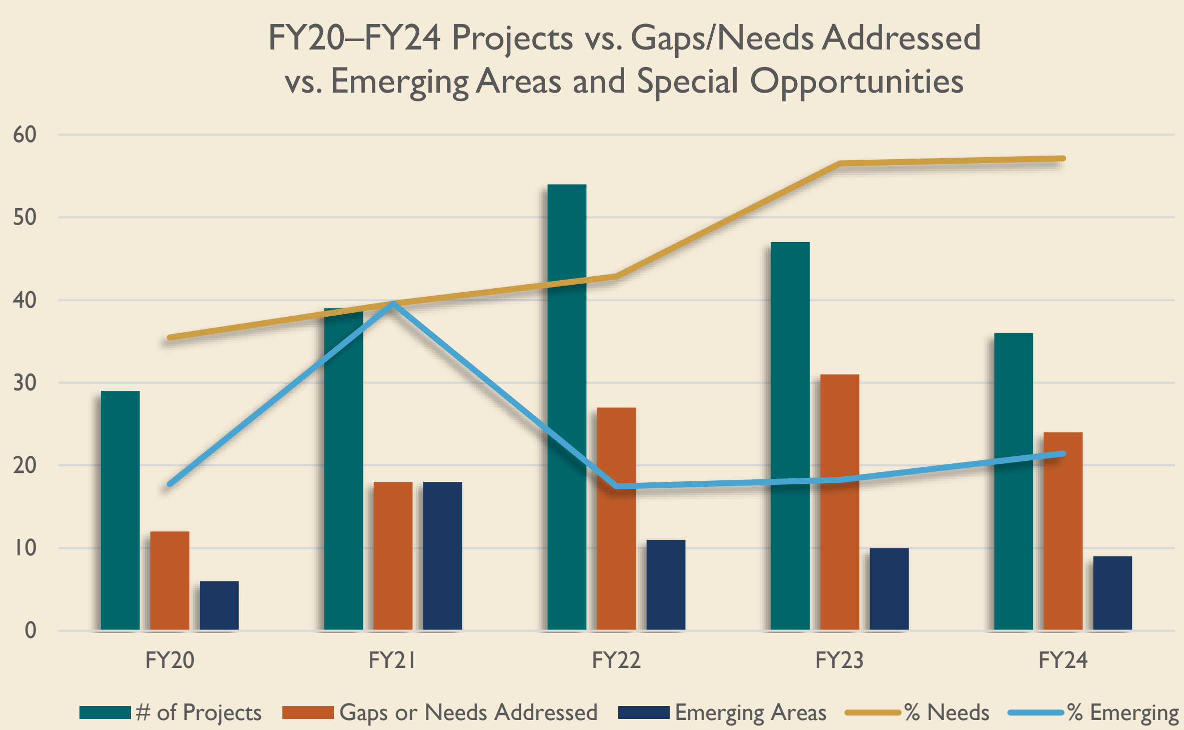

Journal Publications

Publications in peer-reviewed journals showcase the various scientific and technical achievements of our PIs. SDRD had eight publications for FY 2024 including prestigious journals such as the *Nature's Scientific Reports, Journal of Chemical Physics, Results in Physics, Optical Engineering, Physical Review B* and *Physical Review Letters*, as well as the proceedings of SPIE, the international society for optics and photonics, in the Hard X-Ray, Gamma-Ray, and Neutron Detector Physics category.

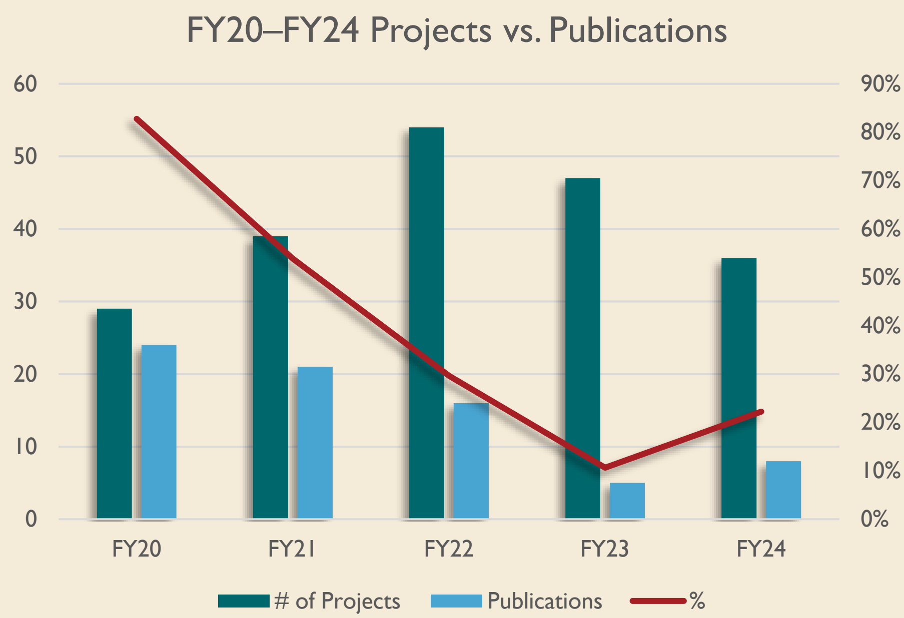

Postdocs and Interns

Early Career Employees are essential to bringing in new perspectives and innovative ideas. The SDRD program brought on one postdoc in FY 2024 and 44 interns which accounted for 37% of the total number of interns at the NNSS.

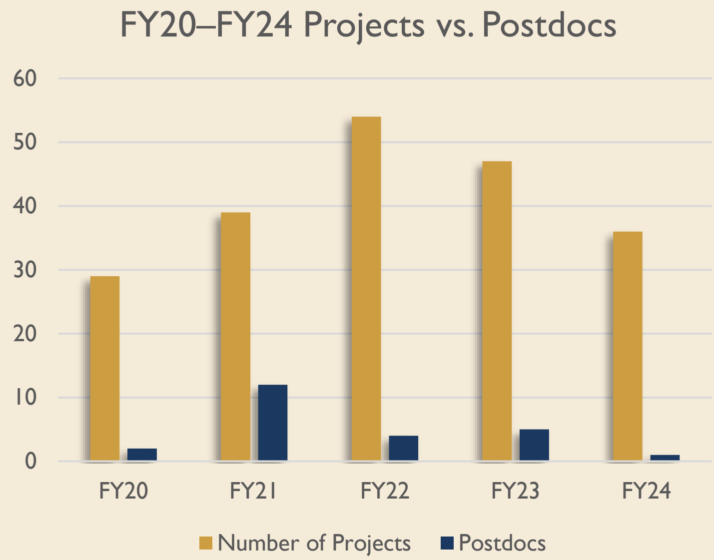

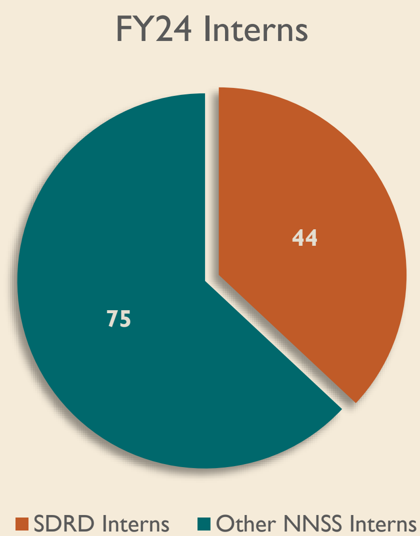

Employee Retention and the NNSS

Employee conversion and retention reveals the desirability to work at the NNSS. SDRD has brought on 229 unique PIs over the last 22 years and has retained 103 for an overall retention rate of 45%.

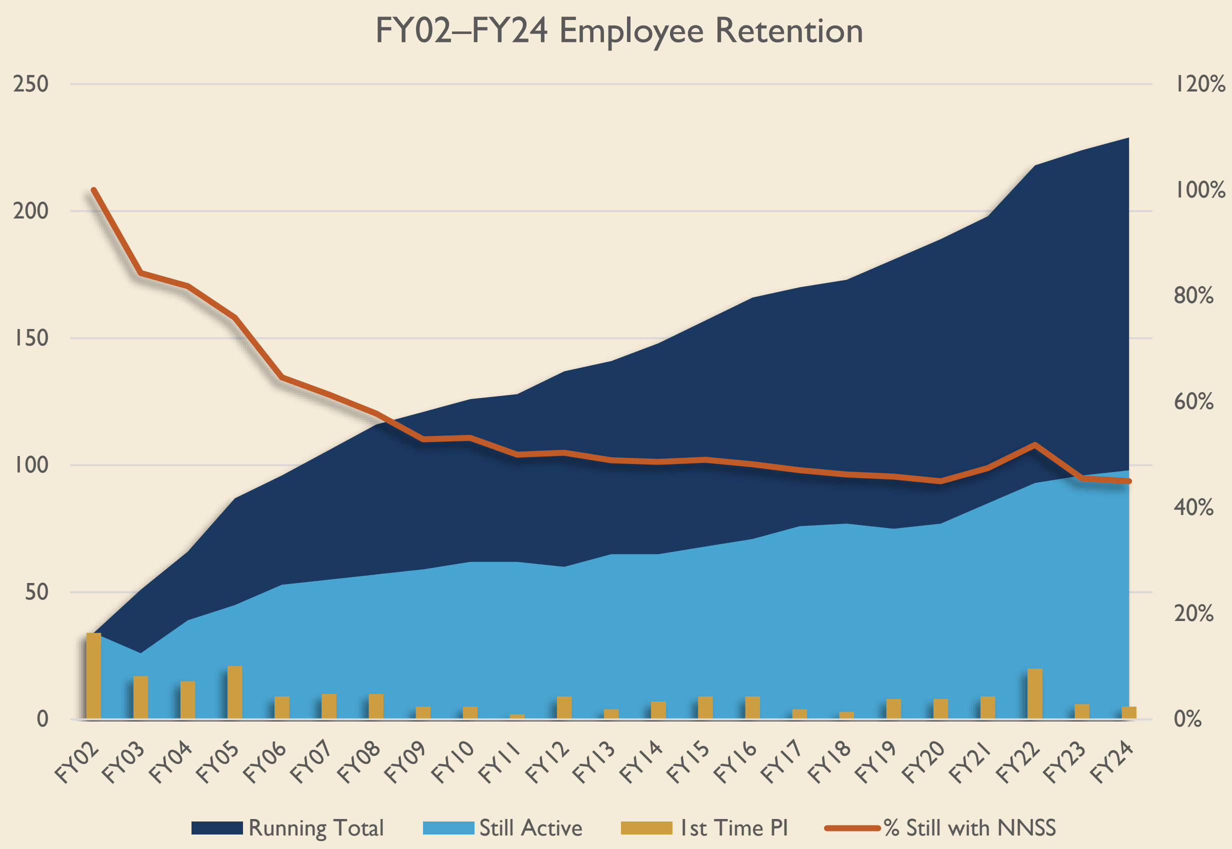

The Top 2%: Distinguished Members of the Technical Staff

The NNSS recognizes the lifetime achievements of its most seasoned scientists and engineers through a promotion to the title of Distinguished Member of the Technical Staff (DMTS). DMTSs are recognized by the NNSS as authoritative sources of information as they provide strategic direction to senior management as well as mentorship to early- and mid-career staff. Of the 20 DMTSs currently at the NNSS, 8 are active participants in SDRD.

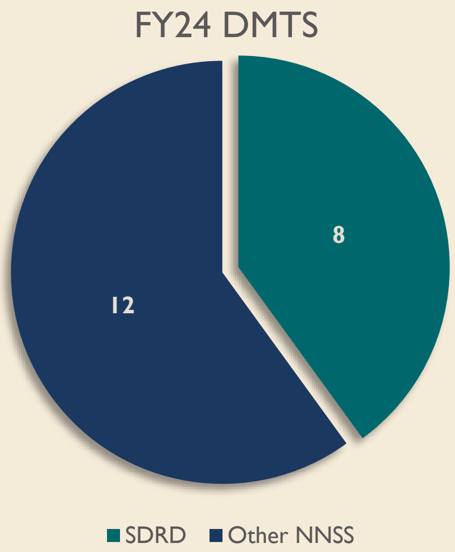

SDRD Impact Stories

SDRD → Programmatic

NNSS Technology Wins an R&D 100 Award

The Electromagnetic Spectrum Management System marks 11th NNSS win

Every year, R&D World holds a competition to determine the year's top 100 innovative technologies. If you take a look at the 2024 winners (released on the R&D World website on August 8), you'll find the NNSS on the list!

Doug Seastrand's Electromagnetic Spectrum Management System (ESMS), technology that was derived from an SDRD project, won an R&D 100 Award in the IT/Electrical category. The decision was made by an esteemed panel of internationally renowned judges in science and technology.

The R&D 100 Awards competition, nicknamed "the Oscars of innovation," focuses on new commercial products, technologies, and materials that are available for sale or license and recognizes them for their scientific and technical significance and innovation.

Congratulations to Doug and his team on this prestigious accomplishment! This achievement is a testament to the NNSS's growing global recognition for its scientific and technical R&D innovations. Read on to learn more about Doug's Electromagnetic Spectrum Management System and how it originated from an SDRD project in 2015.

The Electromagnetic Spectrum Management System: From Idea to Commercial Startup

During the last decade, NNSS Senior Principal Engineer Douglas Seastrand and his team have successfully leveraged project funding from the NNSS SDRD Program to develop patented electromagnetic spectrum management technology. Seastrand worked with Rudolpha "Dolly" Jorgensen, Eric Schmidthuber, Ryan Martin, and Sean Sheehan on the ESMS project. Their work resulted in two patents for technologies to prevent unwanted radio frequency (RF) communications that are useful to the national security and law enforcement mission spaces. This SDRD project, initially developed in 2015 and patented in 2017, opens the way for possible follow-on work, such as exploring modulation control, inserting new or modified modulation, or providing real-time situational awareness of the RF environment.

Doug Seastrand receives his award at the R&D 100 gala.

The team's 2015 one-year SDRD project was titled "Concurrent Transceiver with Ultra-high-speed Fourier Transforms for Unrealized SIGINT Applications" (aka ESMS) and was created to control the RF radio waves propagating through an area. The ESMS system provides a revolutionary approach to controlling RF signals, removing all modulation from every RF signal that is not designated as "friendly," and optionally replacing it with new modulation—thus preventing (or jamming) and controlling all RF communications. The ESMS system selectively allows friendly RF signals to pass without being jammed—including frequency hopping and spread spectrum communication systems. The ESMS technology can near-simultaneously RX [receive] and TX [transmit] to let friendly communications through while blocking all other/unknown communications. ESMS is able to selectively pass or jam any RF signal within its bandwidth, currently up to 8 Ghz.

Conventional jamming techniques have high power requirements. In contrast, the ESMS efficiently tailors each RF carrier output amplitude relative to the signal strength of its received carrier, and the user can determine the hemispherical area of influence to further limit power. ESMS inherently works with all modulation techniques and requires no foreknowledge of the unwanted carrier frequencies.

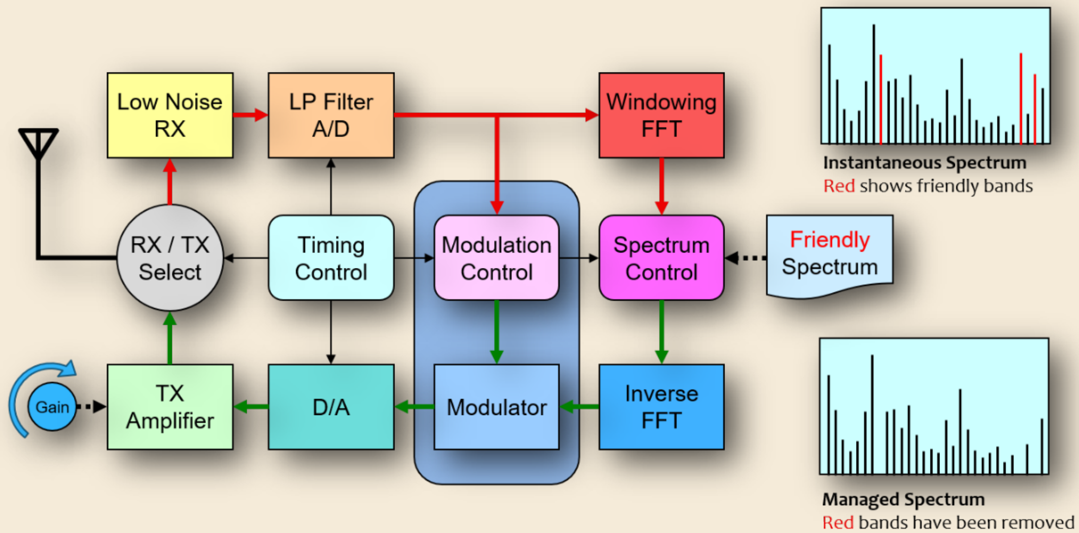

The ESMS rapidly alternates between receive (RX) and transmit (TX) in order to digitize the received RF to produce an Instantaneous Spectrum of all RF carriers. This list of carriers is compared with the Friendly Spectrum to remove them from the Managed Spectrum list. The remaining carriers are considered unfriendly, so they are converted back into RF and retransmitted without their original modulation or with new modulation. The area of jamming influence is dependent upon the RF gain of the TX Amplifier.

It was so promising that, in 2021, Seastrand was nominated and accepted as a FedTech Startup Studio Finalist. FedTech connects scientific work done at the government level with public sector, first-time startup entrepreneurs who plan to grow and monetize inventions for the commercial market using government-generated intellectual property. The vetted entrepreneurs gain access to intellectual property information and federal funding and grants, while the NNSS gains recognition for its groundbreaking work that can be used to improve technology on a large scale. Although other NNSS cohorts were invited to compete for FedTech, Seastrand's invention was the first and only one successfully paired with the optimal entrepreneurs, who have since worked with the NNSS to begin the engineering and commercialization of the ESMS product, forming a startup company. Seastrand was involved in helping the newly founded company to understand the technology and identify potential customers. The startup licensee worked with the mission and operations contractor's (Mission Support and Test Services, LLC [MSTS]) legal department for licenses to advance the technology from a technology readiness level (TRL) of 3 (proof of concept) to TRL 6 (prototype). The startup licensee currently has an MSTS legal agreement for an R&D license to use the technology, and they are in the process of refining the engineering for commercial use.

Patent Notes: Patent filed on Apr 4, 2016. Patent (# 9,559,803 B2) First Awarded on Jan 31, 2017 and Patent (# 9,794,021 B2) Granted Oct 17, 2017. Patent Holders: Douglas Seastrand, Rudolpha "Dolly" Jorgensen, Eric Schmidthuber.

Acknowledgements

SDRD requires a talented team of individuals to ensure success from year to year. Without their support, none of this would be possible.

Special acknowledgment and appreciation go to **Kristen Vernon, Anne Totten**, and **Madeline Gauthier** for technical communications and compiling, editing, and publishing this report; to Kristen Vernon for providing document design; to **Leslie Esquibel**, **Emma Gurr**, **Sally Matthews**, **Kristen Ruocco**, and **Luke Rocha** for project management and cost accounting efforts; to **Michael Baldonado** for information system support; to **Elizabeth Davis**, **Eduardo Morales**, **Sandy Young**, and **Stacey Duffy** for financial data reporting; to **José Sinibaldi** and **Larry Franks** for technical guidance and support; and to our STTA leads and site representatives, and technical review committee: **Stuart Baker**, **Kirk Miller**, **Cleat Zeiler**, **Bruce Dunham**, **Trevor Burris-Mog**, **Daniel Champion**, **Daniel Lowe**, **Edward Daykin**, **Jerry Stevens**, **Marylesa Howard**, **Eric Dutra**, **Amy Lewis**, **Matthew Wallace**, **Scott Suchyta**, **Cameron Hawkins**, **Daniel Frayer**, **Brandon La Lone**, **Dan Clayton**, **Radu Presura**, **Sanjoy Mukhopadhyay**, **James Essex**, and **Rusty Trainham**. Thanks as well to members of our External Advisory Board, **Ryan Camacho**, **Larry Franks**, **Carl Ekdahl**, **Damon Giovanielli**, **Maurice Sheppard**, **Ralph Schneider**, and **Gerry Yonas**, who supply ongoing, valuable recommendations.

Finally, a sincere and special thanks to **Paul Guss**, who served as the SDRD Program Manager over the last few years.

Michael Reed & Cameron Hawkins
SDRD Program Manager & Deputy Program Manager
March 2025

FY24 PROJECT SUMMARIES

Accelerator Beam Science and Target Interactions

ABSTI Projects

Pulsed Optimization with Solid State Utilization of Modulation

Zach Shaw[a]
24-036
Year 1 of 2
Co-Authors: Ivan Aponte[a], Dawson Wright[b], Keegan Kelp[b], Andreas Neuber[b], James Dickens[b], Jacob Stephens[b], and John Mankowski[b]
[a]Nevada National Security Sites
[b]Texas Tech University

Abstract

A novel pulsed power coupling device is to be designed and constructed for the driving of a non-linear load with two individual sources. These sources are of differing impedance, topology, and energy characteristics. This coupling device allows for a secondary pulse to drive a critical point of a non-linear load such as impedance spike or collapse, allow for pulse sharpening of a "traditional" topology with a modern, solid-state source, or even modulation of the overall waveform. To date, prototype versions of each source (Marx and Linear Transformer Driver) have been built and begun characterization. The inductive coupler has reached a Version 1 design, and is being simulated with drivers analogous to the constructed sources. A high voltage, directional diagnostic is currently undergoing assembly to be used to diagnose and characterize the system as a whole. A technique for simulating non-linear 3D magnetic materials in a 1D circuit simulator is also under investigation.

Background

Pulsed power sources are the drivers for many of the Stockpile Stewardship missions test beds. While new driver topologies are still being produced today, their implementation into pre-existing test beds would require a complete project redesign. Our path forward includes a novel approach to allow for the re-furbishing and enhancement of these existing test beds by coupling a classic and modern driver together [SDRD Needs Assessment 2025 (Pages 10-16). Facilities: Cygnus, Gemini, Zeus]. While already proven theoretically feasible, an experimental test bed to determine the efficacy and practicality of this technique is the main focus. Combining like sources is a well-studied concept in pulsed power, yet coupling unlike sources poses specific issues in regards to shielding one source from the other. Inductive coupling has shown success in additive topologies such as Linear Transformer Drivers and Induction Voltage Adders, and is to be studied in depth. One drawback to this technique implementing inductive coupling is that power can couple both ways across the device itself. This would cause issues of floating or exposing the more sensitive solid-state source to high voltages from the Marx, damaging components. Funding allows for the development of critical pulsed power skills, internal collaboration within the NNSS, and external collaboration with Texas Tech University and United States Military Academy (West Point), while helping drive a recruitment pipeline for the next generation of pulsed power engineers. Results of this research initiative allow for options regarding upgrades to all pre-existing mission critical experiments with the need for pulse shaping, or to mitigate the effects of non-linear loads throughout the driving pulse. This technology would increase the operational breadth of current pulsed power driven systems which have been in operation for some time.

Technical Approach

Coupling of like sources has been researched extensively in the form of Inductive Voltage Adders (IVAs) [Wei 2019, Johnson 1987], Linear Transformer Drivers (LTDs) [Mazarakis 2010, Koval'chuk 1997], and even utilizing multiple Marx Generators [Mayes 2001]. IVAs and LTDs share similar concepts, with an electrically isolated annular ring primary coupling to a secondary stalk (or beam) which runs centered through the primary. IVAs utilize multiple sources connected in series to produce a large, additive voltage gradient to be applied to a secondary stalk. LTDs, on the other hand, trigger multiple, independent sources which couple to a secondary stalk via a 1:1 transformer and add via constructive interference.

Our approach utilized this pre-existing LTD technique but developed modified methods to accommodate the coupling of a Primary Source (PS, Marx Bank) and a Supplementary Source (SS, solid-state LTD). Investigators are currently developing coupling methods for processes regarding predominantly high-voltage, and those requiring predominantly high-current. Examples of both processes are a Dense Plasma Focus (DPF), such as Gemini or Zeus, whose processes are current dominated, or a rod-pinch diode application such as Cygnus, where the x-ray generation is dominated by the applied voltage. While established pulsed power sources exist for both applications, interest has been shown by multiple x-ray flash radiography, neutron radiography operations, and scientific staff to modify these pre-existing systems. The coupling of a pre-established PS with a more modern SS allows for manipulation of the applied pulsed power waveform without requiring a whole system redesign.

As an example, it has been proven that the solid-state drivers for the Scorpius Accelerator (an LTD topology) can be modulated to produce somewhat arbitrary output waveforms to the load. Traditionally, pulsed power generators are quite rigid in their waveform and little to no manipulation is achieved without large, pulse sharpening systems, pulse forming networks, or adder topologies. This allows for improvements to amplitude, pulse shape, and rise time, but does not allow for shot-to-shot tailoring of waveshapes to fit the dynamic processes accompanied by a non-linear load. Both example processes mentioned previously have highly non-linear capacitive or inductive loads, which rapidly change the impedance match (i.e., power transfer efficiency) from the source to the load.

The coupling of a PS and SS shall be constructed akin to an LTD or IVA topology, drawing on the concept of an annular ring primary to the stalk of a secondary, composing a coaxial transmission line. Non-linearity of the impedance will cause complex constructive and destructive interference of the two sources driving the changing load, but having a flexible solid-state load can minimize or possibly remove this issue. For a full scale DPF such as Gemini (~1 MJ), care must be taken in protecting the SS from seeing any large reflections from the load. Small scale models are protected with an appropriately specified diode stack, but full-scale experiments with MA or hundreds of kV drivers will require a more well studied approach.

Results

Year one has had a number of accomplishments towards the construction of the test bed:
Members of the NNSS team have designed, developed, and are assembling and testing a four-stage Marx Generator to be used as a primary source (two stages fully assembled and tested). The final design will be composed of four 80 nF capacitors with an erected output of 50 kV (higher voltages possible). To help characterize and troubleshoot the system as a whole, a high-voltage directional coupler is designed and currently undergoing construction. This diagnostic will allow investigators to measure signals propagating in the forward and reverse direction, lending to the characterization of the overall system impedance. These reflection and transmission coefficients (s-parameters) will be used in tandem with the voltage and current measurements to plot impedance variations throughout the pulse. Finally, version one of an inductive coupler has been designed and simulated with analogous sources, providing an in-depth electromagnetic simulation of the system as a whole with a surrogate load.

The Center for Pulsed Power at Texas Tech University (TTU) has designed, developed, and implemented three stages of a solid-state LTD. While only three stages are currently in operation, adding stages is a straightforward process. Experimental and simulated waveforms show good matching, proving variable pulse width, charge voltage, and multi-pulse (burst) capability. In order to better develop the models for these drivers, TTU has also developed a method to simulate 3D, non-linear magnetic materials in a 1D circuit simulation software.

As a collaborative and purely educational endeavor, the United States Military Academy (West Point) is working on this project to develop a MOSFET test bed. Extracting behavior and parasitic elements of FET groups acting as a whole will lead to developing larger and more complex models for large LTD structures while reducing computation time significantly.

Conclusion

Year one has shown that the most critical aspect of this research is in regards to the inductive coupler topology. After simulations have proven foreseen issues with cross talk and protection of one source from another, the PI is exhaustively investigating the current topology with respect to its practicality in the field. Both sources are currently operating as expected, and diagnostics for the test bed have already been decided upon. For year two, the final goal is to have the system working with a surrogate load, while the non-linear load is a stretch goal. Regardless, wave-shaping and sharpening of a pulse on a surrogate load will still experimentally verify the technique is achievable. With respect to programmatic work, confirmation of this technique opens the conversation of test beds the NNSA wishes to have modified for expanded breadth of driver parameters. Whether implemented as a small supplemental system or a complete modification to the existing design, efficacy of this technique will breathe new life into long standing test beds.

References

Hao Wei, Jiahui Yin, Pengfei Zhang, Fengju Sun, Aici Qiu, Tianxue Liang, Jiangtao Zeng, Xiaofeng Jiang, Zhiguo Wang, Jiang Sun, 2019. "Development of a 4-MV, 80-kA-induction voltage adder for flash X-ray radiography." *IEEE Transactions on Plasma Science.* Volume 47, Issue 11, pg. 5030-5036. IEEE Xplore

DL Johnson, JJ Ramirez, CW Huddle, GJ Denison, TL Franklin, LO Seamons, Lee Schlitt, Ian Smith, 1987. "Hermes III Prototype Cavity Tests." *Proc. 6th IEEE Pulsed Power Conf.*. Pgs. 482-485.

MG Mazarakis, JW Poukey, DC Rovang, 1997. "Inductive voltage adder advanced hydrodynamic radiographic technology demonstration." *Sandia National Lab.(SNL-NM), Albuquerque, NM (United States).*

BM Koval"Chuk, VA Vizir", AA Kim, EV Kumpyak, SV Loginov, AN Bastrikov, VV Cheryakov, NV Tsoi, P Moniaux, D Kh"vui, 1997. "Fast primary storage device utilizing a linear pulse transformer." *Russian physics journal.* Volume 40, Issue 12, Pgs. 1142-1153.

JR Mayes, WJ Carey, WC Nunnally, L Altgilbers, 2001. "The Gatling Marx generator system." *PPPS-2001 Pulsed Power Plasma Science 2001. 28th IEEE International Conference on Plasma Science and 13th IEEE International Pulsed Power Conference. Digest of Papers (Cat. No. 01CH37251).* Volume 1, pgs. 504-507.

Publications

Conference Proceedings, Dawson Wright, Keegan Kelp, John Mankowski, Jacob Stephens, James Dickens, Andreas Neuber, Zach Shaw,"Simulation of Nanocrystalline magnetic Cores using Maxwell ANSYS." Not Yet Published, 2024. *2024 International Power Modulator and High Voltage Conference.*

Conference Proceedings, Keegan Kelp, Dawson Wright, John Mankowski, Jacob Stephens, James Dickens, Andreas Neuber, Zach Shaw,"Investigation of Pulsed Nanocrystalline Magnetic Core Behavior." Not Yet Published, 2024. *2024 International Power Modulator and High Voltage Conference.*

Presentation, Keegan Kelp, Dawson Wright, John Mankowski, Jacob Stephens, James Dickens, Andreas Neuber, Zach Shaw,"Investigation of Pulsed Nanocrystalline Magnetic Core Behavior." Oral presentation, 2024. *2024 International Power Modulator and High Voltage Conference.*

Poster, Dawson Wright, Keegan Kelp, James Dickens, John Mankowski, Jacob Stephens, Zach Shaw, and Andreas Neuber,"Simulation of Naocrystalline Magnetic Cores using Maxwell ANSYS." Oral Presentation, 2024. *2024 International Power Modulator and High Voltage Conference.*

Exploration of an Electron Linac-Driven Photoneutron Source Based on Scorpius

Amber Guckes[a]
24-044
Year 2 of 2
Co-Authors: Jesse Andrew Green[a], Kaleab Ayalew[a], James Mellott[a], Elizabeth Bell[a], Allan Ortiz[b], Kevin Yim[c]
[a]Nevada National Security Sites, [b]Los Alamos Operations, [c]University of Nevada, Las Vegas

Abstract

Neutron production can be realized with an electron linear accelerator (linac) and appropriately selected photodisintegration target configuration. Photoneutron sources can be valuable to the stockpile stewardship and global security missions. Specifically, an electron linac-driven photoneutron source could be utilized as a short pulse neutron source to enable diagnostics such as neutron radiography and neutron resonance spectroscopy on subcritical experiments (SCEs). An electron linac-driven photoneutron source currently does not exist at the NNSS. However, the highly anticipated Scorpius machine could be utilized in this way. This project will explore the feasibility of valuable neutron production with Scorpius for neutron diagnostics of importance to stockpile stewardship.

Background

The Scorpius machine is a multi-pulse linear induction accelerator (LIA) with an electron end point energy of ~20 MeV [1,2]. In its intended configuration, the electrons produced by Scorpius will impinge on a Bremsstrahlung x-ray target, enabling x-ray radiography of SCE.
Production of photoneutrons has been studied at the Los Alamos National Laboratory (LANL) Dual Axis Radiographic Hydrotest (DARHT) facility, which is analogous to Scorpius [3,4]. From these studies, an x-ray target designed to minimize unintentional neutron production was realized for Scorpius.
Intentionally leveraging Scorpius as a flash photoneutron source could provide the capability to perform neutron-based measurements of both static and dynamic experiments. Photoneutron energy and yield can be tuned based on target geometry and material to enable measurements such as neutron radiography, fission fragment detection, neutron resonance spectroscopy, and radiation effects studies, which is a possibility that is not currently envisioned for the Scorpius testbed at the NNSS.

Technical Approach

Incorporating photoneutron-producing materials into the existing Scorpius Bremsstrahlung x-ray target or devising an independent photoneutron target will create a viable dual x-ray/neutron source. Various materials such as heavy water, high-density polyethylene, beryllium, tungsten, lead, and tantalum have been used as targets employed with electron accelerators and rhodotrons to produce photoneutrons previously [5-10]. Low-Z materials can be used to optimize the production of slow neutrons, and high-Z materials can be used to optimize the production of fast neutrons [11-13].

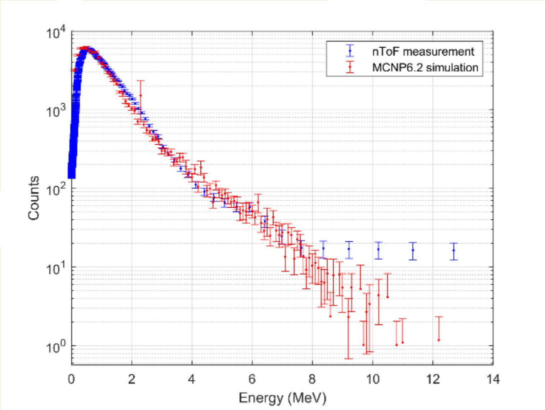

Figure 1. Measured photoneutron energy spectrum created from 20 MeV electrons into a Bremsstrahlung X-ray converter, resultant X-rays impinge on the ¾-inch-thick tungsten photoneutron target; compared to MCNP6.2 simulation normalized to the peak of the measured data.

Our team explored the intentional production of photoneutrons using Scorpius' electron beam parameters by means of Monte Carlo Neutron Particle (MCNP) radiation transport simulations and experimental measurements at the Idaho State University (ISU) Idaho Accelerator Center (IAC). The MCNP work informed the optimum photoneutron target material and dimensions. The measurements were used to predict the neutron yield and energy spectrum expected from Scorpius with the optimized photoneutron target.

A ¾-inch-thick depleted uranium target was found to maximize the total neutron yield. However, due to tungsten material being readily available in the correct thickness, a tungsten target was fielded for measurements at the ISU IAC. The purpose of these measurements was to validate the simulations and provide an experiment-based prediction of the total photoneutron yield and the photoneutron energy spectrum. The IAC's L-band linac operated at 20 MeV electron endpoint energy with a pulse width of 70–100 ps and was used to generate Bremsstrahlung x-rays in a thin tungsten converter. The photoneutron target was centered on the thin target converter. Four NNSS PMD-362 neutron time-of-flight (nToF) detectors were fielded with the L-band linac measurements to infer the neutron energy spectrum. The IAC's S-band multiport linac operated at 20 MeV and a pulse width of 4 µs, maximizing charge on target. It was used in a similar way with the thin tungsten converter and photoneutron target. Neutron activation foils were fielded with the S-band linac for total and thermal neutron yield measurements. The activated foils were then analyzed using a High Purity Germanium (HPGe) detector.

Both neutron energy spectrum and flux measurements were made at the ISU IAC using their L-band and S-band linear accelerators, respectively, having fielded a ¾-inch-thick tungsten photoneutron target. These measurements were used to predict the performance of the Scorpius LIA ahead of its installation and commissioning at the NNSS.

Results

This effort aimed to maximize the total neutron yield and characterize the resultant neutron energy spectrum. Radiation transport simulations with MCNP6.2 provided the basis for the photoneutron target design. Experimental measurements performed at the ISU IAC informed the prediction of a Scorpius photoneutron source performance. With a ¾-inch-thick, 3-inch diameter tungsten target, the measured neutron energy spectrum was like a fission spectrum in shape, but had a peak at 0.55 MeV and maximum energy at ~13 MeV. The predicted total neutron yield was $9.31\times10^{13} \pm 4.66\times10^{12}$ neutrons/pulse. Simulations indicate that using a depleted uranium target yields 2.5x more neutrons than tungsten. This prediction indicates that Scorpius could be used to create useful energies and quantities of neutrons to enable diagnostics such as neutron radiography, fission fragment detection, neutron resonance spectroscopy, and radiation effects studies. Existing short-pulse neutron source capabilities at the NNSS include a deuterium-tritium fueled dense plasma focus (DPF) [14]. For comparison, the DPF can achieve a pulse width of 61.8 ± 30.7 ns and $1.84\times10^{12} \pm 0.49\times10^{12}$ neutrons/pulse.

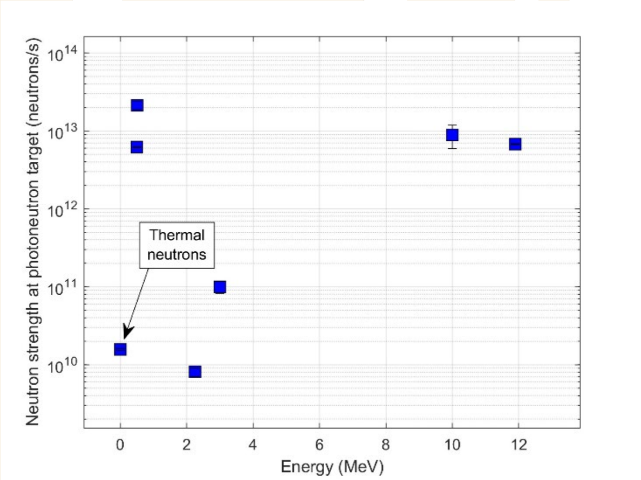

Neutron source strengths as a function of threshold energy determined by neutron activation analysis method; note that the neutron source strengths measured at 10 MeV and 11.9 MeV threshold energy do not agree with the nToF measurement and should be considered suspect.

Conclusion

Our work revealed that neutrons could be produced by Scorpius in useful yields and energies. Looking forward, a specific application should be targeted to refine the photoneutron target design for that application. Such an effort is being proposed as an FY 2025 through 2027 interlaboratory Laboratory-Directed Research and Development project. This team, in collaboration with scientists at LANL, are proposing to prove dual x-ray/neutron radiography based on Scorpius and the efforts under this Site-Directed Research and Development project. Funding notifications will be made before the end of CY 2024.

There is currently programmatic work to investigate multi-probe radiographic capabilities being headed by LANL. Although their current efforts are focused on laser-driven multi-probe sources, there remains interest in accelerator-driven multi-probe sources as part of that effort [15].

References

[1] M. Crawford, 2020. "ASD-Scorpius Overview, LA-UR-20-26293." *NNSS Science & Technology Work-in-Progress Seminar.* Nevada National Security Sites, North Las Vegas, NV, USA

[2] M. Crawford and J. Barraza, 2017. "Scorpius: The development of a new multi-pulse radiographic system." *IEEE 21st International Conference on Pulsed Power (PPC).* Brighton, UK, 10.1109/PPC.2017.8291266

[3] M. Chadwick, T. Brown, and R. Little, 1998. "Photoneutron production in electron beam stop for dual-axis radiographic hydrotest facility (DARHT), LA-UR-97-5174." *Proc. of the 1998 Radiation Protection and Shielding Division Topic Conference: Technologies for the New Century, American Nuclear Society.* Nashville, TN, USA

[4] A.J. Mendez, G.P. Salazar, and M.M. Pickrell, 2021. "Design of the New DARHT X-ray and Neutron Shielding and Measured Results, LA-UR-21-25952"." Los Alamos National Laboratory, Los Alamos, NM, USA

[5] D.L. Duke, 2018. "Short-Pulse Photoneutron Production on Beryllium Using the Mercury Pulsed Power X-ray Source." *osti.gov.*, osti.gov

[6] M. Mamtimin, 2014. "A Study of Electron Accelerator Based Photon & Neutron Production and Applications to Nuclear Transmutation Technologies." Idaho State University, Pocatello, ID, USA

[7] T.K. Tuyet, T. Sanami, H. Yamazaki, T. Itoga, A. Takeuchi, Y. Namito, S. Miyamoto, and Y. Asano, 2021. "Energy and angular distribution of photo-neutrons for 16.6 MeV polarized photon on medium–heavy targets." *Nuclear Instruments and Methods in Physics Research, Section A.* Volume 989, 64965., 10.1016/j.nima.2020.164965

[8] A. Allardice, 2014. "Neutron Production and Transport at a Medical Linear Accelerator." Colorado State University, CO, USA

[9] A. Sumbaev, V. Kobets, V. Shvetsov, N. Dikansky, and P. Logatchov, 2020. "LUE-200 Accelerator—A Photo-neutron Generator For The Pulsed Neutron Source "IREN“." *JINST* . 15, T11006., 10.1088/1748-0221/15/11/T11006

[10] V.W. Yuan, J. David Bowman, D. J. Funk, G. L. Morgan, R. L. Rabie, C. E. Ragan, J. P. Quintana, H. L. Stacy, 2005. "Shock Temperature Measurement Using Neutron Resonance Spectroscopy." *Phys. Rev. Letters.* 94, 125504., 10.1103/PhysRevLett.94.125504

[11] J. Bundgaard, S. Baker, R. Malone, S. Smith, A. Lopez, C. Carlson, J. Castaneda, M. Kaufman, K. Walters, J. Tinsley, A. Durand, V. Geppert-Kleinrath, C. Wilde, J. Tybo, C. Gautier, M. White, S. Winder, R. Nelson, 2019. "Neutron Radiography Efforts." , osti.gov

[12] F. Tabbakh, M.M. Aldaavati, M.S. Hoseyni, 2012. "Induced photonuclear interaction by Rhodotron-TT200 10 MeV electron beam." *Pramana - J Phys* . 78, 257–264 ., 10.1007/s12043-011-0232-y

[13] N. Bennett, M. Blasco, K. Breeding, D. Constantino, A. DeYoung, V. DiPuccio, J. Friedman, B. Gall, S. Gardner, J. Gatling, E. C. Hagen, A. Luttman, B. T. Meehan, M. Misch, S. Molnar, G. Morgan, R. O"Brien, L. Robbins, R. Rundberg, N. Sipe, D. R. Welch, V. Yuan, 2017. "Development of the dense plasma focus for short-pulse applications." *Phys. Plasmas* . 24 (1): 012702., 10.1063/1.4973227

[14] S. Batha, D. Broughton, A. Favalli, C. Huang, R. Reinovsky, T. Schmidt, B. Wyatt, 2022. "Overview of the LANL Multi-Probe Radiography Project." , doi.org/10.2172/1875768

Publications

Presentation, Kevin Yim, Alexander Barzilov, Amber Guckes, Jesse Andrew Green,"Computational study of tungsten and depleted uranium photoneutron targets for a 20 MeV electron linear accelerator." https://caari-sneap.com/sites/caari-sneap.com/files/document/caari-sneap-2024-v240724.pdf, 2024. *27th International Conference on the Application of Accelerators in Research and Industry (CAARI).*

Presentation, Amber Guckes, Jesse Andrew Green, Kaleab Ayalew, James Mellott, Allan Ortiz, Elizabeth Bell, Kevin Yim, Alexander Barzilov,"Prediction of performance for a short, multi-pulse photoneutron source based on the NNSS Scorpius linear induction accelerator." https://caari-sneap.com/sites/caari-sneap.com/files/document/caari-sneap-2024-v240724.pdf, 2024. *27th International Conference on the Application of Accelerators in Research and Industry (CAARI).*

Strategic Initiative: Developing the NNSS Critical Skills in Accelerator Science and Beam Physics

Pitor Wiewior[a]
24-092
Year 1 of 3
Co-Authors: Ivan Aponte[a], Trevor Burris-Mog[a], Ilja Draganic[a], Andrey Esaulov[a], Showera Haque[b], Cameron Hawkins[a], Sean Littleton[b], Evan Scott[a], Zach Shaw[a], Matt Wallace[b], Aaron Covington[c], Jeremy Iratcabal[c], and Brian Franzomi[a]
[a]Nevada National Security Sites
[b]Livermore Operations
[c]University of Nevada, Reno

Abstract

This strategic initiative (SI) was developed to remove gaps in critical skills and accelerator capabilities at the NNSS as well as perform fundamental research and mitigate beam-target interactions. The significance of the $1M budget request is a response to the gap size and the importance of the capabilities and critical skills. Roughly half of the budget will fund a Stanford Linear Accelerator Center (SLAC)-NNSS collaboration to perform fundamental accelerator research, transfer knowledge from SLAC subject matter experts (SMEs) to the NNSS, develop capabilities, and provide opportunities to recruit accelerator SMEs from SLAC (Stanford has a low post-doc conversion rate). The remaining budget will fund collaborations between the NNSS and Los Alamos National Laboratory (LANL) (J-6 and XCP-7) SMEs to develop and perform experiments and computer simulations to mitigate beam-target interactions (i.e., mitigate desorbed contaminants from the target surface and bulk material) and explore techniques to confine targets on multi-pulse linear induction accelerators.

Background

The NNSS has never operated or maintained an accelerator as complex or large-scale as Scorpius, and we must rapidly develop the critical skills necessary to support its operation. Without these essential skills, the NNSS will face significant challenges in fulfilling its mission effectively. Timely skill development is crucial, as Scorpius is scheduled to be operational by 2029, and early preparation will ensure readiness. Scorpius is vital for conducting subcritical experiments with plutonium, eliminating the need for nuclear tests. The ESCE facility will capture high-resolution x-ray images of implosion dynamics in scale models of plutonium pits, which are integral to the primary stage of nuclear weapons. This facility will play a key role in addressing concerns about weapons aging, certifying the performance of newly manufactured pits, and evaluating the impact of new manufacturing methods. Ensuring the surety, reliability, and safety of the nation's nuclear arsenal is essential for national security.

Future Diagnostics for Scorpius

Conserved Quantity	Plume, Plasma	Diagnostic Technique	Beam	Diagnostic Technique
Mass	Density	Two-Color Interferometer (TCI), Thomson Scattering (TS), Filtered Plume Imaging, Shadowgraphy	Current, Current Density	BPMs, Optical Transition Radiation, Pinhole Imaging, Characteristic X-ray Emission
Momentum	Velocity	PDV (Early Times), Spectroscopy (e.g. Doppler shift) Thomson Parabola, Multi-frame Shadowgraphy, Multi-chord TCI, Faraday Cup/Charge Collectors	Transverse Emittance	Pepperpot, Optical Transition Radiation with solenoid scan (near/far)
Energy	Ion Energy, Temperature	Thomson Parabola, Thomson Scattering, Spectroscopy (e.g. line ratios)	Longitudinal Energy Spread	Magnetic Spectrometer, Compton Spectrometer

The planned collaboration with SLAC presented significant challenges, ultimately leading to its cancellation. The initial goal was for this SI to sponsor several post-doctoral positions at SLAC, with the expectation that these postdocs would later join the NNSS. However, the higher-than-expected costs associated with the postdoc in the Bay Area, combined with a budget cut, forced us to reduce the offer to just one position. When SLAC was unable to find even a single suitable candidate, we shifted our focus toward developing our own personnel and strengthening collaborations with Nevada-based academic institutions.

Technical Approach

Topics of Interest Investigated During the First Year of the Project:

1. Beam-Target Interaction and Diagnostics Development:
As the Scorpius accelerator transitions from Initial Operational Capability (IOC) to Full Operational Capability (FOC), the diagnostics for beam-target interactions will become critical. The complexity of these interactions demands a multidisciplinary approach, utilizing diverse diagnostic techniques. A primary goal of the project is the development and testing of methods to probe the expanding plasma and plume between pulses. Diagnostic techniques under investigation include shadowgraphs, schlieren, interferometry, and spectroscopy.

To achieve this, we will collaborate with partner institutions, including LANL/Dual Axis Radiographic Hydrotest (DARHT) and academic institutions like the University of Nevada, Reno, to access unique experimental facilities and foster productive partnerships.

2. Investigations into Multi-Pulse Electron Beam to X-ray Conversion:
We are focusing on the physics of three key regions that impact the conversion of multi-pulse electron beams into x-rays:
- Warm Dense Matter in the Target: The warm dense matter created in the target acts as a short focal length lens, affecting both dose and spot size. Additionally, phenomena such as instabilities and diamagnetic currents must be considered in this context.
- Advanced Ion Mitigation Techniques: High-dose-rate requirements for Scorpius necessitate unique ion mitigation strategies. During beam-target interactions, ions generated by prior pulses can be accelerated by the beam potential, then disrupt the beam and lead to pinching. To address this, we are exploring several technical approaches, including laser target cleaning, gas jets as novel targets, ground cones, cleaned barrier foils, dynamic focus correction coils, and innovative target designs.
- Target Expansion and Dose Reduction: The e-beam causes target expansion, leading to dose reduction due to the loss of conversion material. To better understand the effects of multi-pulse interactions, we aim to measure and model the expansion of Scorpius-specific targets. Our project will focus on Equation of State measurements and computer simulations to predict optimal beam energy, accounting for target expansion. We will utilize CHICAGO on our HPC platform, along with coupled MCNP-LASNEX-LSP codes, and are considering additional simulation codes as necessary.

3. Optimization of Beam Transport in the Injector Region:
The third area of interest is the optimization of beam transport through desorbed species in the injector region, which is critical for maintaining beam quality and performance.

Results

Example 1: Time-resolved interferometer system for simultaneous free- and bound-electron density measurements in an expanding linear induction accelerator target.
The time-resolved dual-color interferometer was fielded at DARHT for density measurements, but data was inconclusive. This project seeks to address possible sources of phase noise in the system and address other possible noise sources.
Challenges: Experiments depend on DARHT schedule which is fluctuating erratically. Some additional procurements necessary in FY 2025.
Path forward:
- Scale up to multi-chord and multi-angle measurements.
- Implement detector arrays.

- Multiple probe beams for simultaneous measurements from different ports.
- Enable time-resolved density reconstruction of expanding target.
- Add visible laser 785/633/405 nm.
- Improve detection: fast digitizers, set ref frequency, direct digitization.

Example 2: Broadband 2D x-ray imager for Scorpius plume diagnostics.
Cylindrical bent convex crystals can be used to:
- Image an x-ray source in the dispersion direction (tested for 0.1 – 10 mm sources)
- Produce 2D image of the source in each spectral line over a broad spectral range

Spectra in which each spectral line is an image of the source enable 2D space-resolved plasma diagnostics, e.g., maps of plasma density and temperature.
Challenge: Experiments depend on DARHT schedule which is fluctuating erratically.
Path forward:
- The imager can be upgraded with time-gated recording, adding the temporal information.
- Perform the measurements on DARHT-II to demonstrate the ability to image high energy x-ray source.

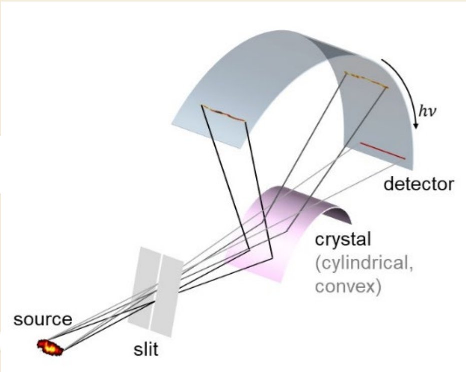

Schematic view and principle of operation of the broadband 2D x-ray imager for Scorpius plume diagnostics. (Courtesy of S. Haque).

Example 3: Target laser cleaning and diagnostics – collaboration with University of Nevada, Reno.

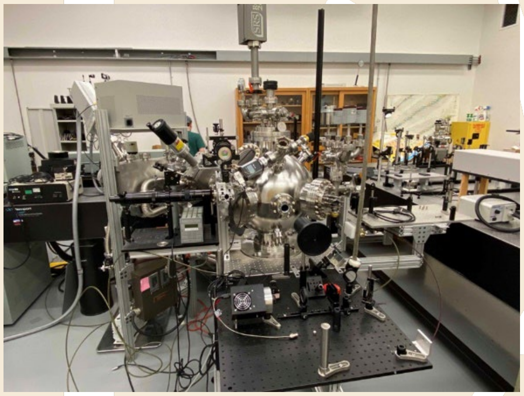
LAPEx apparatus at UNR laboratory. A spherical target chamber occupies the center, with an RGA mounted on top. To the left side of the chamber is a mass spectrometer, while the lasers and spectrometers are located on the right.

Limited laser target cleaning experiments were conducted at LANL, highlighting the need for more systematic studies using varied laser parameters (e.g., energy, pulse duration, wavelength, rep rate, etc.). UNR has a unique apparatus ideally suited for these experiments, along with staff who possess necessary expertise. The first measurements are scheduled for Q4 2024, delayed from Q3 due to the laboratory relocation.
Challenge: The LAPEx lab was recently relocated to the different room within the UNR facility, causing a delay in the original schedule.
Path forward:
- Optimization of laser cleaning of targets, and barrier.
- Develop the spectroscopy measurements to identify ions composition of the plume.
- Study different targets designs.

Example 4: Supercontinuum laser for diagnostics development in the NNSS and partner labs.
A supercontinuum laser (Super K Fianium FIU-15) was procured by SI and will be available for diagnostics development. Succinctly described as “broad as a lamp, bright as a laser”, the supercontinuum source is a marvel of modern laser technology with the turn-key operation. It combines the best of the two worlds: an ultrabroad

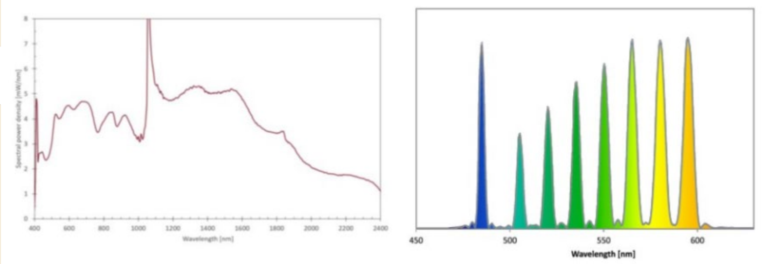
Left: Spectral power of a SuperK FIANIUM FIU-15. The output spectrum covers wavelengths from 400 nm to 2400 nm with approx. 6W of integrated power. The peak at 1064 nm is the residual pump peak of the YB fiber laser. Right: Example of single-lines output spectrum from FIANIUM FIU-15. (Courtesy of NKT Photonics).

spectrum available in the past only from incandescent and fluorescent lamps with a single-mode beam, pointing stability, and brightness attributed to a laser.
Fianium will be used for the multiple optical diagnostics developments, including but not limited to:
- Optical spectroscopy in various configurations (e.g., absorption, emission, CRDS...).
- Shadowgraphs and schlieren imaging of the plume.
- Time-resolved optical methods.

Example 5: Development of Python tools to convert XTR input decks to BMAD accelerator lattice.
We were able to successfully demonstrate that BMAD can be used to model a linear induction accelerator, with results consistent with XTR but also providing more insight into the evolution of the beam distribution. We think this makes a compelling case to extend this capability to model instabilities such as BBU in the next fiscal year.

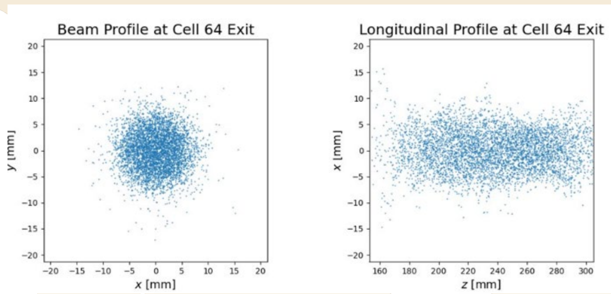

Examples of BMAD simulations. (Courtesy of S. Littleton, NNSS LO.)

Example 6: Development of cluster analysis to computation time for Pulsed Power optimization.

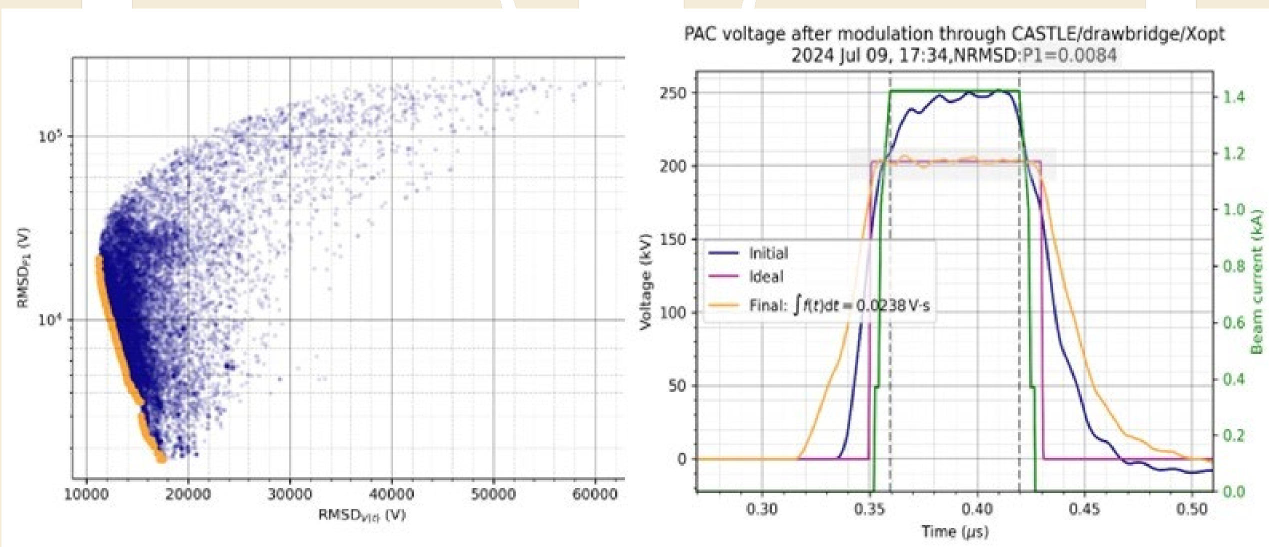

Cluster analysis simulation results. Right: Pareto front (optimal solutions given two objectives). Left: PAC voltage after modulation through CASTLE/Drawbridge/Xopt. (Courtesy of E. Scott and B. Franzoni, NNSS)

Conclusion

Despite the initial challenges with SLAC, the project has successfully progressed.

- In the first year, we significantly reduced the NNSS's skills gap in areas such as numerical analysis, beam parameter modeling, instabilities, beam transport optimization, and multi-head detector modeling. Critical skills in beam physics, envelope equations, accelerator science, and pulsed power have also shown notable improvement.
- The Strategic Initiative played an important role in advancing the Scorpius Computer Modeling Team, which led to the team receiving the 2024 President's Distinguished Performance Award for Innovation. All NNSS recipients of this prestigious award are key contributors to the Strategic Initiative.

- On the experimental front, we initiated a promising collaboration with the University of Nevada, Reno, focusing on target/plume diagnostics, target cleaning methods, ion desorption mitigation, and other experimental physics.
- Lastly, we are pleased with the success of our summer internship program. The Strategic Initiative supported three interns in 2024, all of whom performed exceptionally well. Notably, one of the summer interns is going to work with the ASD team as a casual employee.

Path forward:

1. Enhance Critical Skills: Continue advancing the expertise of NNSS personnel in key areas such as beam physics, accelerator science, and numerical methods, including the application of Machine Learning for Scorpius.

2. Strengthen Collaborations: Further develop and nurture collaborations with our partners, fostering knowledge transfer and productive cooperation:

- With LANL on target R&D, FLAG and CHICAGO Target/Source simulation.
- With UNR on diagnostics for deciphering target-beam interaction, target R&D, plume physics, and Equation-of-State experiments. These initiatives will be instrumental in advancing high-level collaboration between UNR and the NNSS.

3. Build NNSS Expertise - Expand NNSS capabilities in areas critical to ASD:

- Establish a vacuum technology laboratory with a test stand and provide training courses for NNSS personnel
- Develop an optical and laser diagnostics laboratory, equipped with modern technology, to serve as a training ground for diagnostic specialists.

4. Foster Knowledge Sharing

- Introduce a monthly Journal Club in the NNSS as an informal platform for discussing recent scientific advancements.
- Launch a monthly virtual colloquium, featuring invited speakers from leading accelerator facilities and academic institutions. This initiative will provide NNSS personnel with unique opportunities to engage with world-class experts, ask questions, and build valuable professional connections.

Communications and Computing

C&C Projects

Computational Fluid Dynamic Simulations for Critical Infrastructure (CFD-SCI)

Sean Breckling[a]
24-016
Year 2 of 3
Co-Authors: Clifford Watkins[b] and Jacob Murri[b]
[a]Nevada National Security Sites
[b]Special Technologies Laboratory

Abstract

While the NNSS has individuals with Computational Fluid Dynamics (CFD) expertise, little is available as a capability for Global Security needs. This project will use case studies to solve two relevant simulation challenges. The approach will be iterative, using our computational skills and our ability to perform physical sensing experiments for validation in surrogate testbeds. Target research includes validating a mitigation technique for insufficient breathable air in occupied spaces found in public transportation (Strategic Partnership Projects focus), and simulating air flow in high hazard chemical production facilities whose air handling is coupled to the environment through intentionally drafty buildings (Nonproliferation focus). While these simulation/verification use cases will provide much needed understanding of both vulnerable environments and movement of nonproliferation materials into the environment, a more global result will be developing a core S&T capability for airflow simulation as it applies to our sensing needs.

Background

In FY24, we focused our efforts on delivering a fluid model sufficiently efficient to execute in a digital twin environment. Cliff Watkins and Sean Breckling had identified this potential scope under the SET/Osiris project and worked with venture management to chalk out a plan. To make execute volumetric flow computations of SET in a practical amount of time at the nominal prevailing atmospheric conditions, significant model reduction and simplification is required. The classic simplification strategies (e.g., Large Eddy Simulations, Reynolds Averaging, etc.) are options, but they require fresh full-scale computations every time the user adjusts a relevant flow setting. While there exists newer model-reduction methodologies that leverage Proper Orthogonal Decomposition (POD), they too suffer from the inflexibility of the spatial discretization.

Technical Approach

The main innovation in year two was identifying that POD-based model reductions, as such, are not encumbered by much of the restrictions common to models defined by partial differential equations, but by the variations in the data they're based upon. Therefore, if a POD-based reduced order model (ROM) could be defined on a sub-region of the domain likely to present complicated flow, then it could be possible to selectively apply surrogate models in lieu of directly computing results in that localized region. Such a capability would stand to greatly reduce the overall computational complexity of a full-facility model, since the only regions of the flow computed directly would be laminar regions far away from the dynamic forcing, sharp boundaries, or buoyancy effects.

A similar notion was explored by Chung et al. at Lawrence Livermore National Laboratory (LLNL) [1], wherein they trained a collection of POD-ROMs of the linear Stokes model, and attached them together like blocks. This approach demonstrated that separate ROMs can be connected at an interface, and produce results that adhere to the combined model. What this version lacks is the generality to move objects freely. If two ROMs can be attached, then certainly it must be possible to submerge a ROM into a larger full-order computation.

While this notion solves the model reduction problem in theory, there were significant technical hurdles. It is not guaranteed that the flux of fluid momentum across the surrogate model's interface with the global model would be stable. Mismatches of this variety are often called *traction* mismatches and can potentially destroy all physical relevance of a numerical simulation.

The second innovation was the implementation of a new data-assimilation (fusion) technique to force results from the CFD codes to correspond to measurements of important flow quantities (velocity, temperature, and pressure). A recent paper by Karnakov et al. [2] demonstrated that high-quality reconstructions of flow quantities are possible with a surprisingly limited amount of measurement data. This procedure is based on automatic differentiation, with a stochastic gradient descent optimization method.
This technique potentially offers two distinct new capabilities: 1) The ability to better model complicated boundary conditions at facility interfaces (e.g., the way heat is distributed on a piece of active equipment), and 2) The ability to train the POD-ROMs on reconstructed flow data, as opposed to simulations of the Navier Stokes equations.

Results

In the summer of FY24, University of California, Los Angeles (UCLA) graduate student and NNSS intern Jacob Murri worked in concert with Sean Breckling and Cliff Watkins to address the traction mismatching issue. A promising technique was devised and demonstrated at both the NNSS summer intern review and the 2024 SDRD program review. Software based on this new technique is being guided through the record of invention process.

To extend the result to 3D, the simplest path forward is to discretize the 3D space using a hexahedral meshing technique. This variety of mesh uses quadrilateral facets, which eliminate the possibility of non-conforming interfaces between the surrogate subdomain and active computational mesh components. Most freely available meshing software construct tetrahedral meshes. Sandia National Laboratories has software called "CUBIT" that is freely available for government contractors. We are actively acquiring a license for this software now.

Additionally, Sean Breckling was able to reproduce the results from Karnakov et al. for two-dimensional flows at moderate Reynolds numbers. This result is promising, given that a successful reconstruction of the flow was accomplished with such little data-- namely, the absence of any enforced boundary conditions. This success is the basis for the subcontract sought in FY25, wherein we hope UCLA will be able to extend Karnakov's result by recovering fluid momentum and pressure forces from a distribution of temperature estimates.

Conclusion

In FY25, we intend to construct the rudiments of the 3D POD-ROM for the SET facility. To this end, the 3D model of the facility must be converted into a fully and dynamically discretizable mesh of the negative space. The first objects of interest to be reduced into a submerged ROM include the downward HVAC vents and support pillars, given that they are fixed.

A subcontract with UCLA will be established, wherein students will give us a much clearer understanding of the promise of Karnakov's inversion schemes. Namely, they will consider flow reconstructions from quantities easily measured by easy-to-acquire commercial off-the-shelf sensors (heat, pressure, humidity, etc.).

The fully realized 3D models must be codified in codes that are easy to run on LLNL HPCs.

References

[1] S. W. Chung, Y. Choi, P. Roy, T. Roy, S. E. Baker, 2023. "Scalable physics-guided data-driven component model reduction for Stokes flow." *OSTI.*, https://www.osti.gov/servlets/purl/2246718

[2] P. Karnakov, S. Litvinov, and P. Koumoutsakos, 2024. "Solving inverse problems in physics by optimizing a discrete loss." *PNAS Nexus.* 3.1., https://academic.oup.com/pnasnexus/article-pdf/doi/10.1093/pnasnexus/pgae005/56347037/pgae005.pdf

Measurements for Combined Gamma-Ray and Video Modalities

Chris Burt[a]
24-024
Year 3 of 3
Co-Authors: Eric Moore[a], Johanna Turk[a], Shreyas Kamath[a], Micheal Mortenson[b], Matthew Swan[b], Nicholas Eisenberg[b], Michael Willis[c], and Gomez Wright[c]
[a]Special Technologies Laboratory, [b]Nevada National Security Sites, [c]Oak Ridge National Laboratory

Please see CUI summary for more information.

AR/VR CBRN Solutions for Emergency Responders

Brian Richardson[a]
24-081
Year 3 of 3
Co-Authors: Henry Holstein[b] and Larry Hess[c]
[a]Nevada National Security Sites, [b]NNSA/CTOS Navaro Subcontract, [c]Hess Systems Inc.

Abstract

The first year of this project resulted in a functional prototype external probe for use with the Virtual Radiation Training through Ubiety System (VIRTUS) with successful demonstrations of detecting the probes geolocation within a given space and simulated surface contamination survey. In the second year we focused in 3 areas. 1st was to develop software to ingest probe location and sensor data into VIRTUS. 2nd was to develop software and hardware to allow for system setup, monitoring, and troubleshooting. 3rd was to continue developing probe location accuracy and increase detectable range in a GPS [Global Positioning System] denied environment. The third year continued software development and hardware refinement. This included continued development of the Graphical User Interface, smaller format printed circuit boards (PCB) to fit inside 3D printed probe housings, and continued programming within VIRTUS to ingest all available sensor and geolocation data.

Background

Counter Terrorism Operations Support (CTOS) conducts training for emergency first responders, the National Guard, and other agencies for both Response and Prevent Radiological/Nuclear missions. CTOS uses a combination of real radioactive sources and a radiation simulation training system. VIRTUS is an Android smartphone-based application for training the operation and tactics of various radiation detectors. It recreates the controls, indicators, and display elements of each detector. It has a GPS-based scenario system in which instructors can position point sources and contaminant deposition fields onto a map. Once the scenario is propagated to trainee devices, the simulated radiation meters will react appropriately to the virtual radiation levels present at their GPS location. Simulated dosimeters will also accumulate the total virtual dose to which the phone/trainee has been exposed. VIRTUS will also react to Bluetooth Low Energy (BLE) radio beacons that can be configured to represent different radioactive sources. This allows for limited indoor and mobile source training scenarios.


Beta-Gamma probe


Pancake probe

VIRTUS is not without some limitations. VIRTUS is constrained by the accuracy of commercial smartphone GPS receivers. These devices typically have a positional error margin of about 3 meters (9 feet) under ideal conditions. This means that a phone's GPS-calculated position can be 3 meters or more off from their actual position on the ground. The presence of nearby buildings can degrade the accuracy even more. Usually GPS will not function at all indoors. Additionally, the GPS position will often "drift" inside that 3-meter inaccuracy zone. So, while standing still, the reported position can be off 3 meters in one direction, then seconds later it can be 3 meters off in the other direction.

This means that a VIRTUS user is unlikely to precisely locate a virtual point source.

These VIRTUS limitations are primarily limitations of commercial smartphone sensor technology. A potential solution is to augment the system with additional sensor hardware. GPS technology is continuously improving, so it stands to reason that cutting-edge receivers would be available by themselves long before they are integrated with a commercially available smartphone. An attached device with a newer GPS chip could provide greater accuracy. Enhancements in technology that provide accurate location accuracy within a GPS-denied environment will expand our ability to support training in difficult areas such as airports, sports arenas, and other indoor environments.

Finally, having the additional hardware in “probe” form could help make training more realistic. It would more closely match the operation of a radiation meter with an attached probe.

Technical Approach

This research and development project is focused on enhancing the VIRTUS application with the addition of custom-built “probe” hardware. There were two main efforts, the first being development of the actual hardware and the second being integrating that hardware with the VIRTUS software.
External simulated probes were developed to mimic the feel and operation of real equipment. Three different probes were created that mimic the size, shape, and function of real probes: beta – gamma, pancake, and 100 cm^2.

The Inertial Navigation System (INS) is intended to be included in all the probes. The INS includes the inertial measurement unit (IMU) and the Global Navigation Satellite System (GNSS) module. The prototype version consists of commercial parts managed by an Arduino device via a serial (I2C) interface.

Development of a custom INS device was started that integrates the functions into a single compact PCB.

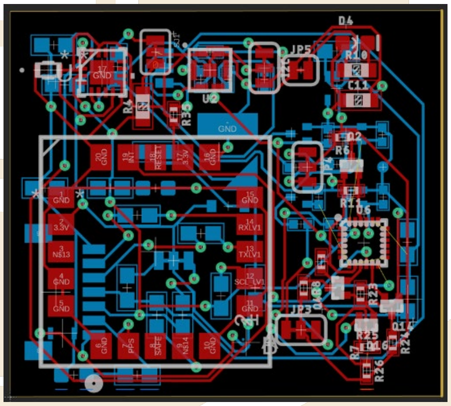

Combined PCB design

Probe sensor technology

IMU includes:

- 3 axis Gyroscope
- 3 axis Accelerometer
- 3 axis Magnetometer
- Digital Motion Processor
- GNSS module
- Proximity Sensor
- Radio Frequency Identification (RFID) sensor
- Bluetooth emitter tag
- Barometer

The focus was four on components: GNNS, RFID, proximity sensor, and Bluetooth emitter.

The first probe was designed to mimic a Geiger-Mueller (G-M) “pancake” detector probe. The internals of the prototype consisted of an RFID scanner and a proximity sensor. When the probe detects an RFID tag, it engages the proximity sensor and reports the distances for several seconds after detection.

The second prototype was designed to mimic the Beta-Gamma probe for a PDR-77 meter. It included a Bluetooth emitter.

The third probe was designed to mimic the 100 cm^2 probe. It had a much larger inside volume and could contain the COTs PCBs for all planned sensors. In addition to the RFID scanner and proximity sensor of the pancake probe, this prototype probe had room for an enhanced GNSS chip, IMU, Bluetooth emitter, and a barometer. For this effort only the RFID scanner, proximity sensor, and GNSS chip were utilized.

100 cm^2 probe

The controller connects the probe and VIRTUS device. The controller combines the navigation and sensor data from the connected probe and the geolocation data from the anchors.
Anchors calculate accurate geolocation within a GPS-denied environment by creating lines of bearing (LOB) to the probe. The Anchor includes: a Bluetooth beamforming receiving antenna; a Raspberry Pi Zero 2 W computer; and an external WiFi antenna.

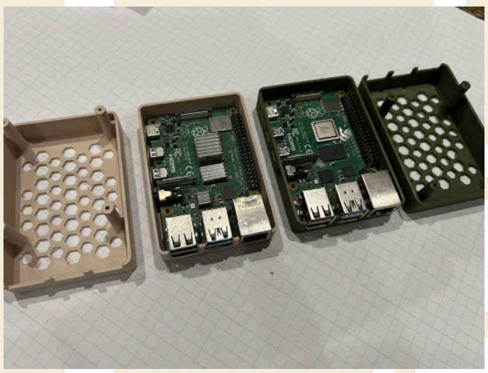

Bridge and gateway

The bridge relays anchor configuration messages between the Graphical User Interface (GUI) and the Anchors. It receives the anchor LOBs and uses them to geolocate a probe. It sends the probe location data to the GUI and the controllers to be integrated into the navigation data sent to the VIRTUS device.
The mesh network is a WiFi network that uses the BATMAN routing protocol. In the mesh network every device (anchor, controller, bridge, gateway) acts as a node in the network.

The GUI is used for setup of the anchors in the test area.
A library was added to the VIRTUS software to connect to USB devices and receive serial data.

Results

A solid mesh network visibility of nearly 500 feet between anchors was achieved.

Accurate probe location within the GPS-denied environment was within 1 meter of the actual location.

A library was created in VIRTUS to receive probe and location data.

Anchor

Ingesting the GNSS data into the VIRTUS device was relatively straightforward.

While the laser rangefinder is fairly accurate, the actual RFID detection, which lets the probe know a source is present in the first place, is very inconsistent. VIRTUS currently does not distinguish between different RFID tags. While it can technically tell them apart, there is no way to configure a property within the tag to convey radiation source properties to VIRTUS. Also, in an ideal solution, the RFID sensor data would be fed into the VIRTUS radiation simulation, which does contain some basic alpha radiation transport functions.

A basic GUI was created for prototype system testing to locate and orient the anchors within the GPS denied test environment.

Conclusion

VIRTUS is a very useful training tool despite the limitations of underlying smartphone technology. The development of these custom-built USB probes and their associate geolocation system has great potential to mitigate many of those limitations. Although the initial prototypes had varying issues, the latest probe iteration contains several useful sensors that would provide training benefits. They do, however, require further development for full functionality. The VIRTUS code has been updated to communicate with that probe hardware. Further development work is required to solve some of the current problems with the probe system. Beyond fixing those problems, there are other potential enhancements that have not yet been tested.


RFID cards and tags

VIRTUS is a very capable training tool currently in use by NNSA/CTOS, training first responders in radiological/nuclear mission spaces. This project demonstrated that the addition of external probes with more accurate sensors greatly improves the capability of the system and the effectiveness of the training. CTOS primarily uses VIRTUS to train National Guard troops for post nuclear detonation response operations in the fallout zone. This increase in capability and location accuracy would greatly improve the realism and quality of the training CTOS delivers. It would expand our capability to train in more places where real sources are not appropriate or permitted. It would increase the target audience to include federal response agencies and State/Local/Tribal/Territorial first responders, and help prepare the nation's response agencies for a major radiological or nuclear incident in support of the national planning scenarios.

Cloud-Based Meta-Analysis with Adaptive Learning for Massive Sensor Networks

Carson Schuetze
24-117
Year 1 of 3
Co-Authors: Ryan Roman and Michael Reed
Nevada National Security Sites

Abstract

This SDRD will empower the nuclear search mission to perform with efficiency & accuracy like never before. Migrating sensor analytics to a cloud-based architecture will facilitate statistical meta-analysis & adaptive learning of radiation detection systems, sensors, & alarming metrics across space and through time. The use of a dense, highly-curated historical archive will enable us to use machine learning to identify equipment abnormalities, optimize parameters for meta-analysis, & continuously adapt. Ultimately, the mission needs to meet include: Increased threat detection probability without increasing false alarm rate by meta-analysis, increased analyst sensor throughput by autonomous anomaly adjudication, anomaly prioritization by meta-analysis scoring metrics, & optimizing sensor time on-target by machine learning. The project also embodies the rare opportunity to collaborate & innovate among NLV, RSLN, and RSLA scientists of all career levels.

Background

Current radiation detection algorithms use a single sensor to run simple time-series analyses. These systems employ edge-computing models in which one sensor is unaware of others, devoid of historical context, and has no in-field adaptive learning capability. Increasing amounts of gear and manufacturer diversity means we now have more sensors, less context, and less expertise. Using ~1B ground-truth data points, including ~2K adjudications, we will use meta-analysis and machine learning to rapidly assimilate all data to optimize sensor time on-target, identify non-performant gear, and refine automated anomaly prioritization and adjudication. The edge-based sensor analytics paradigm routinely misses subtle radiation anomalies that don't trigger alarms, suffer from a pervasive lack of context that curtails performance, and require intensive analyst oversight that scales linearly with the number of sensors. During real-world events, human analysts become overwhelmed and exhausted. This mission is in desperate need of contextual analytics, autonomous adjudication, and anomaly prioritization.

Currently, sensors in our sensor networks work as independent agents. Each triggers an alarm without using information available to the other. If each sensor in a network is calibrated with a specified false alarm rate (FAR), then the false alarm rate for the network scales linearly with the number of sensors. This is referred to as the multiple comparisons problem in statistics. Naïve scaling of the specified FAR may control network FAR but can also come at great cost to overall power of the detection algorithms used. Our current work has explored methods to improve the alarming performance of the network in its current state.

Technical Approach

Probability Space

Nuisance-Rejection Spectral Comparison Ratio Anomaly Detection (NSCRAD)

The anomaly detection problem can be viewed through the lens of statistical inference where we consider the anomaly to be our alternative hypothesis. Indeed, this is the underlying framework for NSCRAD, which is the primary metric for alarming in our sensors. NSCRAD performs the following:

1. Removes the expected contribution of nuisance sources of gamma radiation using subspace projection.
2. Updates background distributions using a Kalman Filter.

3. Compares our observation to our updated background distribution using Mahalanobis distance.
4. Constructs an alarming metric determined by the assumed distribution of the distance metric and a quantile determined by the specified alarm.

In step (4), the alarming metric is designed in such a way that an alarm is triggered if NSCRAD is greater than one.

NSCRAD has historically been shown to perform well relative to other detection algorithms and robustly over various scenarios. We wished to leverage the 'built-in' feature engineering of NSCRAD to help a new probabilistic network wide alarming algorithm.

Multiple Equivalent Threshold Alarms (META)

The META algorithm was designed by scientists at the Remote Sensing Laboratory (RSL) as a general approach to the multiple comparisons problem. Statistically, the method can be described as:

If $X_1, \dots, X_n$ are iid with CDF F_X under H_0, then we can construct a test of $m \leq n$ thresholds

$$argmax_{\{k_1 \geq \cdots \geq k_m\}}\, p_\pi(1|H_1)\ s.t. \sum_j b[1 - F_X(k_j); n, j] \leq \alpha$$

where

- $b(\cdot;\cdot)$ is the binomial probability mass function
- π is the alarming rule, where $\pi = 1$ if for any $j = 1, \dots, m$

$$\sum_{i=1}^{n} 1[x_i \geq k_j] \geq k_j$$

Intuitively, META constructs quantile buckets and triggers an alarm if we fall into the larger ones at too high a frequency. The optimal selection of thresholds is difficult and still an ongoing problem. Current implementations can still yield greater than intended FARs.

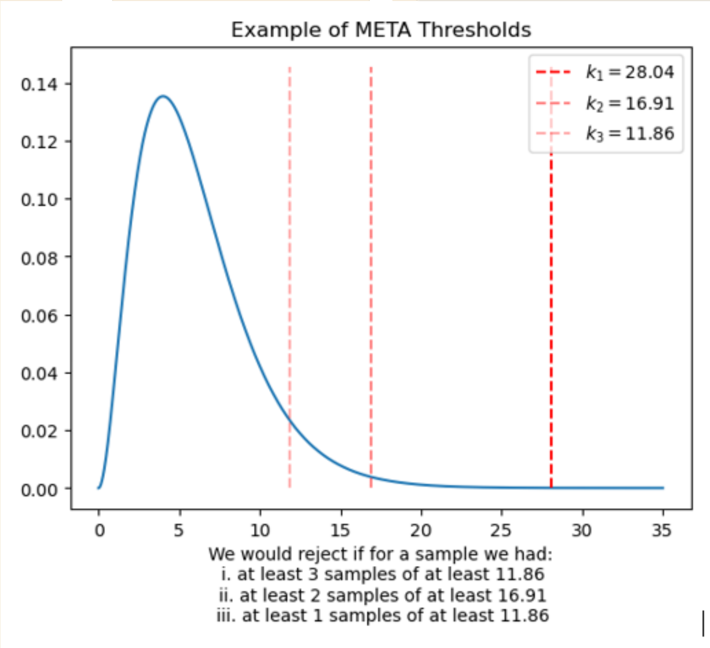

Due to its nuisance-rejecting and filtering properties, we can treat NSCRAD background measurements from multiple sensors as the random sample described in META.

We still need to determine the distribution of NSCRAD outputs. Using NSCRAD sample data gathered by aerial measuring systems for Super Bowl 58, we estimated the CDF using the empirical distribution. Since the empirical distribution converges to the true distribution, it follows that its quantiles also converge. This should imply that META results assuming the empirical distribution are equivalent to those when assuming the true distribution (if enough samples have been gathered). Simulation results are consistent with our intuition.

Over a variety of distributions, we could see that the thresholds constructed in META over the empirical distribution would converge to those constructed in the actual distribution.

The figure below compares the thresholds generated from a $\Gamma(3,2)$ distribution to those generated by $\widehat{F}_n$, the empirical distribution.

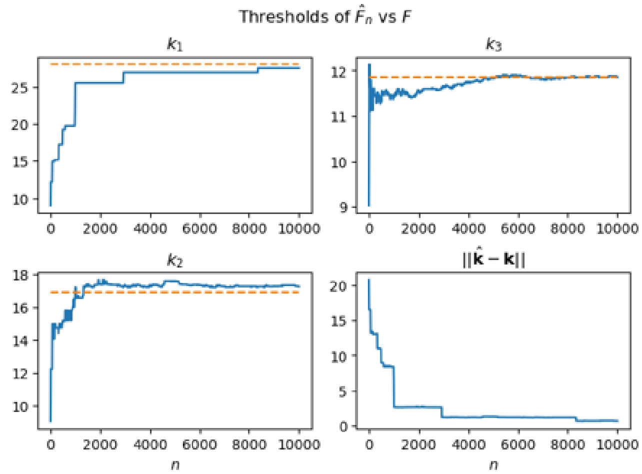

Results

Overview

We began with a literature review to determine feasibility, review similar research, and gather ideas for applicable techniques. This resulted in a starting list of methods to appraise, including: neural networks (NN), kriging, Kalman filters, sequential probability ratio test, Poisson-clutter split algorithm, etc. Concurrently, we began approaching the technical work with a set of 5 toy problems to introduce the concept in a digestible format and have a jumping off point. We gathered a small, simulated test dataset for use on the toy problems and a large dataset from Super Bowl 58 for use with more intricate algorithms. We are currently testing our work's performance with the real data, which includes spectra, location, alarm metrics, and adjudications. Another use for this data set is part of a collaboration with Site-Directed Research and Development (SDRD) project 23-024. We are modifying their existing convolutional neural network (CNN) framework to identify isotopes present during an alarm and to autonomously adjudicate nuisance alarms. In addition, we designed standard onboarding materials for C&DS scientists coming into the NA-80 mission, to introduce clarity and efficiency into the process. This includes both classroom-based training and hands-on learning. After spending the first two months of this SDRD onboarding team members with little to no experience in NA-80, I determined we focused too much on concepts that had no bearing on these scientists' contributions to the mission, which ultimately led to burnout and a longer onboarding process. With our new onboarding materials, we can have C&DS scientists onboarded into an NA-80 project in one week or less. Finally, we welcomed an intern on board and identified scope for him for the summer. It is only his second full week at the time of writing this, but I believe he will make an important impact in the project's outcome.

Statistical Analysis

To test the performance of META as a network alarming algorithm, we conducted a numerical experiment. Abstract hyperparameters intensity, scale, and decay were used to represent isotope effect of NSCRAD, velocity of source pass, and standoff distance, respectively. Source passes occurred at the same time for each sensor. For each hyperparameter setting, four detectors were used with 10,000 runs lasting 100 steps each. Simulation outputs were drawn from a generative model fitted from historical data. The image below shows some sample outputs from nine runs at various hyperparameter settings.

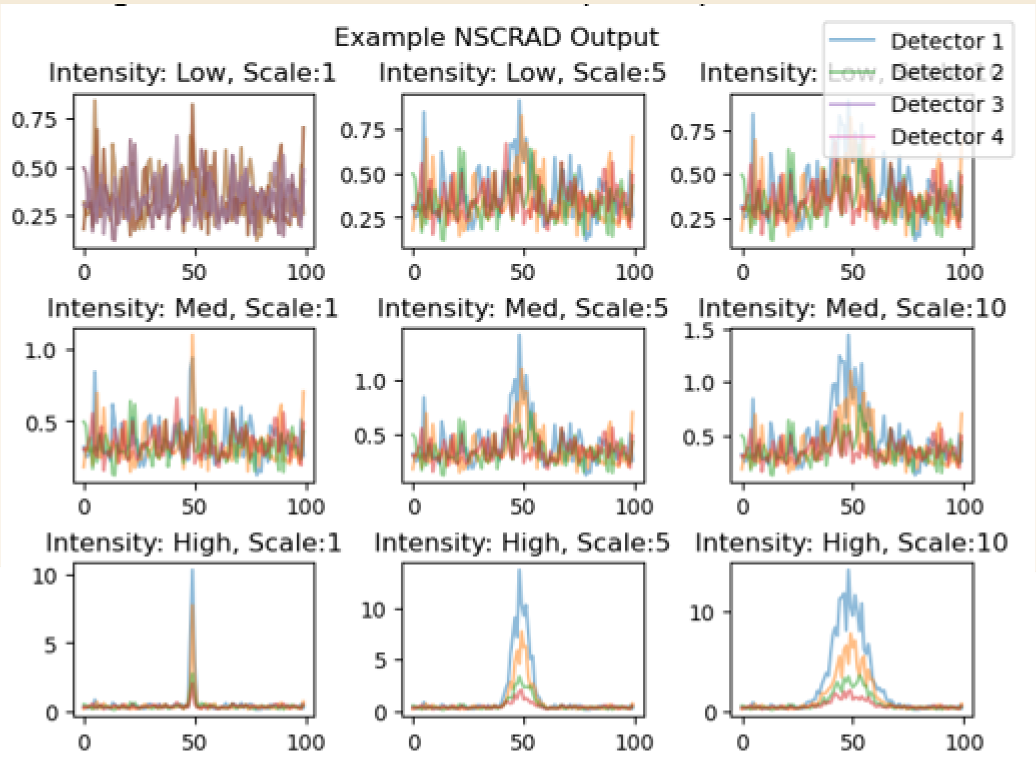

Two network alarming methods would be tested: a naïve method which triggers an alarm whenever any sensor triggers an alarm in each step (NSCRAD > 1) and META. Results from the simulation are consistent with intuition. The image below provides a high-level summary.

		Base FAR	Test TAP
Source	**Alarm Type**		
High	META	3.816	0.666
	Naive	4.284	0.646
Low	META	3.816	0.110
	Naive	4.284	0.001
Med	META	3.816	0.299
	Naive	4.284	0.241

Some remarks on this simulation:

- META does improve our network FAR but is still higher than intended. Improvement in threshold derivation should resolve this issue.
- META achieves significant boosts in power relative to a naïve alarming rule in situations with weaker signals. The naïve approach cannot trigger an alarm without observing NSCRADs over 1.

We have demonstrated large relative gains in performance using information from multiple sensors simultaneously in our simulation on initial investigation. Our findings suggest we can continue to improve alarming for sensor networks with the use of multi-modal and spatial-temporal data, as well as algorithmic improvements.

Machine Learning

In addition, we began collaboration with Chris Burt's NoVA SDRD to use their existing machine learning pipeline to train models for this project. The NoVA team has worked to re-categorize the Super Bowl 58 dataset to feed into a CNN. They are using synthetic data to generate samples in different conditions (e.g., shielding, distance), which act as augmentations, find an ideal representation for an isotope via encoder and projection network, and use the ideal representation to classify. Then we will be able to use this pipeline to perform autonomous anomaly adjudication and equipment abnormality identification.

Conclusion

We have seen great improvements in detection methods by migrating to probability space: decreased FAR, increased detection rate, and ability to detect weak signals not previously detected. In addition, we have made good progress in the machine learning aspect of this project, which will allow us to provide classification based on spectral data, perform autonomous adjudication, and identify equipment abnormalities by stacking models.

Path Forward for Fiscal Year 2025

Q1: Collect more real-world historical event data sets. Create informed prior distributions for background.
Q1-3: Collaborate with NoVA team: optimize and implement machine learning model.
Q1-3: Develop multi-modal alarming systems.
Q1-3: Populate code repo.
Q3-4: Implement new metrics in AVID and perform field testing. Planned event with mobile Radiation Systems Incorporated system and drive by known locations of alarms we would like to automatically adjudicate, etc.
Q4: Begin collaborating with A8 team (NA22) on Cloud infrastructure and computing capabilities.

Dynamic Experiment Diagnostics

DED Projects

Thermal Transport Detection of Phase Boundaries at Elevated Pressures

Gerald Stevens[a]
24-022
Year 2 of 2
Co-Authors: Brandon La Lone[a], Ruben Valencia[a], Paulius Grivickas[b], and Allison Kuelz-Ackerman[b]
[a]Nevada National Security Sites
[b]Lawrence Livermore National Laboratory

Abstract

We are developing a new experimental technique to double-shock-heat a compressible metal and use the resulting hot layer of liquid metal to heat a thin metal coating on a lithium fluoride (LiF) window, driving the material across a phase boundary. A similar technique was designed in a prior project (STL-031-21), and re-solidification of cerium was observed at the melt boundary—results[1] were published in *Physical Review B*. The new technique described in this report offers the potential to explore high temperature melt boundaries typically inaccessible on a powder gun.

Background

Static high temperature and pressure phase boundary determination is typically performed utilizing diamond anvil cells and x-ray diffraction. These experiments take place over long timescales from seconds to minutes. Dynamic determination of phase boundaries is difficult, and historically has utilized small changes in interface wave speed at boundaries to suggest a transition has occurred. We are using a method familiar to most from high school chemistry classes. As you cross a phase boundary by heating a material (e.g., boiling water), the rate of change in temperature of the water hesitates and 'plateaus' at the boiling point temperature.

Technical Approach

We shock, release, and re-shock a compressible material such as cerium, tin, or antimony and have that layer of hot liquid-metal heat a thin (micron scale) film of metal under investigation against a transparent anvil at constant pressure, while thermal diffusion heats the film across phase boundaries. A schematic of an impactor/target configuration is shown in the figure below. This approach allows us to investigate phase boundaries at high pressure on single-stage gun experiments.

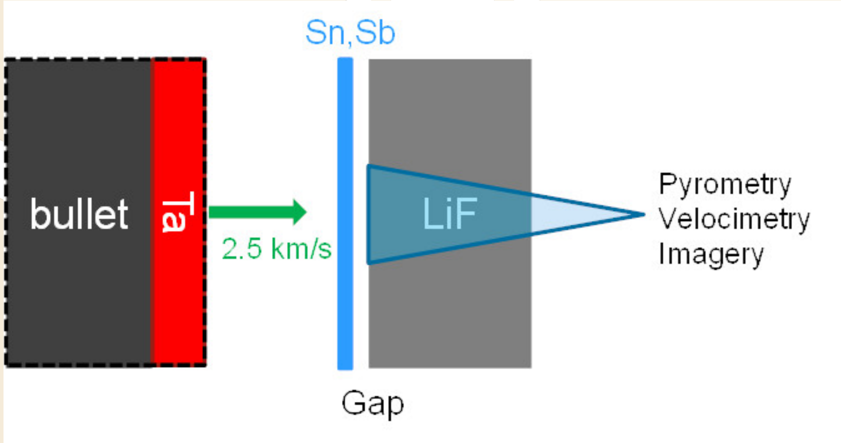

Schematic of double shocked technique. A high speed (2.5 km/s) tantalum impactor strikes 1 mm of a compressible metal (Sn, Sb, or Ce), which transits a small (25 – 200 μm) gap and impacts a thin metal layer coating on a LiF anvil. The goal is to observe phase transitions in an iron coating, however most experiments were performed without the metal coating in order to test the technique with high speed photography and pyrometry.

Results

We demonstrated the feasibility of our novel technique to reach high temperatures. We developed 2-dimensional hydrodynamic simulations that highlight a difficulty we encountered due to surface imperfections developing into large features that penetrate the metal film under investigation. Further efforts focused on mitigating these issues, and our final experiments gave temperature histories consistent with 1-dimensional thermal diffusion hydrodynamic calculations. Our models will inform future designs and efforts to continue the work to find phase boundaries in iron.

Conclusion

We have several approaches to mitigate the instability growth issues we faced in this work. First, reducing the gap will not allow such large features to develop prior to impact and second-shock heating of the hot layer. Next, we could 'ring up' launch tin across the gap. We may also shift our approach from shock, release, and re-shocking a metal to using a single shock on a two-stage gun with collaborators at Sandia National Laboratories. Despite these difficulties, our results are of interest to the shock-physics community that has been performing temperature measurements of thin film samples, and fiscal year 2025 experiments will provide additional insight into these phenomena.

Publications

Journal Article, T. M. Hartsfield, B. M. La Lone, G. D. Stevens, M. T. Beason, J. K. Baldwin, and W. D. Turley,"Temperature, enthalpy, and kinetics of cerium resolidification under dynamic compression." https://doi.org/10.1103/PhysRevB.108.L140101, 2023. *Physical Review B.*

Digitized Nanosecond Silicon-Germanium Photomultipliers for Prompt Radiation Detection

James Mellott
24-069
Year 1 of 3
Nevada National Security Sites

Abstract

The Digital single-photon avalanche photodiode (SPAD) Array Photomultiplier revolutionizes dynamic radiation sensing by leveraging the digital nature of discrete photons. By subdividing the sensor into smaller areas with faster temporal resolution, it preserves binary photonic sparsity and eliminates the constraints of analog integration. This cutting-edge technology combines a high-resolution SPAD array with a read-out integrated circuit (ROIC) for rapid digital photonic transfer. On-chip storage capacitors hold the captured information until readout, enabling nanosecond-speed readouts and interleaved temporal sampling. With exceptional temporal resolution and dynamic range, this innovation obviates the need for traditional tubes or digitizers. The Digital SPAD-Array Photomultiplier opens up new frontiers in radiation detection, offering precise quantum measurement, streamlined workflows, and vast scientific possibilities.

Background

Photomultiplier tubes (PMTs) are considered obsolete in the commercial industry. Hamamatsu recently announced the end of life for one of our most used PMTs, the Mod5 R5946. The performance of that PMT is unmatched in terms of gain and linearity. Our goal is to design an avalanche photodiode (APD) array and read out circuitry that will be fast enough to measure prompt radiation. If we are successful, we will be able to replace PMTs and expensive digitizers with small and relatively inexpensive application-specific integrated circuit deigns and microcontrollers. Our work is unique because commercial applications of solid-state replacements are typically designed for 1550 nm light and are much too slow for use in prompt radiation detection. The typical application for radiation detection using APDs is long exposure counting. If we cannot find a suitable replacement for PMTs in the next 10 years, I believe we will have to rely on very poor performance PMTs to collect our data for prompt detection experiments.

Technical Approach

We are utilizing silicon germanium (SiGe) APDs to push the quantum efficiency of silicon APDs up to 80+% at 400 nm. Commercial industry is interested in 1550 nm light for communication. This means any advances in APD technology do not work for our experimentation needs here and at the labs.

In order to be used for prompt detection, these APDs need to be small, fast, and reset quickly. Typically, APDs are passively quenched, which results in higher dark counts and longer reset times.

Fortunately, on another project at the University of Nevada, Las Vegas (UNLV) in 2018, I was part of a group that designed, simulated, and fabricated some SiGe APD test structures using a 350 nm process. Unfortunately, funding ran out before we could test the structures. But this is where this Site-Directed Research and Development project begins. We had to wire bond 45 different APD structures and test them individually. Most of this work was performed at UNLV by Abraham Castaneda and Angsuman Roy. Unfortunately, we were not able to test any of the active quenching test structures as it was forward biasing the substrate due to how the structures were laid in the design.

Results

As stated previously, we tested 45 different APD structures and topologies. The best performing passively quenched circuit achieved a 160-mV output and a 171-picosecond pulse width. This nearly meets our stretch goal of less than a 100-picosecond pulse width. We were able to test so many structures because we designed and fabricated a printed circuit board that utilized a QFN [Quad Flat No-leads] package socket. This allowed us to quickly swap in new wire bonded chips. We also developed an algorithm to control several benchtop pieces of equipment to do parametric sweeps for characterizations. We varied SPAD bias, quench resistor value, and LED power.

Conclusion

We know moving to solid state is the future. It is difficult because commercial industry isn't pursuing innovation in our field of interest. We know we can handle more flux with an array of single photon avalanche devices. We will need to develop our own devices and supporting circuitry for read-out. Moving forward, we are going to develop an active quenching topology to further increase the time response and reset times to achieve less than 100 pico-second full width half max and less than a 1 nano-second reset time for the SiGe APDs. These arrays will be usable for prompt radiation detection, but they can also be used for long exposure counting experiments. For fiscal year 2025, we will be designing and fabricating four 16 x 16 arrays. We have one year to get a functional prototype. The arrays will be two active quenching topologies and two passive quenching topologies.

Intensity Based Laser Velocimetry Measurements

Brandon La Lone
24-079
Year 1 of 1
Co-Authors: Dale Turley, Eric Larson, Jason Mance, Matthew Staska, Jerry Stevens, Ruben Valencia, and Brent Frogget
Special Technologies Laboratory

Abstract

We have built an optical velocimetry system almost entirely composed of commercially available telecom-based 1550 nm lasers and components. This system has the potential to be more robust and simpler to field and operate than existing velocity interferometer for any reflector (VISAR) [1] and photonic Doppler velocimeter (PDV) [2] systems and be faster and more sensitive than these traditional diagnostics. A prototype was assembled and fielded in a dynamic experiment. The experiment was designed to cross-compare performance against legacy techniques and anticipated improvements were demonstrated. Though the demonstration was a success, some pathology was observed that will need to be fixed before the system can be routinely fielded.

Background

The goal of this project was to develop and test a new type of velocity recording system for dynamic experiments. Existing optical velocimetry techniques are based on Doppler shift of light reflected from a material surface accelerated by a shock wave. We have developed an alternative method that encodes velocity into intensity (iVISAR) of a reflected optical signal and has the potential to return data otherwise not possible with legacy systems. The proposed system could be used in place of existing VISAR systems where either the velocity changes are too rapid (sub 10 ns) or are too high (> 20 km/s) for PDV to measure. This system has many potential advantages over legacy VISAR systems which are no longer built or supported by NNSS because of personnel attrition. The proposed system is almost entirely composed of commercially available telecom-based 1550 nm lasers and components and has the potential to be more robust and simpler to field.

Technical Approach

We have devised an optical velocimeter technique that can translate velocity of a moving surface to the intensity change in light reflected from the surface of a shocked material. Velocity based interferometer systems rely on the Doppler shift of reflected light caused by the motion of the reflecting surface. When the reflected light fills an interferometer and is mixed in the two legs of the optical cavity, the resulting mixed waveform will change frequency when the reflecting surface moves. The change in frequency of the resulting signal can be analyzed to determine the new velocity of the target material. VISAR systems use an unbalanced interferometer cavity through which the Doppler shifted light is passed. In this way the velocity signal is encoded into the phase of the interference. Traditional VISAR systems use green light (532 nm) and non-telecom optical components and require recording multiple detector channels (typically 4) carefully balanced in amplitude and phase before a sample begins to move. Because the starting points for each channel are precisely tuned to be out of 90 degrees out of phase from each other, the data recorded during a dynamic event can be analyzed and ambiguity caused by turn over points (peak and valleys) in the oscillating signal can be resolved. PDV systems are all contained in optical fiber and a single experiment channel is mixed with a reference beam resulting in a beat frequency being creating between the Doppler shifted light and a reference laser. The resulting signal is analyzed using Fourier transform techniques to extract a velocity within the time band of the Fourier analysis. The VISAR system requires an expert to operate and assemble. The PDV is easier to assemble and operate, but the response time can be limited to the selected time band of the analysis method required to determine a velocity. VISAR systems can in principle have better time response x velocity resolution products than PDV systems but at greatly increased complexity and cost.

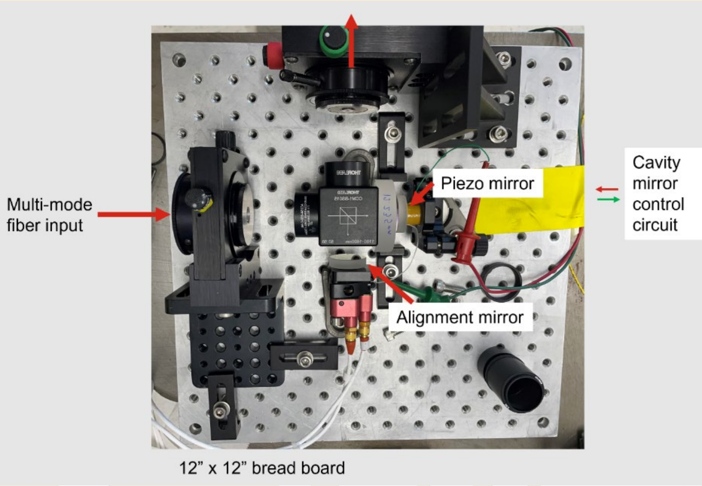

Assembled prototype intensity based velocimeter (iVISAR) cavity

The iVISAR concept used a compact optical interferometer (12" x 12"). The figure shows a picture of the iVISAR cavity brassboard including fiber inputs and bulk optics. The control circuit for automated cavity optimization is not shown. The signal returning from the experiment is split using a 90/10 fiber splitter (not shown in the figure). The 90% leg is transmitted into the cavity. The 10% leg goes to a high-speed detector to allow normalization of signal changes not caused by a velocity change. The cavity is unbalanced as in a traditional VISAR but only slightly, (about 65 ps for our prototype). The output of the cavity is split again with 90% going to a high-speed detector and 10% to a low-speed detector to allow active tuning of the cavity prior to the experiment. The goal of the low-speed detector is to tune the interferometer contrast to the 50% point for the combined waveforms prior to initiating the dynamic experiment. This is achieved by sending the signal of the low-speed detector into a control circuit that adjusts a piezo control of one of the cavity mirrors. This active feedback loop to stabilize the starting phase of the interferometer is unique to the iVISAR and is the main difference between our system and a traditional VISAR. By having the starting phase at the midpoint, the transmitted intensity through the cavity is proportional to changes in velocity (over a range of velocities).

Results

A compact intensity based velocimeter was designed, and a prototype system was built and laboratory tested. The system includes 1550 nm telecom components, a compact optical interferometer, and a customized electrical circuit for feedback control of an in-cavity mirror to optimize and stabilize the interferometer starting phase. The overall system was tested in a dynamic experiment and cross-compared with traditional PDV and VISAR. The intensity based velocimeter was able to detect the separation between the elastic and plastic waves propagating in a shocked thin (~100 micron) aluminum target, while traditional PDV was not. However some pathology was observed which needs to be addressed before the system can be reliably fielded on future dynamic experiments.

Conclusion

The success of this project could impact many specialized dynamic materials studies that include fast small velocity change phenomena typically encountered in experiments at Z, NIF and other specialized impactor or explosive experiments. The intensity based velocimeter developed under this project has the potential to replace existing VISAR systems throughout the weapons complex, through a simpler and lower cost design.

References

[1] L. M. Barker, and R. E. Hollenbach, J. Appl. Phys. **43**, 4669 (1972)

[2] O. T. Strand, D. R. Goosman, C. Martinez, T. L. Whitworth, W. W. Kuhlow, Rev. Sci. Instum. **77**, 083108 (2006)

Direct Measurement of Metal-Hydride Formation during Ejecta Particle Transport in Reactive Gases Using Raman Spectroscopy

Jason Mance
24-090
Year 2 of 3
Co-Authors: Brandon La Lone, Thomas Myers, Rick Allison, Chusia Moua, Eric Larson, Jerry Stevens, Dale Turley, and Mark Morey
[a]Special Technologies Laboratory

Abstract

There are important and unresolved questions about the properties of ejecta that are relevant to the weapons community. These questions have been and still are an ongoing topic of emphasis in the NNSS experimental program. Results of recent studies suggest that ejecta properties are likely influenced by chemical reactions when propagating in reactive gases. However, the presence of these reactions has thus far only been inferred through pyrometric temperature measurements. No direct evidence has been presented. We are proposing experiments that can provide direct evidence of these chemical reactions.

Background

Excess heating of ejecta in reactive gases has been observed and attributed to metal-hydride formation. These chemical reactions may affect ejecta transport properties, and determining whether that is the case is important to the weapons community. Deducing temperature from pyrometry requires assumptions about emissivity—Raman spectroscopy, on the other hand, can provide temperature independent of emissivity. Therefore, Raman spectroscopy combined with pyrometry should define emissivity.

Technical Approach

We utilized the following method to capture Raman measurements for temperature: Laser light was scattered off of a target and the resulting data was captured on a line graph. Raman shifted lines on that graph have stokes and anti-stokes lines, and the ratio of intensity of lines defines temperature.

Static measurements that were taken on an aged cerium metal surface gave a Raman signal. Peaks are distinguishable in a single shot, using a 10 ns laser pulse – this result is promising for dynamic experiments. To determine what compounds are in aged cerium and which one contributes to the Raman spectrum, we sent aged cerium out for XRD analysis. It was determined that CeH2, CeO2, Ce and Ce(OH)3 are primary ingredients. Pure Ce is not Raman active, and CeH2 and CeO2 are Raman active. There is no published Raman data available for Ce(OH)3. We purchased cerium oxide and cerium hydride powders from American Elements and captured Renishaw Raman measurements on various combinations of these powders.

Results

Raman measurements showed a strong signal in CeO and no signal in CeH. We were surprised to find that there was no Raman signal on hydride powder. Even after building a sealed chamber, with the cerium placed in a chamber at 180C and purged with H_2, there was still no Raman signal. We hypothesized that perhaps the presence of CeH_2 in samples causes a loss of Raman signal (CeH_2 is metallic and thus has no penetration depth for Raman). Measurements on CeH and CeO powders showed no discernible Raman signal on CeH powders – all peaks appeared to be from CeO contamination or the cuvette sample holder cell. When measurements were taken on CeO powder on Sn into oxygen, a fundamental 532 nm reflection was detected but Raman peaks disappeared (radiance background was approximately 3000 K). When we took measurements on CeO powder on Sn into helium, the radiance background was negligible (using helium provided lower ejecta temperatures) and there were still no Raman peaks. For CeO powder on DT Sn into helium, there was a very low 532 nm reflected signal. This might have happened be because the laser signal may have been obscured. For aged Cerium into helium, Raman was 295 K and radiance was approximately 3000 K. But the Raman peaks, which we initially thought came from ejecta, ended up being a Raman signal in the collection fiber.

Conclusion

After the above attempts, we tried to enhance the Raman signal using CARS but there was not enough peak power with ns lasers. We think, however, that fs lasers could work. When we tried static CeO and CeH fluorescence, a signal was not detected. Trying LaH powder also showed no Raman signal.

Although our attempts were not successful in , we see a two potential paths forward for future work. 1) CeO shows a strong absorption feature at 430 nm that may be detectable in the radiance spectrum. 2) CeH is very absorptive while Ce is partially reflective. Future experiments could focus on looking for ejecta to turn black while travelling through hydrogen (i.e., dynamic reflection and radiance spectral measurements). Both of these avenues of experimentation may yield results.

Temperature Study of Compressed Porous Metals

Brandon La Lone
24-144
Year 1 of 1
Special Technologies Laboratory

Abstract

Scientists from Lawrence Livermore National Laboratory (LLNL) (Will Schill, Mike Armstrong, and Jon Belof) are investigating temperature rise from shock compression of porous materials. They are particularly interested in the compression and heating of reactive materials for advanced munitions development (conventional weapons development). Simulations suggest that temperatures reached upon compression of aluminum or magnesium foams could be 15,000 K or higher, even on a single stage powder gun, but experimental validation is needed. The aim of this feasibility study is to collaborate with LLNL on the design, construction, execution, and data analysis of powder gun experiments on metal foam targets to be conducted at the Special Technologies Laboratory (STL) in FY 2024. This work will challenge our ability to make very high temperature radiance and reflectance measurements which can benefit future work. This work will strengthen our collaboration with LLNL scientists and open new avenues for future DOD sponsorships. Also, this work is directly related to ongoing shallow bubble collapse studies of relevance to NA-10 programs.

Results

None. Project was not able to move forward.

Enabling Technologies for Autonomous Systems and Sensing

ETASS Projects

Mass-Selective Photoionization Detector

Manuel Manard[a]
24-002
Year 2 of 2
Co-Authors: Rusty Trainham[a], Richard Allison[a], and Roark Chao[b]
[a]Special Technologies Laboratory, [b]University of California, Santa Barbara

Abstract

We will design, build, and test a proof-of-concept instrument that couples a photoionization (PI) lamp with an array of ion traps to provide mass spectra of chemical species in real time. The unit will be designed so that the mass analysis region can be deactivated, allowing the ion current to be used to monitor for analytes of interest in a low power state. Once ions are sensed, the mass analysis region of the system would be energized to generate mass spectra. Mass analysis would be facilitated by an ion trap array that has been developed as part of a previous research effort. The array uses Paul-type (radio frequency [RF]-field) ion traps that have trapping regions measuring hundreds of microns in diameter. The array is integrated into the design of a printed circuit board (PCB), so all circuitry needed to provide the electric fields to the various component of the traps are in place.

Background

Small, field-portable systems capable of providing analytical specificity for chemical detection are of interest to multiple government agencies. Inexpensive instruments capable of providing real-time chemical analysis with reasonable sensitivity and selectivity are desired for man or drone-based deployment. Real-time chemical analysis is possible. However, the sensors used are non-specific. PI detectors are used for this purpose but only inform the user if a chemical with an ionization potential ≤ the ultraviolet (UV) photon energy is present. Recent advances have been made in reducing the size of mass analyzers, making their use in portable systems possible to achieve analytical specificity in the field. However, additional development is required before a ruggedized, fieldable platform is realized. Accordingly, a device coupling the simplicity of PI detectors with the selectivity of mass analyzers would be a significant achievement toward in-field chemical analysis.

Technical Approach

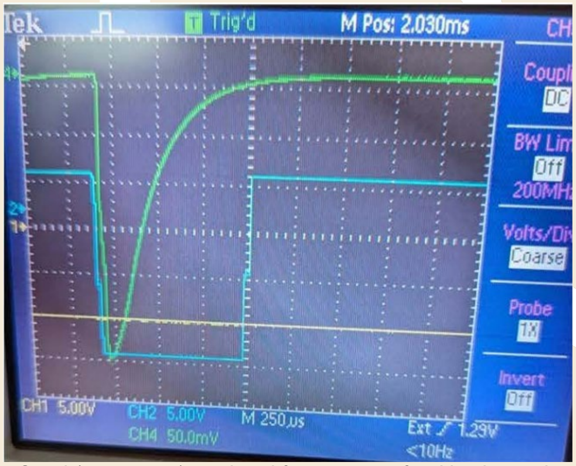

Signal (green trace) produced from ions confined by the mesh ring electrode which is a 20x increase in intensity compared to the original design. The negative voltage pulse drawing ions out of the trap is shown in blue.

A PI lamp functions by generating UV photons, which results in the ejection of electrons from chemical species having ionization potentials less than the energy of the photons, leading to ion formation. A Paul-type ion trap functions by confining ions in a region of space between three electrodes using a combination of direct current (DC) and RF electric fields. Two end cap electrodes, which typically have a conical geometry, are positioned above and below a ring-shaped electrode. The DC component of the field is applied to the two end cap electrodes, confining ions axially, and the RF is applied to the ring electrode. The RF frequency and amplitude are chosen such that the confining and anti-confining directions of the oscillating voltage (RF) shift at a rate faster than the time required for ions to escape the trap, leading to radial confinement. A mass spectrum of the ions is obtained by altering the trapping field in a way that destabilizes the trajectories of the ions based on their mass-to-charge ratio (m/z). Ions are then sequentially ejected from the trap as a function of m/z and are detected.

Results

During year two, new concepts were explored for improving the efficiency of UV photons penetrating into the trap leading to an increase in the population of confined ions. Here, a modified ring electrode was fabricated and integrated into the design of the prototype ion trap. The ring was made of a stainless-steel mesh. The modification resulted in a 20x increase in trapped ion signal strength relative to the original design.

The increased signal strength allowed the limit of detection (LoD) of the system to be measured. The LoD was determined using a trace concentration gas calibration system, developed by Kin-Tek Analytical Inc. The system uses permeation tube sources and mass flow controllers to mix a small flow of the analyte contained in the permeation tube into a large flow of the dilutant gas (N_2). This leads to mixtures that contain the gas of interest at concentration ranging from 100 ppm to single ppb levels. For these experiments, isobutene (IP = 9.2 eV) was used as the test gas and its concentration in the flow of N_2 was stepped down until no ion signal was observed when the ions were extracted from the trap. Ultimately, an LoD of approximately 10 ppm was measured for the system.

A picture of the PCB containing the ion trap array. A quarter is also shown for scale.

A printed circuit board (PCB) containing an array of ion traps for integration with the PI lamp was designed and fabricated as part of this effort. The PCB measures 1 inch in diameter, 0.0625 inches thick and contains an array of 25 ion traps. The diameter of the individual traps is 500 µm. The array mitigates the reduction in sensitivity resulting from the reduced size of the traps caused by Coulomb repulsion (smaller traps necessarily hold fewer ions). The PCB simplifies the design of the system and could lead to a device that could be inexpensively produced.

Conclusion

A proof-of-concept instrument that couples a PI lamp with a Paul-type ion trap to provide mass spectra of chemical species was designed, built, and tested. Data was acquired that showed the presence of ions, generated by the PI lamp, confined in the trap. A modified ring electrode, made of a stainless-steel mesh, was fabricated and integrated into the design of the prototype ion trap to allow more UV photons to penetrate into the trapping volume. The modification resulted in a 20x increase in trapped ion signal strength. A limit of detection of approximately 10 ppm was qualitatively measured for the system. A PCB containing an array of 25 ion traps, with diameters of 500 µm, was designed and fabricated. The PCB measures 1 inch in diameter and 0.0625 inches thick.

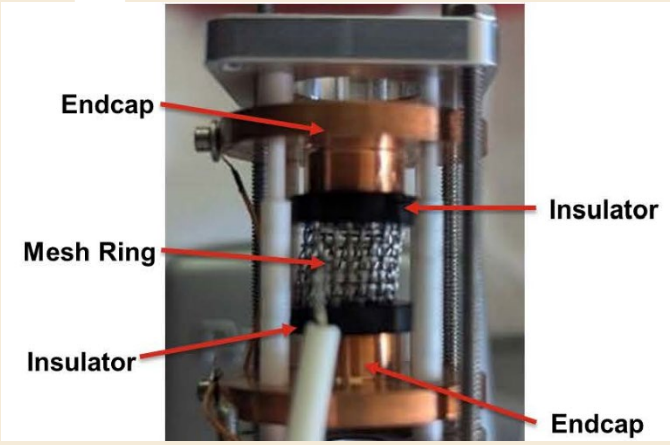

Prototype ion trap using a stainless-steel mesh as the ring electrode.

Low SNR, High Clutter UAS Detection and Tracking

Ian McKenna[a]
24-009
Year 2 of 2
Co-Authors: Mary O'Neill[b], Tristan Richmond[a], Michelle Zimmerman[a], and Andrew Song[a]
[a]Special Technologies Laboratory
[b]Keystone International

Please see CUI summary for more information.

Multi-Modal Remote Vibrometer for Infrastructure Interrogation

Steven Koppenjan[a]
24-010
Year 3 of 3
Co-Authors: David Baldwin[a], Paul Taylor[a], Eric Larson[a], Ebrahim Saberinia[b], and Giovanny Vazquez[b]
[a]Special Technologies Laboratory, [b]University of Nevada, Las Vegas

Please see CUI summary for more information.

Optical Comb Techniques for Hyperfine Spectroscopy

Rusty Trainham[a]
24-014
Year 2 of 3
Co-Authors: Manuel Manard[a], James Bounds[b], and Alexandre Kolomenskii[b]
[a]Special Technologies Laboratory, [b]Texas A&M University

Abstract

Measurement of atmospheric noble gases for radioactive isotopes, in particular, radio-xenon, is an important tool in the detection of nuclear proliferation activities. We can currently measure isotopic abundances of xenon samples by means of optical hyperfine spectroscopy. The current apparatus utilizes a large, complex, and expensive Ti:sapphire laser, so we propose to simplify the laser and the detection scheme by implementing a Doppler-free dual-frequency optical comb technique. This would utilize a fixed frequency diode laser, an electro-optic modulator, and a spectrum analyzer. The current experiment sits on a large laser table in the laboratory. However, with the diode laser it can be downsized to fit on an optical breadboard on a rolling cart. Potentially, it would have no moving parts (except for the wheels on the rolling cart). This would make for a more robust concept for field implementation within a van or aircraft.

Background

This investigation has determined that it is possible to detect and quantify isotopic ratios of noble gases by means of laser hyperfine spectroscopy, and that it can be done with a compact apparatus suitable for field deployment. Noble gases are chemically inert and difficult to confine, so they inevitably leak into the environment. Noble gas radioactive isotopes and isomers of interest possess odd half-integer nuclear spin that couple to atomic fine structure to create hyperfine substructure. The hyperfine structure can be probed by laser spectroscopy, and it can serve as a spectral signature to identify the isotope or isomer. Advantages of laser spectroscopy over traditional nuclear coincidence counting are that radiation shielding is unnecessary, measurements can be performed in a matter of minutes rather than hours, and laser interrogation of a radioactive atom can be done multiple times before the atom undergoes nuclear decay. A disadvantage of using laser spectroscopy is that Doppler broadening masking the hyperfine structure must be overcome by means of a Doppler-free spectroscopic technique.

In the interest of reducing the mechanical complexity of the technique and apparatus, we have investigated the use of optical modulation of fixed laser frequencies as a calibration fiducial and as an active means of interrogating hyperfine structure.

Technical Approach

We measured atomic hyperfine structure of natural xenon's two isotopes with hyperfine structure (129 & 131) and determined that identification and isotopic absolute abundance measurements are possible by probing the 6s to 6p transition in the 820 nm to 850 nm wavelength range. Frequency combs on the laser light were used to calibrate the energy scale during the wavelength scans and also for sweeping over resonances using a fixed laser wavelength and an electro-optic modulator to impose laser sidebands. The laser system consisted of a Spectra Physics Matisse Ti:sapphire ring laser driven by a Coherent Verdi V8 pump laser. The optical setup consisted of an rf-discharge gas cell filled to a few hundred milli-Torr of natural xenon. The radio frequency (RF) discharge formed a plasma to populate the first excited state (6s), which is metastable. Counter propagating pump and probe laser beams interrogated the 6s to 6p optical transition, and the technique of saturated absorption was used to overcome the Doppler broadening that obscures the hyperfine structure. Both absorption and fluorescence emission measurements were performed.

For the energy scale calibration, an Rb frequency standard was used as a reference to modulate a rainbow laser (of broad spectral width), whose beats were recorded during frequency scans. Since portable Rb frequency standards are commercially available and relatively cheap, they are ideal for absolute measurements in field operations. For sideband frequency scanning, we employed a Pluto software defined radio (SDR) and a 20 dB microwave amplifier to drive a Thorlabs electro-optic modulator to impose upper and lower sidebands on the laser light, with attempts to modulate the sidebands themselves. Enough RF power was applied to the modulator to put sufficient energy in the first sideband to probe hyperfine resonance, but the RF power was kept low enough to suppress sidebands beyond the first. In scanning measurements using the upper sideband, the technique showed promise, however harmonic distortion in the output of the Pluto SDR created artifacts in the hyperfine data. The artifacts should be absent by using a higher quality SDR with lower harmonic distortion.

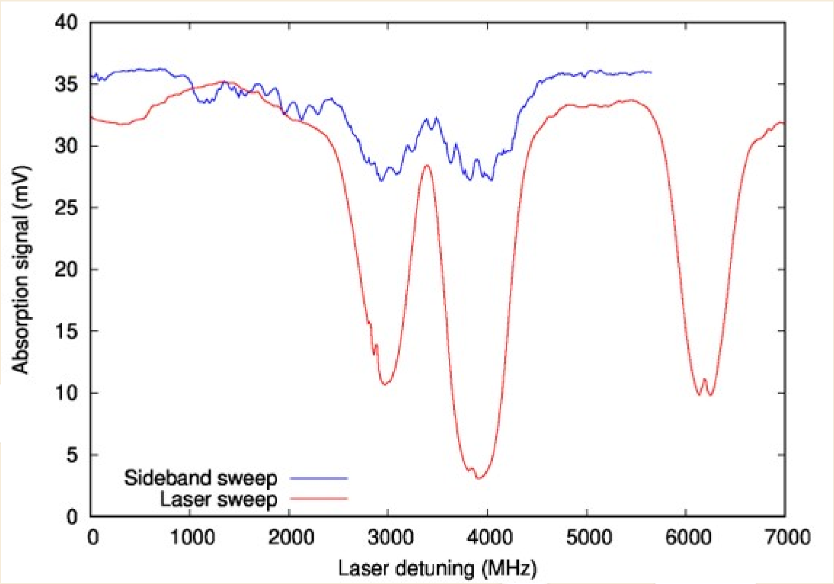

Data comparison between traditional laser frequency scanning and fixed frequency laser variable sideband scanning.

Results

The frequency comb was successfully applied as a "ruler" to measure hyperfine energy shifts with high precision. As a sideband frequency scanning mechanism, the preliminary results suggest that the method has utility, even though the preliminary data collected with a hobbyist grade Pluto software defined radio show artifacts due to sideband harmonic distortion. Better radios are commercially available and would be expected to produce higher quality data.

Conclusion

Although the project was delayed by lab renovation, multiple procurement issues, and a four-month work stand-down at the Special Technologies Laboratory, preliminary results point to the utility of the combs method for scanning hyperfine structure and for quantifying the energy shifts. The method can be used for isotope ratios measurements of species possessing hyperfine structure. These include radioactive isotopes and isomers of the noble gases. The apparatus employing the method can be made compact, portable, and low powered, thus making it suitable for field applications.

Publications

Journal Article, J. Bounds, A. Kolomenskii, R. Trainham, M. Manard, H. Schuessler, "Hyperfine structure and isotope shifts of xenon measured for near-infrared transitions with Doppler-free saturated absorption spectroscopy,." https://doi.org/10.1016/j.sab.2023.106635, 2023. *Spectrochimica Acta Part B: Atomic Spectroscopy,* 202, 106635 (2023).

Surface Gas Sampling Payload for Autonomous Underwater Vehicles

Cameron Priest
24-034
Year 2 of 3
Co-Authors: Jonny Reitinger, Roy Abbott, Kevin Lee, and Chris Burt
Special Technologies Laboratory

Please see CUI summary for more information.

Microwave Detection through Thin Films

Hilary Tarvin[a]
24-075
Year 2 of 2
Co-Authors: Arianna Sanchez[a,b], Kevin Reuwer[c], Kevin Thomas[a], Melissa Wright[a], Carson Schuetze[c], and Jessica Farnsworth[c]
[a]Remote Sensing Laboratory, Nellis, [b]University of New Mexico, [c]Nevada National Security Sites

Please see CUI summary for more information.

Spatially Aware Multi-Modal Directional Radiation Detection Swarms

James Essex
24-114
Year 3 of 3
Remote Sensing Laboratory, Nellis

Abstract

This project explored several spatial awareness technologies including inertial measurement units, RGB-depth cameras, and lidar technologies to combine inputs from multiple sensors and estimate radiation source locations from detector measurements. Spatial awareness along with enabling protocols for radiation data exchange between sensors allowed for the application of more robust methods for source detection and localization. Multiple algorithmic approaches were tested and the results are presented here.

Background

All existing radiation detection systems utilize alarming algorithms that are temporal, and the localization of a potential threat currently requires manual methods and operator skill. If alerted using existing systems, the operator can rotate using body shielding to affect count rate or use a finder mode with tones that increase as the count rate increases. In access-restricted environments, it is not currently possible to locate a source without long dwells using sophisticated and expensive instrumentation. These methods are slow and error-prone, require post-processing, or, in some tactical situations, are not practical or safe.

Technical Approach

In the first year of this effort, we tested spatial sensing capabilities and developed the software layer to map relative positions of devices into a common local coordinate system. Our approach to this effort will be to utilize similar methods to those used with the HoloLens [1], but we will adapt the spatial sensing to the new Inertial Measurement Unit (IMU), RGB-depth camera-based Simultaneous Localization and Mapping (SLAM), and Ultra-Wide Band (UWB) modules with new modular gamma and neutron detectors.

In the second year of this effort, we will continue to optimize pedestrian-based spatial awareness technologies and sensor fusion algorithms, and tune localization solutions using both gamma and neutron directional detection systems. Several data collection campaigns will be executed in a variety of environments that represent the spectrum of operational conditions of interest (i.e., static environments too crowded with people). These tests will characterize the performance of the spatial awareness suite to enable error estimates associated with localization.

Results

The team has used an assortment of sensors to leverage strengths of each while mitigating any pitfalls. Often, SLAM is used on robotic systems which can calculate their position based on odometry from wheels. The system developed by the team is hand-held or worn by an operator, so the type of odometry available to robots is not readily available. Indeed, the team primarily used Lidar Inertial Odometry (LIO) along with Visual Inertial Odometry (VIO) to estimate the pose of the sensor system. The lidar can use an algorithm such as iterative closest point (ICP) to estimate the pose of the system. The system created for this project uses a 3D lidar to generate position estimates in three dimensions. Additionally, the map generated by a 3D lidar gives a more intuitive feel when viewed. The lidars used have a 360-degree field-of-view, which speeds up map generation. A 2D lidar may also be used to generate a floor plan map, but it loses some flexibility since some features are not available.

For this project, several stereo cameras from different vendors were tested. The authoring team used various combinations and configurations to meet the needs of varying operational scenarios. Stereo cameras work on a similar principle to human vision. The field of view is limited because both cameras need to have a view of the target environment. To circumvent this restriction, the team experimented with fusing the output of multiple stereo cameras to increase the field-of-view. Cameras also provide increased situational awareness since they have a much faster update rate (60 fps) and may provide a live feed. The lidar and stereo camera systems are both integrated with inertial measurement units (IMUs) that assist in the SLAM process. This helps smooth the motion by combining the sensor's data (lidar or camera) with acceleration data to calculate the estimated position. In fact, the IMU is the "inertial" part of LIO and VIO techniques.

Conclusion

This effort is novel because all previous radiation anomaly detection efforts have focused solely on detector response and have not been capable of exploiting precise spatial coordinates of each measurement or angular indications from a multi-detector system. In addition to increasing the sensitivity of anomaly detection, we will develop algorithms for determining optimal data for inclusion into existing localization algorithms.

The development of this technology represents: 1) a practical solution to mapping radiation measurements in GPS-denied environments, and 2) the potential to equip current overt radiological search teams with a capability to localize a radiation source.

The team developed a practical solution to mapping radiation measurements in GPS-denied environments, and the potential to equip current overt radiological search teams with a capability to localize a radiation source.

References

[1] Essex, J., C. Okada, A. Podovich, M. Reed, A. Guild-Bingham, and D. Haber., 2018. "Adaptive Source Localization Using Augmented Reality." *FY 2018 Site-Directed Research and Development Annual Report.*, https://doi.org/10.2172/1559295

Selective Isotopologue Capture from Whole Air with Porous Crystalline Solids

Mark Morey
24-131
Year 1 of 1
Co-Authors: Manuel Manard and Jacob Mansbach
Special Technologies Laboratory

Please see CUI summary for more information.

Neutron Technologies and Measurements

NTM Projects

Cryogenic Deuterium Pellet Injection for Enhanced Neutron Output of a Dense Plasma Focus

Daniel Lowe[a]
24-011
Year 3 of 3
Co-Authors: Michael Blasco[a], Parker Winters[a], Martin Pagali[a], Chris Hagen[a], Steve Molnar[a], Larry Robbins[a], Rand Kelly[a], Gary Huffines[a], Giovani Acevedo[a], Jeeno Doria[a], Isaac Robinson[a], Megan Lawrence[a], Rafael Castro[a], Trey Gebhart[b], Jeremy Chittenden[c], and Brian Appelbe[c]
[a]Nevada National Security Sites, [b]Oak Ridge National Laboratory, [c]Imperial College

Please see CUI summary for more information.

Additive Manufacturing of Structural and Pixelated/Discriminating Scintillators

Adam Wolverton
24-019
Year 2 of 2
Co-Authors: Jim Tinsley and Robert Buckles
Nevada National Security Sites


Stereolithographic Resin Prints attached to the build plate.

Abstract

Plastic scintillators are commonly used in radiation detection devices throughout the world. The Nevada National Security Sites (NNSS) use scintillators for prompt radiation detection in high energy experiments that generate large fluxes of pulsed radiation. Increased light output and faster decay times are desired. These attributes are directly affected by the formulation of the scintillator, machining, polishing, and coatings on not only the scintillator, but also light guides in the optical path. Additive manufacturing (AM) of plastic scintillators has recently been shown to produce performance comparable to cast materials. Resolution at micron levels allows us to rapidly prototype new formulations, shapes, and sizes of scintillators without the cost and machining associated with it. This work examines the use of commercially off-the-shelf (COTS) clear resins as a medium for mixing various concentration levels of dopants such as Anthracene, 2,5-Diphenyloxazole (PPO), and 2,5-Bis(5-tert-butyl-benzoxazol-2-yl)thiophene (BBOT).

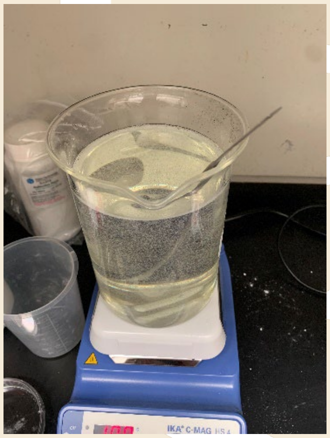
Mixing PPO and BBOT scintillant powders into clear printing resin.

Background

Scintillators have been used in radiation detection for many decades and tend to come in a variety of flavors that exhibit differences in light yield and timing performance. Fabrication of said scintillators involves casting, machining, and polishing to get the right optical finish and geometry for the application at hand. Because of the process to fabricate scintillators, cost can increase dramatically. An example is the large hexagonal scintillator that will be used in Neutron Diagnosed Subcritical Experiments (NDSE). This is one of the largest casted/polished scintillators made for the NNSS and because of that, it posed technical challenges and an increase in cost to meet mechanical and optical specs required. Each one of these ~60Lb scintillators roughly costs $9,000.00 to make. Utilizing AM can greatly reduce on machining, resulting in cost and time savings. Another desirable feature of AM is mixing additives to the COTS resin to change the scintillating properties of the material and print out custom scintillators with improved light yield and timing performance.

Technical Approach

This project deploys several AM technologies/methods of printing to explore the possible. We utilized Stereolithographic (SLA), Fused Deposition Modeling (FDM), and Direct Metal Laser Sintering (DMLS) to investigate its uses in the development of structural, pixelated, and discriminating scintillators. We mixed several resins with increasing concentrations of the scintillant/wave shifting powders. PPO and BBOT were mixed in at several concentrations. We printed several witness pieces as test articles to measure optical transmission, fluorescence spectrum, and fluor decay time. We compared our test articles to the EJ-232 scintillator as a control, which we readily use in many detector designs. These AM scintillators were placed in

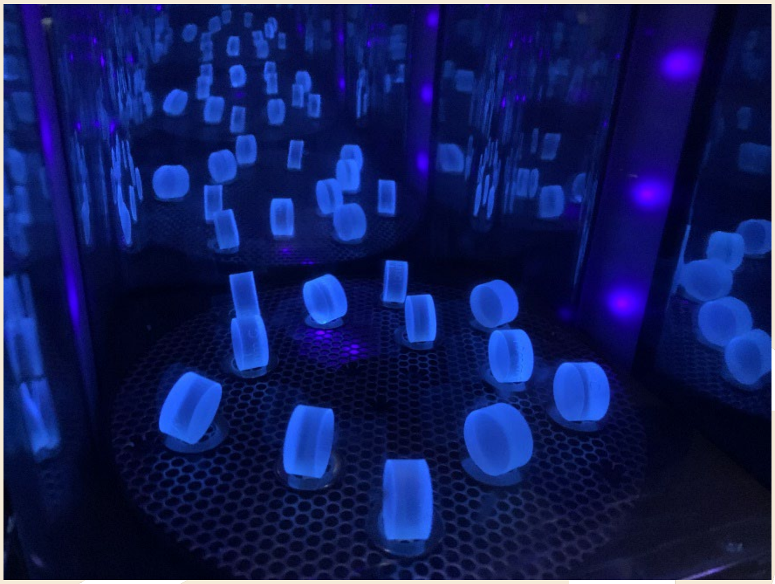

Samples glowing under UV light.

a detector test fixture for gamma calibrations, allowing us to measure scintillator sensitivity to Co-60 gamma radiation. We will present results from increased dopant concentrations and their effect on gamma sensitivity, fluorescence decay time, and optical transmission. Further improvements in performance of the resins will reduce costs associated with machining and polishing and will speed up the development time of new and interesting scintillators. The fine detail found in current state-of-the-art AM systems allows for truly mixed materials and engineered structures not available by other means. We are extending these rather nascent advances into the engineering of shapes that function as structural components, gradients in material index (by composition) to improve optical coupling, and combinations of spatial and spectral aspects to increase discrimination.

In collaboration with Eljen Technologies, we had scintillating fibers made out of Polystyrene (PS) and Polyvinyl Toluene (PVT), which we used to attempt FDM printing of a scintillating filament. We developed the profile to be used for this filament to be printed properly to prevent warping and delamination of the layers, and explored in-fill percentages to determine the best option for polishing.

Exploration of pixelated scintillators lead to DMLS printed samples of high-resolution capillaries in tungsten. The idea is that if we could print clear channels, we could cast scintillator material in the channels and utilize this assembly in radiation imaging as a coded aperture. This will be explored in greater depth with a follow-up Site-Directed Research and Development (SDRD) project.

Results

We were invited to give an oral presentation at the SCINT 2024 Conference hosted by the University of Milan - Bicocca. At this meeting, we presented results from increased dopant concentrations and their effect on gamma sensitivity, fluorescence decay time, and optical transmission. The resin-based SLA prints provided transmission of about 80% from 425nm out to 800nm wavelengths. We saw a 20% increase in transmission when comparing undoped clear resin to resins with scintillant mixed in. FDM samples of PS and PVT yielded similar transmission but at around 405nm, which is our typical wavelength of interest in measurements. Using a Fluorometer, we measured normalized emission of the samples at an excitation wavelength of 300nm. The undoped resin sample sees very little scintillation, but with the additives, we are able to see the scintillation of the wavelength shifters that were added and saw about a 5x increase in light yield. Compared to EJ-232, we see almost a tenth of the light with our SLA printed samples. Using a Co-60 source and a Carry 5000, we measured scintillation decay time of the SLA and FDM samples. The EJ-232 scintillator has a fluor decay time of about 1.6-2ns Full-Width-Half-Max (FWHM). We were pleasantly surprised to measure a very sharp timing response and saw sub ns FWHM measurements as low as .7ns. PS provided a bit slower fluor decay at about 3.2ns FWHM. In collaboration with EOS, we used DMLS to print a high resolution

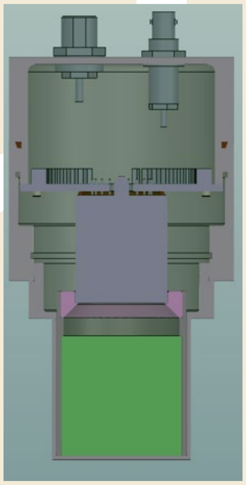

CAD model of detector housing

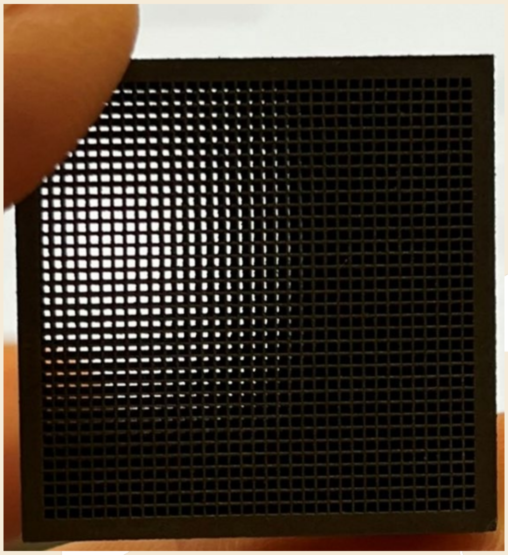

DMLS Tungsten Sample with 500-micron capillaries.

(250 micron) capillary sample out of tungsten metal powder. We did not have time to pursue casting with scintillator material, but this has led to further work in another SDRD and hopefully an Interlaboratory (IL) Laboratory-Directed Research and Development (LDRD) project.

Conclusion

In conclusion, we were successful in additively manufacturing scintillators for detecting radiation utilizing stereolithographic and FDM techniques. Although there is clearly a disparity in light output comparing AM samples to COTS scintillators, the sub-nanosecond decay time could prove useful in measurements with higher gain photodetectors for prompt radiation experiments. FDM printing is an avenue to explore further. With this method, we can form filament that can be printed and provide a much higher light yield with a nominally fast FWHM timing response. Although it is printable, these objects tend to lack mechanical strength, and improvements can be made in the materials. Development of tungsten high-resolution capillaries using the DMLS has sparked a lot of interest in the imaging community and will be explored further in fiscal year 2025 with a new SDRD looking at neutron imaging using CASPA Coded Apertures, and we are hopeful for further funding and collaboration through an IL LDRD.

Publications

Presentation, Buckles, Robert A.; DiBenedetto, John A.; Tinsley, James R.; Wolverton, Adam J., "Additive manufacturing of structural and pixelated/discriminating scintillators." https://icon.nv.doe.gov/otcs/llisapi.dll?func=ll&objId=38614987&objAction=Open&nexturl=%2Fotcs%2Fllisapi%2Edll%3Ffunc%3Dll%26objId%3D38611218%26objAction%3Dbrowse, 2024. *SCINT 2024 - 17th International Conference on Scintillating Materials and their Applications.*

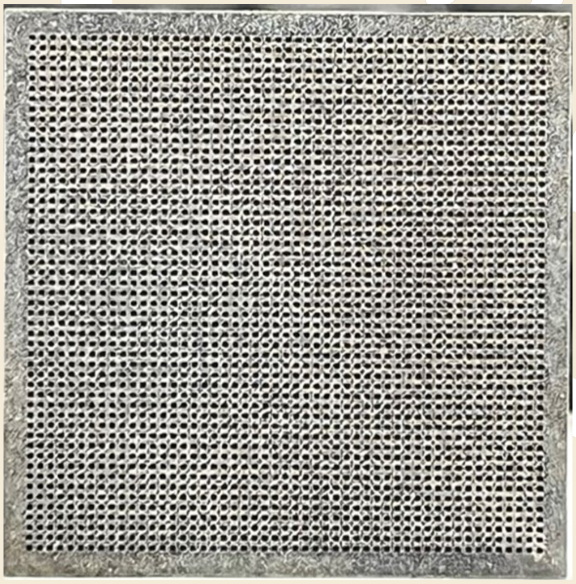

DMLS Tungsten Sample with 250-micron capillaries.

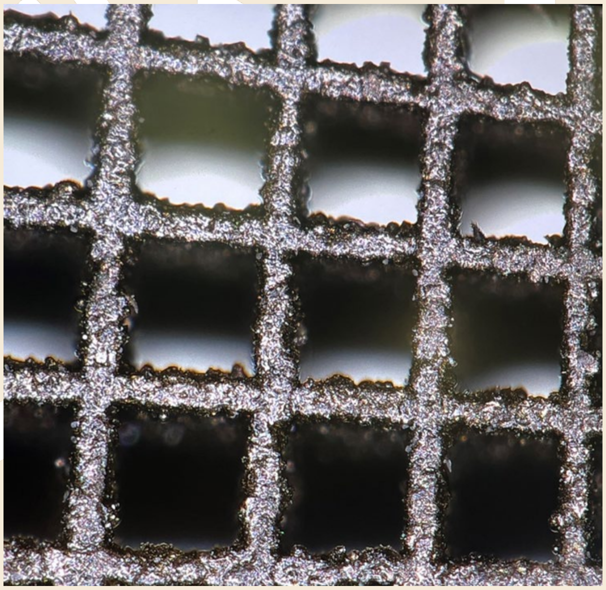

Micrograph of 250-micron capillary sample

Staged Z-Pinch and Variable-Energy Laser Ablation-Driven New High-Yield Neutron Source

Eric Dutra[a]
24-096
Year 2 of 3
Co-Authors: Matt Wallace[a], Showera Haque[a], Daniel Lowe[b], Zach Wolff[a], Piotr Wiwior[b], Aaron Covington[c], Jeremy Iratcabal[c], Jeremy Chittenden[d], and Brian Appelbe[d]
[a]Livermore Operations, [b]Nevada National Security Sites, [c]University of Nevada, Reno, [d]Imperial College

Please see CUI summary for more information.

Ultrafast High-Dynamic-Range Photomultiplier Trials

Robert Buckles
24-119
Year 2 of 2
Nevada National Security Sites

Please see CUI summary for more information.

Radiographic Systems Imaging and Analysis

RSIA Projects

Novel Photon-Counting Detector Concept for High-Resolution Radiographic Imaging

Stuart Miller[a]
24-032
Year 2 of 3
Co-Authors: Jacob Marks[a], Showera Haque[b], and Luke Hovey[a]
[a]Los Alamos Operations, [b]Livermore Operations

Abstract

Neutron imaging has many important applications including those related to global security such as Defense Nuclear Nonproliferation (DNN) and near-field detection. There are also many industrial applications in nuclear detection technology (NDT) and radiography. Imaging neutrons is challenging due to their high penetrative power, which typically leads to low quality images with poor spatial resolution. We propose to develop a new imaging detector that will improve on both detection efficiency and spatial resolution. The innovative concept includes a thick transparent scintillator that is viewed by multiple cameras with lens coupling. The high-frame-rate cameras are synchronized together with a short frame time to view individual scintillation events from multiple angles; this allows 3D spatial coordinates to be determined with great precision. The *x*, *y*, and *z* values for thousands of frames and millions of events are compiled to form the 2D image. This innovative concept has potential to impact not only global security applications, but also a broad array of others.

Background

Typical radiographic imaging systems utilize a scintillator that converts the incident radiation (X-rays, gammas, neutrons) into optical light photons that are then detected by the light-sensitive detector. Normally a quantity or exposure of the incident radiation produces a lot of optical photons that are integrated in the pixels of the 2D imaging detector such as a CCD or CMOS camera or even film to form an image. Here the best scintillators are those that have high absorption for the incident radiation and that produce the most light. However, there exists a trade-off between the scintillator thickness and the resulting spatial resolution due to the inherent light-spread that occurs within a thicker scintillator. This trade-off can be ameliorated to some degree by using scintillators with columnar form so that thicker layers can pipe the light to the detector, but the trade-off still exists. Here we are investigating a new approach in which high-speed cameras are used to detect individual scintillation events within a thick transparent scintillator volume. Two or more cameras are used in order to view the events within the scintillator from two or more angles. This provides the means to determine the location of the individual events with very high precision, and these locations can be used to artificially construct the image. This, in turn translates into high spatial resolution which applies for all of the events within the entire scintillator volume. Thus, the trade-off between the scintillator thickness and spatial resolution is substantially reduced.

Technical Approach

The technical approach of this project was to first demonstrate the validity of this imaging concept. With this objective in mind, the following technical goals were identified:

1. Identify and acquire suitable transparent scintillators for first imaging tests,
2. Work with Xcitex to customize their software for automatic frame processing, providing *x*, *y*, and *z* coordinates,

3. Perform Geant4 simulations with various scintillator configurations with gammas and neutrons of a range of energies,
4. Demonstrate 3D scintillator event imaging concept with gammas or X-rays,
5. Develop image construction methods to convert the 3D event location data into a 2D radiographic image, and
6. Choose components for neutron detector prototype design.

At the beginning of this project, we investigated several transparent scintillators as well as cameras to determine which will work best for this application. We showed that CsI:Tl, LYSO:Ce, and GAGG:Ce were all suitable, and produced bright spots that could be visualized above the background. We also found that EMCCD cameras performed the best for imaging scintillation events, and two cameras were purchased for the project.

Software developments are an important part of this project as well. This includes software for automatically detecting scintillation events and providing data on their location in 3D space. For this, we are working with Xcitex, a company that has developed software for 3D motion tracking with multi-camera images. A subcontract was placed with them to modify their software specifically so that scintillation events could be automatically processed to provide *x*, *y*, and *z* location information. Automating the process is essential to the program since it is not practical to go through thousands of frames to manually locate scintillation events. Geant4 simulations were performed with various configurations in order to demonstrate the theoretical performance of this concept with X-rays, gammas, thermal and fast neutrons. While this imaging method eliminates the dark noise and read noise of the camera, the shot noise of the incident radiation is still present as well as scatter from the object and within the scintillator itself. These can be accounted for through these simulations with each species.

This new imaging technique also requires new methods to form the actual radiographic images. With normal radiographic imaging detectors the images are formed by simply integrating for the required exposure time, or adding multiple image frames together. Here, however, the *x* and *y* coordinates of the scintillation events are used to construct the image. A script was written in Python to project the *x* and *y* locations into artificially generated images based on the number of events at each *x* and *y* location. In addition, *x* and *y* coordinates can be chosen at different depths (z ranges) in the scintillator allowing for energy-selective imaging.

For the initial demonstration of this concept, we started with alphas because they produce bright spots and do not penetrate into the scintillator. For the initial developments of the software, this is more straightforward since all of the events are located in one plane at the surface of the scintillator.

Results

In the second year of this project, great strides have been made in software developments. This includes both the software for automatically locating events as well as for the construction of the images from the location data. With these successful developments, we were able to produce the first 2-camera images using an alpha source and a CsI:Tl scintillator crystal. This is a great accomplishment as it demonstrates the viability of this new imaging concept. The figure below shows the resulting image along with a comparison to a standard integrated image acquired with one camera.

The second year accomplishments were as follows:

- GEANT4 simulations were refined from the previous year to demonstrate imaging technique with X-rays, gammas, thermal and fast neutrons.
- Image construction methods were further developed and improved to make 2D radiographs from scintillation event location data provided by both simulations and actual data.

- Software developments at Xcitex can now automatically locate and provide *x* , *y*, and *z* location data for events that are located in one plane.
- The first ever high-resolution 2D radiograph has been produced to successfully demonstrate this imaging concept.

Alpha images of an NNSS aluminum phantom. A standard integrated image acquired with a CsI:Tl film and one EMCCD camera (*left*). A similar single-camera image constructed from centroiding individual scintillation events (*middle*). The constructed image from the new imaging system, acquired with a CsI:Tl crystal 15 mm thick and two cameras (*right*).

Conclusion

At the end of the second year, we have successfully demonstrated that this new imaging concept works, which is a major milestone. The automated software is far from perfect at this stage, so we can expect a significant improvement as the software is refined during the final year. The first images were using alphas; however, the GEANT4 simulation results suggest that this will work equally well with gammas and neutrons.

In the last year of this project, the focus will be on further development of the software and also in demonstrating the concept with neutrons and gammas. The challenge with the Xcitex software is to automatically correlate an event seen in one camera with the same event viewed in the other camera. While this has been demonstrated with the image produced in Figure 1 below, further refinement and improvements need to be made in the third year. In addition, the image construction software, which is in development at LAO, will also be refined and improved.

In order to demonstrate imaging with neutrons and gammas, the entire system must be made travel ready. To accomplish this, a portable system will be designed that will house the two cameras and the scintillator inside a dark box. The design will be made as versatile as possible to accommodate different imaging areas and camera angles. It will also include mirrors so the cameras can be offset to allow them to be shielded from direct exposure to the source radiation to avoid damage.

The next steps will be to take the imaging system to various locations in order to acquire data. This will include going to Los Alamos National Laboratory to visit Scott Watson's lab for imaging with a Co-60 source. There the imaging system will be fully evaluated including with the imaging metrics such as spatial resolution and detective quantum efficiency.

Data Fusion: Reconstructing 3D Hydrodynamic Scenes Utilizing Both Radiography and Momentum Diagnostics

Jordan Pillow
24-052
Year 1 of 2
Nevada National Security Sites

Abstract

Reconstructing hydrodynamic scenes from a single x-ray projection has been an analytical mainstay of stockpile science for decades. Both the classic and current best practices rely on solving a full-rank, but highly ill-conditioned system of equations. Recent developments to the Asay Window (AW) momentum diagnostic have proven it feasible to reliably resolve substantially larger quantities of areal mass. As a result, an analyst may now consider the AW diagnostic as an additional collection of projection views from the experimental axis. Combining these data may potentially allow for new reconstructions that potentially surpass all previous methodologies.

Background

The primary goal for this project is to obtain more accurate 3D volumetric density reconstructions for subcritical experiments by "fusing" radiographic and AW data and analysis.

In radiography, there are multiple processing steps that the raw image must undergo before arriving at a final volumetric density estimate, the primary ones being dark field subtracting, dose normalizing, flat field correcting, converting pixels to areal density, and Abel inversion. See [1] in the NLV share drive for more details. Each processing step introduces sources of error that we must quantify using the methodology from the National Institute of Standards and Technology [2]. These errors propagate into final density estimates, and we expect the AW data will help minimize these uncertainties.

The AW diagnostic can give reliable estimates of volumetric density at the finite number of Photon Doppler Velocimetry (PDV) probe points. The uncertainty comes when we interpolate among the probes to get a more complete picture. Radiography can inform this interpolation and reduce errors. We refer the reader to [3] for more information on AW analysis.

Technical Approach

The project is split into three stages: (1) Asay-window-informed radiography analysis, (2) Radiography-informed Asay window analysis, and (3) Asay window and radiography data fusion. Breaking the project up in this way allows us to fully understand how the diagnostic can inform and improve the analysis of the other. After fully understanding both directions, we expect there to be a clear path forward on the true "data fusion" problem.

This year, we mainly focused on part (1). We assumed the AW analysis produced highly accurate volumetric density measurements at the sparse number of probe locations. Using this data as ground truth information, we modified the inverse Abel problem for our radiography analysis in order to take this additional information into account. The forward Abel transform is a special case of the Radon transform, where 3D -> 2D projections are performed by summing the discretized 3D object's voxels. This mimics radiographic image acquisition, where Beer's law has been applied to the "photon-counting" image to get a picture of the object's x-ray attenuation.

The Abel transform assumes the object is axially symmetric, which makes calculations easier. If a 3D object (width x length x height) is axially symmetric, then it can have a 2D representation (radius x height). Therefore, we are able to work with matrix equations such as AX = B, where A is the n x n Abel operator, X is the n x m 2D representation of the 3D object, and B is the n x m 2D attenuated image of X. The inverse Abel problem is to estimate X, the 3D object, given B and A.

Using a Bayesian framework for the inverse Abel problem (see [4] for more details), we can obtain uncertainty estimates in our final 3D volumetric reconstructions. This year we modified the work in [4] to include the sparse AW points as ground truth information, which reduces the widths of the uncertainty bars in the reconstructions, especially for smaller radii. Future work would be to incorporate uncertainties in the AW measurements within the Gibbs sampler.

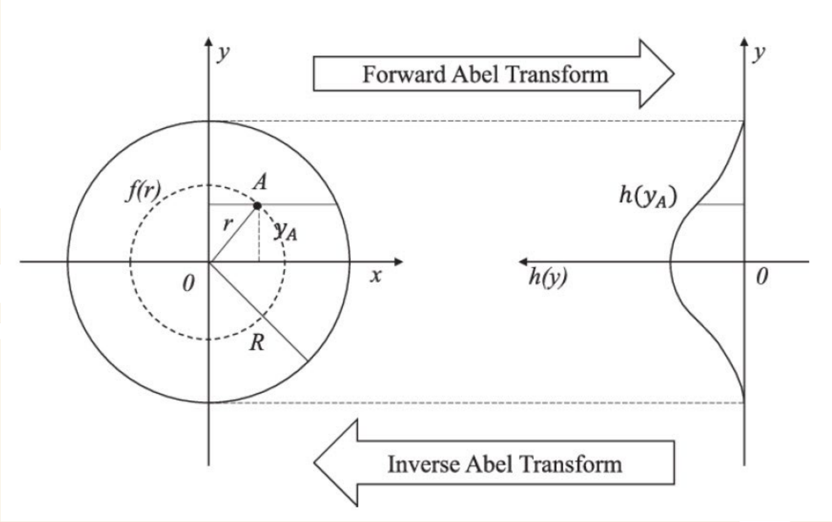

Diagram of the forward Abel transform (projecting 2D data onto 1D plane) and inverse Abel transform (taking 1D projection back to 2D)

We will also collect experimental AW and radiography data for our analysis. We will use the C3 gas launcher to collect AW data. If we can find an available radiography source, we will incorporate that into the C3 launcher experiments. If not, radiographs will be collected using Cygnus at PULSE. The target profiles we plan to use are in the image below.

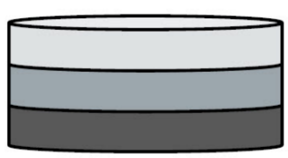

Target 1: *Stack of flat disks with varying densities.*

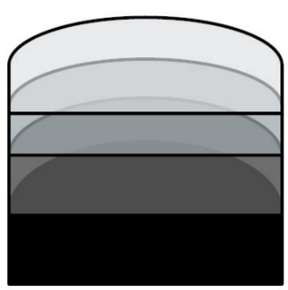

Target 2: *Concentric domes with varying densities.*

Results

With the help of our summer intern, we successfully implemented a Gibbs sampler for the 1D inverse Abel problem with sparse ground truth points.

Two experiments were performed at the C3 gas launcher the last week of September 2024. AW data was collected for the flat stacked coins target.

Conclusion

We have made good progress on the "AW-informed radiography analysis" piece by using the Gibbs sampler that incorporates the AW data. The sampler yields a mean reconstruction along with credibility intervals to quantify uncertainties. We have real AW data from the C3 gas launcher experiment with the stacked flat coins. We will analyze this data and estimate the volumetric density of the target. We will also image the target at PULSE and apply the Gibbs sampler approach with the real data. We will repeat this process later in the fiscal year with the more challenging "concentric metal domes" target.

This fiscal year we will also focus on the "Radiography-informed AW analysis" problem. Analyzing the C3 data should give us ideas on how radiography could help this analysis. Twin Peaks AW analysis has already given us a couple ideas, like accounting for the target's trajectory and outward expansion.

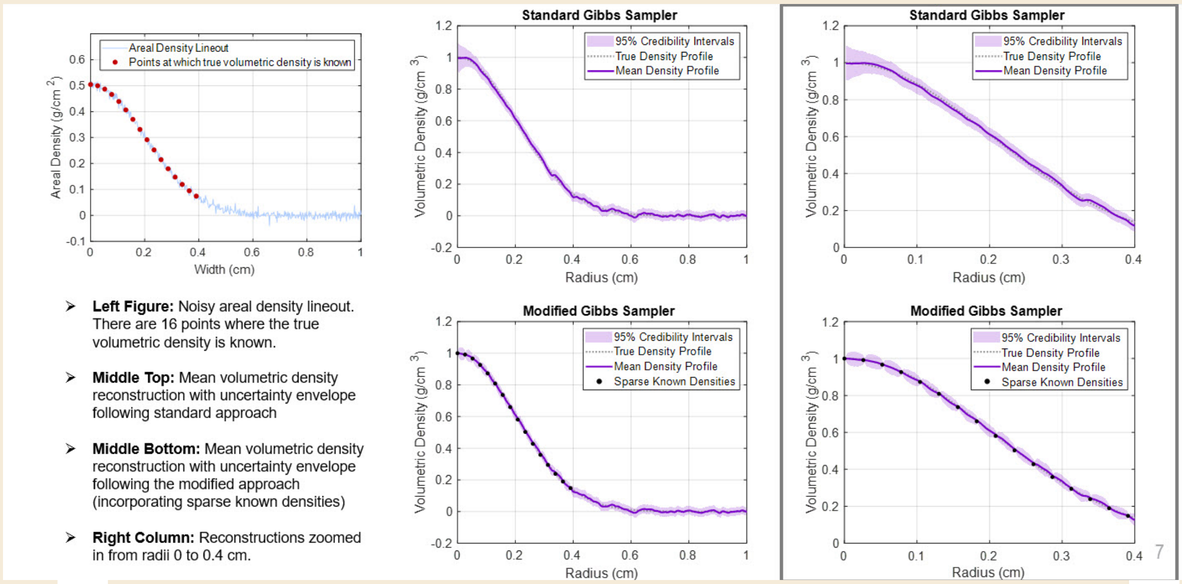

Bayesian Abel Inversion with sparse known data

We will continue to collaborate with Arizona State University for help in developing better algorithms for parts of radiographic image processing (e.g., deblurring and the inverse Abel transform). These steps must be performed as best as possible, or errors will propagate to our final estimates.

References

[1] Margaret Lund, 2022. "Data Analysis for Radiography in the DOE." , S:\NLV\Share\Pillow_JA\Data Fusion SDRD\References\Radiography\Data Analysis for Radiography in the DOE_V2.docx

[2] National Institute of Standards and Technology, 2017. "Uncertainty of Measurement Results." , https://physics.nist.gov/cuu/Uncertainty/index.html

[3] Daniel Champion, Sean Breckling, Garry Maskaly, Fady Najjar, Paul Steele , 2022. "Extending the Asay window measurement model to high areal mass ranges." , https://www.osti.gov/servlets/purl/1875060

[4] Marylesa Howard, Michael Fowler, Aaron Luttman, Stephen E. Mitchell, Margaret Hock, 2016. "Bayesian Abel Inversion in Quantitative X-Ray Radiography." *SIAM Journal of Scientific Computing*. Vol. 38, No. 3, pp. B396-B413., https://doi.org/10.1137/15M1018721

Solid-State Spectrographic Camera for HED and Pyrometry Applications

Amy Lewis
24-064
Year 3 of 3
Los Alamos Operations

Abstract

High-speed, nanosecond-scale, time-resolved radiance and pyrometry type measurements are essential to characterize advanced HED tests at Z and the National Ignition Facility (NIF). Streak cameras suffer from poor detector efficiencies, variation in temporal resolution from shot to shot, limited spectral range, and overall sensitivity. A solid-state solution will provide a reliable, cost-effective option with improved performance. The proposed solid-state spectrographic camera will incorporate a complementary metal oxide semiconductor (CMOS) sensor with a novel shutter distribution architecture to create an imager with 100ps resolution. A prototype design was submitted to the Sandia MESA foundry as a ride-along to reduce cost and realize a functional ROIC.

Background

A solid-state spectrographic camera capability would benefit many programmatic mission priorities in the following areas: high explosive (HE)-driven ejecta temperature measurements for melt equation of state (EOS) of ejecta or bulk materials in dynamic shock tests to inform physics models, HE and detonator performance tests, EOS for Insensitive High Explosive (IHE) tests or high temperature pyrometry on gas gun tests. Dynamic high-temperature measurements currently with traditional streak camera systems are also a critical diagnostic at Z, Omega, and NIF in the HED program.

Streak cameras have been workhorses in the weapons program for underground testing and subcritical experiments as well as for university research. Very few flexible solid-state solutions exist for the wide variety of streak camera experiments. If successful, this camera design will provide a significant opportunity for the NNSS to provide a state-of-the-art diagnostic system tailored to HED experiments.

Technical Approach

This high-speed solid-state streak camera concept utilizes a standard two-dimensional FPA architecture with a global electronic shutter. Standard FPAs collect spatial information in both the X and Y dimensions using an M rows x N columns array of pixels. This concept substitutes the spatial information in the X direction for temporal data, thus realizing an FPA that captures N, 1-dimensional images (of M rows of pixels). In this concept (figure, *right*), an externally triggered, high-speed global shutter is generated, replicated, and then distributed to every row in the pixel array simultaneously starting at the leftmost column of the array (column0). Every column of the

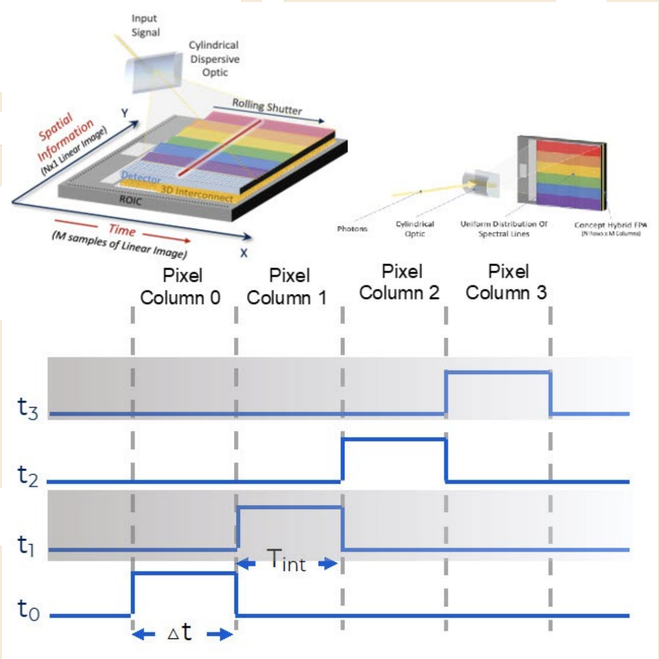

S4 Concept Timing The rolling shutter distribution creates a streak-like imager.

pixel array contains a delay element that will delay each subsequent column by a programmed delay time. Therefore, each column captures a 1-dimensional image (of M rows) of spatial information while delaying the subsequent column shutter (image) by a delta-T on the order of 100-150 ps.

A time-varying input signal of photons is dispersed evenly across the image plane of the sensor using a cylindrical optic. A trigger synchronous to the experiment is issued to the FPA, and the image capture sequence begins. A rolling shutter propagates across the image plane capturing linear images of the input signal starting at T_0 and ending at T_N. Read-out of the sensor pixel array is performed, and M, 1XN images of the time-varying input signal are collected. Consistent input impedance on every pixel is enabled by each pixel having a single signal connection to a corresponding photodiode via three-dimensional interconnect. The scalable architecture is limited to the size of the two-dimensional FPA. Kathy Opachich, Hanna Shelton, and Minta Akin (LLNL) provided feedback for initial use case considerations.

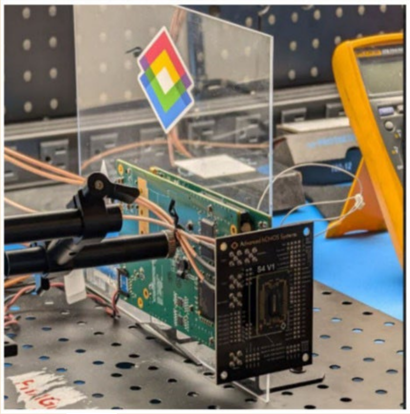
ROIC Testing Arrangement ROIC performance was tested in this benchtop arrangement.

Results

In year one, the team developed a detailed camera architecture enabling a proof-of-concept design. The team modeled the ROIC, detector, and system to predict performance under various input conditions and stimulus. The target design specifications for the new imager are presented in figure (*left*). In year two, the ROIC design was fully tested and submitted to the MESA foundry. Additionally, the design and layout of a corresponding photo-diode array was completed and submitted to the MESA foundry for fabrication. A camera test bench for the FPA was designed.

The third-year effort evaluated the solid-state streak imager designed in years one and two in a benchtop demonstration of the ROIC (see table below). The three-year proposal yielded a first-in-the-community

Table: Design Specifics

SPECIFICATION	TARGET	MEASURED*
T_{delay}	125- 150 ps	122 ps
Dynamic Range	1000:1	
Full Well	100k e^-	119k e-
Noise Floor	< 100 e^- (RMS)	~58 e- (with photo diode, perhaps a bit better)
Linearity	> 10%	> 10% to 0.5V
Pixel Size	30 um X 30 um	By design
Spatial Channels	31	By design
Temporal Samples	512	By design
Detector Type	25 um, Silicon	By design
Detector Sensitivity	4-6 keV, X-Ray 380-880 nm, Visible	
Pixel Array Size	0.93mm X 15.32mm	By design

*Measured and in some cases inferred

solid-state streak camera with resolution suitable for dynamic experiments (in the 100ps range) with a plan to achieve HED time scales in a second, programmatic iteration.

216 devices were fabricated across nine full wafers of Kraken parts. Ten S4 ROICs were packaged to evaluate device performance with bench level testing. All packaged parts passed functional tests (Figure *previous page* and *below*).

Part Number	VDD/VSS nBiasEn (mA)	VDD/VSS (mA)	CASCBOT (mV)	CSRCBIAS (mV)	CASCTOP (mV)	BGREF (mV)	TSENSE (mV)	Trig In to Trig Out (ns)	Trigout to RepTree Out (ns)	Min Record Len (ns), VDD=3.2V	Min Record Len (ns): Rep-Tree-Out to 512-Delay, VDD=3.6V	Jitter Pk-Pk TrigOut - 512 Out Delay	Min Record Len (ns) : Rep-Tree-Out to 512 Delay Out, VDD=4.0V	Jitter Pk-Pk TrigOut - 512 Out Delay	V_P Tune (Ohms)	VAB (Ohms)	TC_Access In	VRST (Ohms)	ColTestIn (Ohms)	~~PDBIAS (mA)~~	Grade (D
S4-09-01BS1																					
S4-09-01BS2																					
S4-09-01B03	1.5	13	803	2057	1607	903	1225	9.49	0.338	80.6	70.96	0.1	63.78	0.07	26M	26M	26M	1M	26M		A
S4-09-01B05	1.3	13	792	2054	1581	904	1242	9.36	0.357	79.24	69.72	0.1	62.59	0.08	26M	26M	26M	2M	26M		A
S4-09-01B06	1.7	14	789	2066	1576	905	1271	9.43	0.422	81.45	71.43	0.14	64.41	0.08	26M	26M	26M	8M	26M		A
S4-09-01B08	1.5	15	808	2041	1610	934	1330	9.56	0.391	82.46	72.25	0.11	65.2	0.08	26M	26M	26M	1M	26M		A
S4-09-01B12	0.8	15	801	2036	1598	888	1212	9.51	0.364	80.52	70.64	0.1	63.72	0.07	26M	26M	26M	8M	26M		A
S4-09-01B15	1.3	14	803	2049	1604	923	1315	9.54	0.34	80.73	70.73	0.09	63.78	0.07	26M	26M	26M	7M	26M		A
S4-09-01B16	1.5	15	801	2050	1601	928	1349	9.38	0.296	76.21	67	0.1	60.54	0.06	26M	26M	26M	8M	26M		A
S4-09-01B17	1.4	14	795	2059	1587	914	1349	9.25	0.319	76.09	66.83	0.09	60.38	0.08	26M	26M	26M	6M	26M		A
S4-09-01B20	1.4	15	798	2044	1595	925	1379	9.4	0.305	77.01	67.58	0.11	61.08	0.07	26M	26M	26M	7M	26M		A
S4-09-01B22	2	15	803	2058	1603	907	1255	9.33	0.33	77.24	67.92	0.09	61.41	0.08	26M	26M	26M	8M	26M		A
Simulation - Typical			730	2330	1450	970	1880		0.303	75.26			63.49	0.02							

Part Number	Read Noise with KTC removed (uVrms)	Measured Total Noise (uVrms)	inferred KTC component (uVrms)	inferred Sense Cap From KTC (fF)	inferred charge gain (uV/e-)	Vrst Sweep (Vgain)	ColTestIn Sweep (Vgain)	Bleed Rate (1000'carriers/sec)*, Vrst =0.3V, Vcap=0.5V	Bleed Rate (mV/sec), Vrst =0.3V, Vcap=0.5V	Vtune Max RL (us) : vtune=2.25V, vdd=3.3V	BGTrim Sweep, Digital Value @ Bgref = 0.972V	Vrst SW On Resistivity Ohms Vab@ 3.3V	Vrst SW Off Resistivity Ohms Vab@ 3.3V	Test Circuit : Vab=3.3, 100uA, Mstart (Ohms)	Test Circuit : Injected Signal (# of offset pixels)	Vdd=4V Burnin 24Hours; Before-After IDD Current (mA)
S4-09-01BS1																
S4-09-01BS2																
S4-09-01B03	247	530	469	19	8.50	1.09	0.5	148	625	1.07	113	154	23.2M	625	41	0mA
S4-09-01B05	254	525	459	20	8.16	1.09	0.5	118	498	1.08	23	155	23.2M	609	30	0mA
S4-09-01B06	251	508	442	21	7.54	1.11	0.5	65	274	1.09	23	153	23.2M	622	31	
S4-09-01B08	251	560	501	17	9.68	1.11	0.49	120	507	1.1	67	152	23.3M	638	49	
S4-09-01B12	263	701	650	10	16.32	1.09	0.5	128	540	1.1	115	154	23.4M	625	25	
S4-09-01B15	257	644	590	12	13.48	1.09	0.5	114	481	1.1	66	153	23.3M	602	46	
S4-09-01B16	247	527	466	19	8.38	1.08	0.5	101	426	0.98	37	153	23.2M	599	10	
S4-09-01B17	254	513	446	21	7.68	1.09	0.5	114	481	0.84	21	156	23.1M	587	0	
S4-09-01B20	242	522	463	19	8.27	1.07	0.5	110	464	0.85	35	153	23.3M	597	21	
S4-09-01B22	242	473	406	25	6.38	1.1	0.49	86	363	0.89	19	155	23.1M	592	0	
Simulation - Typical	242	301		16.4	4.20	1.00	1.00	-		0.67				635	0	

ROIC Functional Testing Tabulated ROIC tests results show all test devices are functional.

Conclusion

A successful S4 concept was designed at Advanced hCMOS Systems and fabricated in the Sandia CMOS7 process. Ten S4 ROICs were packaged and tested to evaluate functional performance. All packaged devices were found to be functional and initial performance results were taken (non-photometric) and compared to simulated and target specifications. All non-photometric design specifications were met and validated/inferred with measurements taken on the ten packaged ROICs. Photometric testing is pending hybridization of

KrakenV2 ROICs to Si photodiodes. The S4 package developed is compatible with Lawrence Livermore National Laboratory (LLNL)/Sandia National Laboratories camera systems. S4 ROIC test data collection was taken with a LLNL camera system interface to enable faster system development. Stockpile Stewardship's Detectors and Instrumentation project will provide a programmatic soft landing for this work. As the Kraken V2 imager is hybridized, S4 will be, too. JASPER's spectrometer is a good target application. A technology disclosure was submitted at NNSS in October 2024.

References

A.E. Lewis, S. Baker, L. Claus, A. Corredor, L. Fegenbush, Z. Fitzpatrick, M. Jones, K. O'Flarity, M. Sanchez, K. Walters, 2021. "New Design Yields Robust Large-Area Framing Camera," *Review of Scientific Instruments.* 92(8):083103.

L. Claus, L. Fang, R. Kay, M. Kimmel, J. Long, G. Robertson, M. Sanchez, J. Stahoviak, D. Trotter, J. L. Porter, 2015. "An Overview of the Ultrafast X-ray Imager (UXI) Program at Sandia Labs," *Proc. SPIE.* 9591, 95910P. https://doi.org/10.1117/12.2188336.

Material Identification in Radiographic Images of Dynamically Formed Metal-Explosive Mixtures by Tuning the X-Ray Source Spectrum Using Multiple Anodes

Brandon La Lone[a]
24-070
Year 2 of 2
Co-Authors: Daniel Sorenson[b], Ruben Valencia[a], and Stuart Miller[b]
[a]Special Technologies Laboratory, [b]Los Alamos Operations

Abstract

The goal of this project is to identify and quantify the amount of a particular atomic element, in a mixture of elements, on a dynamic experiment. We use two-angle flash radiography for the material identification where the radiographic sources have different anodes which alter their x-ray spectrum. Unlike other efforts to use x-rays for material identification, this project takes advantage of the characteristic x-rays. In one x-ray diode we use a tantalum anode and in the other we use a gold anode. The target element is zinc. The characteristic L-lines of tantalum are just below the zinc absorption k-edge and the L-lines in gold are just above the zinc k-edge. Therefore, zinc more strongly absorbs the gold x-rays than the tantalum x-rays, whereas every other element (except Ta) more strongly absorbs the tantalum x-rays. This allows us to identify zinc in a background of other elements, even elements with similar Z. We demonstrate this effect on static targets to show the viability of this approach.

Background

The ability to correctly identify and quantify materials in x-ray radiographs has several applications within the weapons complex. It could be used for part inspection and for dynamic experiments. The main interest of this work was using x-rays to identify materials in mixed ejecta fields. When an explosively driven shock wave reflects from the free surface of a metal, the metal surface can particulate into ejecta particles. In some instances, it may be possible for the explosive products, or other materials, to breech the metal and mix with the ejecta. These mixed ejecta fields are of interest to our work.

Technical Approach

The approach taken in this work is to compare the x-ray transmission through an object at two different, closely spaced, monochromatic energies. If the energies are chosen carefully, they can straddle either side of the absorption k-edge of a particular element. For that one element, the higher energy x-ray source will be more strongly absorbed than the lower energy source (because of the k-edge); whereas for every other element the lower energy source will be more strongly absorbed. By comparing the transmission values through the scene from both x-ray sources, the one element can be uniquely identified and quantified.

Rather than using truly monochromatic x-ray sources (which may be possible at a synchrotron source in the future), we take advantage of the characteristic x-rays (nearly monochromatic) emitted from an x-ray diode. The energies of these characteristic lines are created by inner shell electronic transitions and are specific to the anode material in the diode. We chose to find characteristic line energies near 10 keV because this is a good energy for ejecta measurements which are often in the 2-20 mg/cm^2 range of areal density. We decided to use tantalum and gold anodes to look for the presence of zinc. The zinc absorption k-edge occurs at 9.66 keV and its attenuation coefficient changes discontinuously there from a value of 35 cm^2/g below the edge to 254 cm^2/g above the edge. Tantalum has characteristic L-lines at 8.1, 8.2, 9.3, 9.65 and 10.9 keV, mostly below the zinc k-edge. Gold has characteristic L-lines at 9.63, 9.7, 11.4, 11.6, and 13.4 keV, mostly above the k-edge. In addition to the lines, the x-ray spectrum also contains a large Bremsstrahlung component, which for our use is an undesirable background.

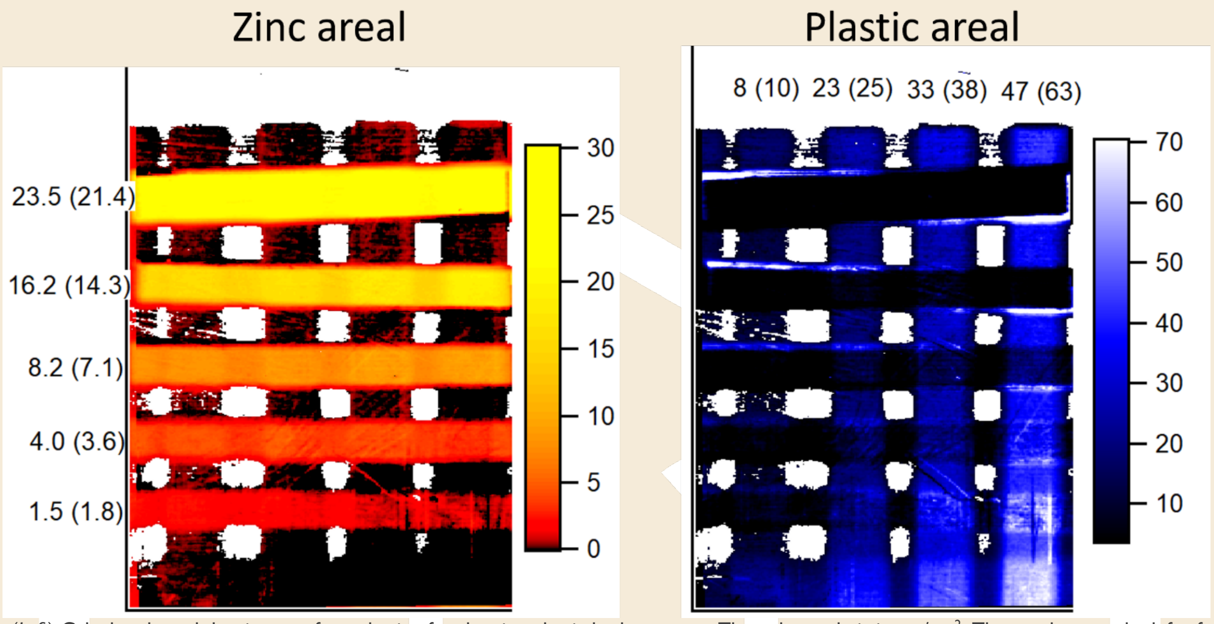

(*Left*) Calculated areal density map for only zinc for the zinc plastic basket weave. The color scale is in mg/cm^2. The numbers to the left of each strip are average values for that strip from the calculation. The numbers in parenthesis are the known areal densities of the zinc strips for comparison. (*Right*) Calculated areal density map for only plastic for the zinc plastic basket weave. The color scale is in mg/cm^2. The numbers above each strip are average values for that strip from the calculation. The numbers in parenthesis are the known areal densities of the plastic strips for comparison.

Gold and tantalum anodes were machined and installed into two different "Super Saver" x-ray sources at the Special Technologies Laboratory (STL). These are 380 kV flash x-ray sources with a rod-pinch diode design and a nominally ~30 ns pulse width. The x-ray heads are separated by a couple of inches so that images formed on the detector are physically separated as well. The test objects are placed between lead shield so that the two images from the two different heads do not overlap. To test both the concept and the analysis methods, we chose to image foil targets consisting of horizontal strips of zinc and vertical strips of plastic.

Results

Areal density reconstructions of the x-ray images are shown in the image of this summary. Using the dual anode approach, we are able to correctly identify the presence of zinc with a mixed element target. The methods also did a reasonably good job of quantifying the amount of zinc in the mixed zinc/plastic target, with measured areal density values from the x-rays agreed to within +- 10% of the known values from the foil thickness measurements. The plastic areal densities were also quantified though with greater uncertainty. Though not shown here, we were also able to correctly identify and quantify zinc in a mixed target of zinc and tin, to illustrate this material identification method is not sensitive to the Z of the elements in the mixture.

Needle-Washer Diode for Dynamic X-Ray Diffraction on Actinides at Z

Showera Haque[a]
24-107
Year 1 of 2
Co-Authors: Dale Welch[b], Matthew Wallace[a], Zachary Wolff[c]
[a]Livermore Operations, [b]Voss Scientific, [c]Nevada National Security Sites

Abstract

Sandia's actinide science experiments on Z require pulsed x-ray diffraction. The existing x-ray sources are insufficient for this task: the laser-driven sources cannot reach the photon energies required and the Marx-driven coaxial diode is not intense enough. The leading option is an upgrade of the coaxial diode with a needle anode and a washer cathode successfully used on dynamic materials experiments driven by the Thor pulsed power generator. The improved system needs to produce an order of magnitude higher intensity, higher photon energies, and a small source size. Prior optimization work has been trial and error and led to small improvements; this approach is time consuming, costly, and does not identify a development path. Here we propose a computational study of the processes and parameters responsible for the x-ray emission in the coaxial diode, to guide the development of an x-ray source suitable for dynamic materials studies of actinides on Z.

Background

The system used for dynamic x-ray diffraction at Sandia has been designed [1] and upgraded [2] by Dane Morgan (NNSS). The diode is inspired by [3], who adapted for line emission, by trial and error, a commercial diode optimized for bremsstrahlung, consisting of a needle anode and a washer-shaped cathode. The actinide science experiments are complicated because of the high atomic number and the fact that they are performed in containment vessels. Multi-keV photon energies are required to penetrate the high-Z material, and quasi-monochromatic radiation (typically Kα lines) is needed for the diffraction measurements. Commonly used anode materials are Mo (17 keV) and Ag (22 keV) and there are only a few materials with higher energy line emission that are both conductive and can withstand the electron energy deposition for multiple shots. An x-ray optical element is required to transport the radiation from the source to the sample inside the containment vessel, and the preferred solution is a polycapillary optic, equivalent to a light guide. These have generally small acceptance angles, so they require small sources, and become less effective as the photon energy increases. Finally, to account for the distance to the sample and for the losses in the polycapillary, the x-ray source needs to be very intense. This can be achieved by a combination of increasing the voltage and current of the driving Marx generator and optimizing the diode configuration. The pulse duration, which has to be much shorter than the phase change rate, is determined primarily by the power pulse from the Marx, but it can be shortened by anode plasma closing the anode-cathode gap. This proposal focuses on developing a computational model of the diode to optimize the emission parameters, to address the effects of higher electron beam power, to select effective diagnostics for plasma formation and evolution, and to identify configurations suitable for multi-pulse operation.

In the diode used for x-ray diffraction [2], the anode is a needle with a rounded tip that reaches partially into the circular opening of a washer-shaped cathode. Applying a voltage across the anode-cathode gap causes electron emission from the cathode regions where the electric field surpasses the threshold for explosive emission, typically 200 kV/cm, and electron acceleration toward the anode. The subsequent electron deceleration in the anode material produces bremsstrahlung radiation. The incident electrons and the bremsstrahlung photons also ionize the anode atoms leading to characteristic line emission, which is of interest for x-ray diffraction diagnostics. The diode is designed to reduce the impedance of the Marx generator load, to increase the emission current and reduce the electron impact energy on the anode, thus favoring the characteristic line emission over the bremsstrahlung background [1]. The most intense emission line, Kα, is typically used for measurements, while the next most intense line, Kβ, is attenuated with filters [2].

Technical Approach

In addition to radiation, the electrons deposit enough energy to ablate the anode surface. Taking the values from the COMSOL simulation shown in the figure, the electrons deposit approximately 100 J on the tip of the anode, with a rate of 10^{12} W/cm^2, which is sufficient to vaporize and ionize approximately 0.1 mm of material in the tip region. This leads to a gradual reduction in emission intensity from shot to shot [2]. The anode plasma expansion, together with plasma ejected from the cathode [4], eventually fill the anode-cathode gap and may reduce the duration of the x-ray pulse. Unless this plasma can be cleared on sub-microsecond time scales, multi-pulse operation of this diode is not possible.

The Marx-driven needle-washer diode is a simple device, but the still-superficial description above shows the complexity of the interconnected phenomena responsible for the characteristics of its x-ray emission. A simplified model, like the COMSOL one shown in the figure, is clearly insufficient for predictive and optimization purposes. A better model of the system should include power flow from the Marx to the diode; electron emission at the cathode; electron trajectories from cathode to anode considering the relativistic effects and electric and magnetic inter-particle interactions; x-ray generation by energetic electron and photon bombardment; plasma formation at the anode and the cathode and their evolution; and anode erosion. The Chicago particle-in-cell code with hybrid capability includes well-tested models for these processes and is the code of choice for this project. NNSS already owns a license, and the code is running on the Los Alamos Operations (LAO) Athena cluster.

Chicago will be used to create a complete model of the diode operation and to study the parameter interdependence, with the goal of optimizing the x-ray emission. The most difficult task is attempting to keep the anode-cathode gap plasma free, as a prerequisite for multi-pulse operation. If the time scales are favorable, and unless other processes will be found to contribute to the gap closure, one option could be to create a depression in the anode tip so that the plasma outflow is directed axially, through the washer cathode opening. This would keep the plasma out of most of the electron acceleration space and would delay the plasma closing the anode-cathode.

Results

A model of the needle-washer diode was constructed in Chicago, and we were able to run hydrodynamic and Monte Carlo simulations of the diode performance. To begin the computational study, needle length and drive impedance were the parameters we chose to vary because we had existing data to compare to the code's output. Needle lengths varying from 1.6–2.1 cm and drive impedances between 40 Ohm–75 Ohm were tested initially. We looked at the electron-photon Monte Carlo calculations to see how combinations of needle length and pulsed power drive affected K-alpha fluence. Understanding the sensitivity of the spectral output to needle length in particular can have a big impact on reducing shot-to-shot variation as the needle length incurs significant damage after just one shot.

A hydrodynamic simulation, which takes plasma formation into account, was performed for varying anode lengths. The main takeaway from these results was that plasma was formed and lasted within the anode-cathode gap region for 50 ns and longer. This is significant, as it can impact multi-pulse diode operations where we may require a second x-ray pulse hundreds of nanoseconds after the first one from the same diode.

The third case study we looked at using Chicago was using a structured anode, with a high Z core such as Mo surrounded by a lower Z shell. This type of design was considered so that the high energy K alpha radiation was limited in origin to a smaller region of the anode tip while keeping the diode impedance and electrical properties the same. The initial results showed that indeed the K alpha fluence emitted by the diode was from a smaller source size. However, we will need to continue to optimize for brightness while looking at the robustness of this type of anode in practice.

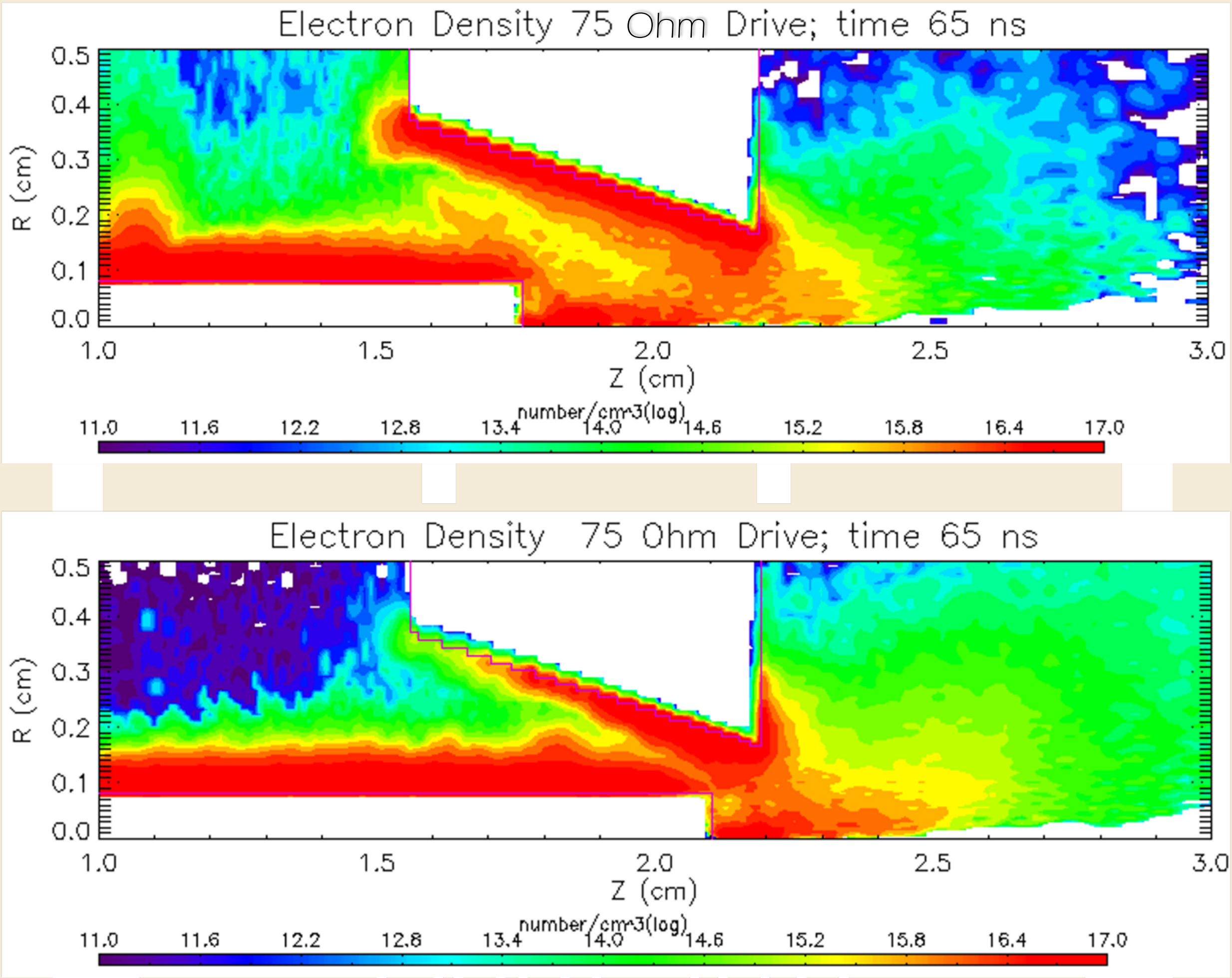

Chicago simulation of the diode with two different anode lengths showing a map of the plasma electron number density as the color scale. These simulations show that at a snapshot at 65 ns, plasma exists between the anode-cathode gap. For the shorter anode (*top*), the plasma density is lower, highlighting a possible plasma mitigation technique.

Conclusion

Using our basic model of the needle-washer diode in Chicago, we are able to capture broad characteristics of the diode performance that we have observed in the lab, like photon fluence as a function of anode length. Work remains in the following year to refine the model and to devise experiments so that we can benchmark the simulations. Once benchmarked, we can more confidently use the model to drive diode design modifications.

References

[1] D. V. Morgan, D. Macy, G. Stevens, 2008. "Real-time x-ray diffraction measurements of shocked polycrystalline tin and aluminum." *Rev. Sci. Instrum.* 79, 113904., https://doi.org/10.1063/1.3030855

[2] T. Ao, D. V. Morgan et al., 2022. “A compact x-ray diffraction system for dynamic compression experiments on pulsed-power generator." *Rev. Sci. Instrum.* 93, 053909., https://doi.org/10.1063/5.0074467

[3] Y. M. Gupta et al, 1999. "Experimental developments to obtain real-time x-ray diffraction measurements in plate impact experiments.” *Rev. Sci. Instrum.* 70, 4008., https://doi.org/10.1063/1.1150026

[4] Q. Johnson, 1980. "“Flash x-ray tube for diffraction studies on a two-stage light-gas gun." *Rev. Sci. Instrum.* 51, 741-749., https://doi.org/10.1063/1.1136306.

Assessment of Single-Sided Radiographic Imaging Concepts for Future Development of a Compact Manned-Portable Radiographic Device

Luke Hovey
24-127
Year 1 of 1
Los Alamos Operations

Abstract

Single-sided radiographic imaging is an alluring prospect for a compact radiographic source to identify possible threats of nuclear weapons or dirty bombs for situations where traditional throughput radiography is not feasible. Given that, this technique poses its own unique challenges such as a low signal from back-scattered particles. To assess the feasibility of this for future development of a portable device, we run a set of simulations in Geant4 varying the target shell composition and incident particle sources and compare the flux ratios for the neutron cases and the three combinations of x-ray Bremsstrahlung sources and find that in all but one case, the prospects for accurate material identification are promising, with the neutron sources having the best prospects due to their relatively high signal and low noise compared to the x-ray sources.

Background

Nuclear response teams are at the forefront of our nation's efforts in deterring the illicit transport of nuclear weapons, dirty bombs, and special nuclear materials (SNMs) into our country. While they have many tools at their disposal to carry out this objective, they lack a compact manned-portable radiographic device that could be transported anywhere (such as by helicopter). The Baker et al. (2023) report on Workshop on Radiographic Imaging and Applications Research and Development Recommendations for Field Radiography (WORIA) identified the utility and need for radiographic standards for single-sided radiographic imaging (SSRI) and is closely tied with their highest priority research and development recommendations of Detectors for Penetrating Field Radiography (section 1.2.1). The 2023 WORIA is written with multiple national laboratory partners, led by NNSA NA-22, and identifies mission critical needs and gaps in current field deployment capability to provide input for the fiscal year 2025 Defense Nuclear Nonproliferation (DNN) R&D National Laboratory Call for Proposals.

SSRI is a very challenging problem in the emergency response environment but leveraging our team's background we expect to find potential solutions. The main advantage of SSRI is that the detector and source are effectively in the same location, which allows for it to be more compact when compared to traditional throughput radiography. SSRI also allows for material identification since x-ray attenuation, and hence back-scatter, are dependent on the elemental composition of the target. By operating at two or more successive beam energies, a user/algorithm can use the relative decrement between the radiographs to identify the presence of SNMs.

Technical Approach

We performed our simulations with the particle transport code Geant4 to model back-scatter radiography. For our preliminary results we used a target that was a spherical shell with an outer radius of 15 cm and a shell thickness of 2 mm with a source-object distance of 1 m. We ran simulations using target shell materials of isotopic mixtures of U and Pu, along with pure Fe and Ta with the target's fill volume being composed of 1 atm air, which was also used for the world volume composition. For the particle source, we considered fixed energy DD and DT neutron beams at 2.45 MeV and 14.1 MeV respectively, and three commercially available x-ray Bremsstrahlung sources from Golden Engineering (Golden sources XR-150, XRS3, and XRS4). We used source-blur functions with full-width-half-maximum values of 10 mm and 3 mm for the neutron and x-ray sources respectively. Additionally, we modeled the beam as a cone-beam with a total opening angle of 20o. We chose the FTFP_BERT physics list to handle decay and hadronic processes but replaced its electromagnetic physics list with the G4EmLivermorePhysics, which is computationally less expensive than the packages G4EmStandardPhysics package and performs nearly identically for x-ray energies less than 1 GeV. Due to Geant4 not having the neutron capture cross section data for Pu, we omitted the DD and DT neutron simulations where that is the target's shell composition. To boost the low signal of the detected back-scattered particles, we used geometry-based biasing where tracks that were backscattered and directed towards the tally volume tracks were split into separate new tracks by a factor 20 or 10 based upon whether the backscatter occurred within the target volume or not respectively and assigned a weighting that was the inverse of the number of splits multiplied with the current weighting of the particle track that is split. We biased and collected hits for both neutrons and x-rays for our neutron sources, but only x-rays for our three Golden sources. For our sample of 18 simulation configurations, we ran 108 input particles and created 2D histograms of their tally detection positions for the total number of hits and for hits that had passes through the target sphere weighted with each hit's track weighting upon detection. In reality this would be approximated via flat-fielding, but such steps are unnecessary with perfect information that simulations afford. Then we project each 2D image into 1D radial profiles for our preliminary analysis and compare the ratios of the DD vs. DT neutron sources (figure, *top left*) and the ratios of the XR-150 vs. XRS3 (figure, *top right*), XR-150 vs. XRS4 (figure, *bottom left*), and the XRS3 vs. XRS4 (figure, *bottom right*) Golden x-ray sources with each radial profile being normalized with their total respective dose for the 108 incident particles.

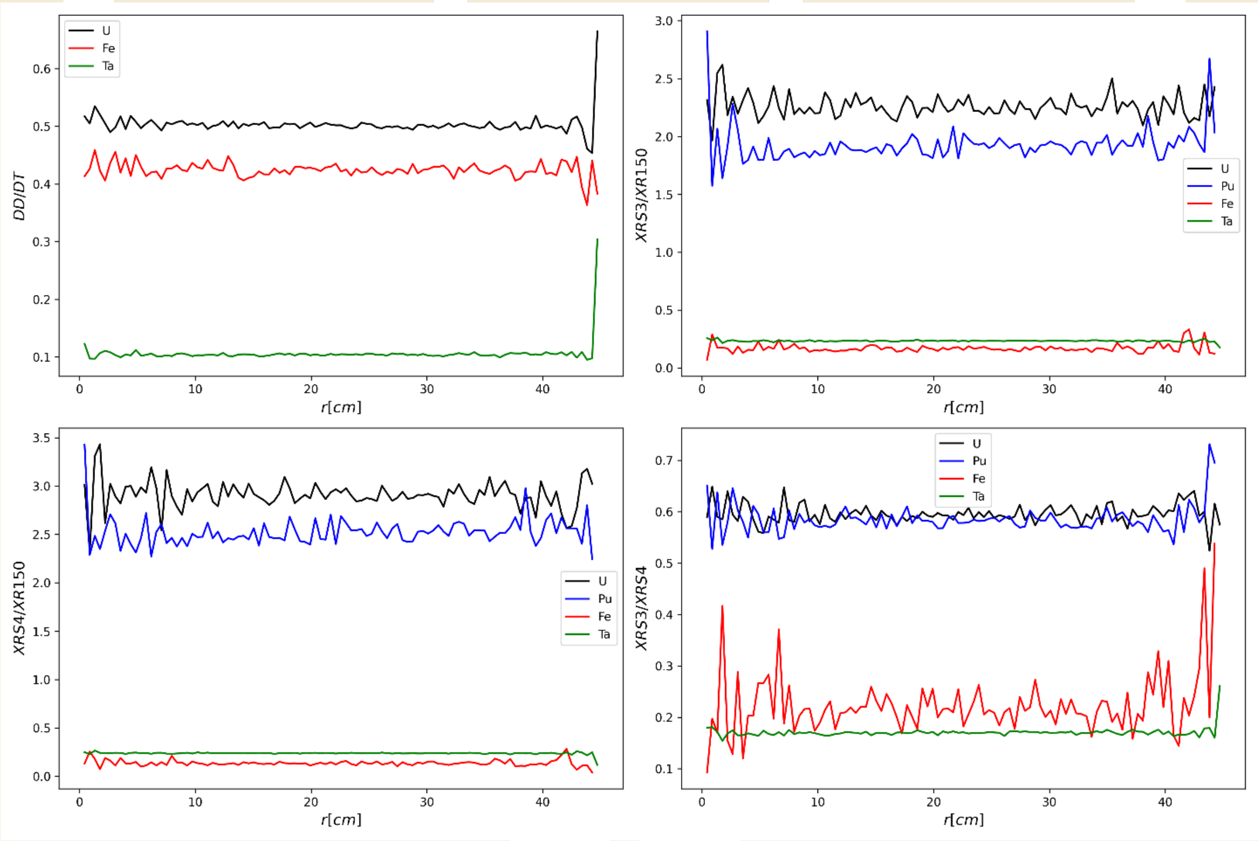

Comparison of the radial flux profile ratios for targets shells composed of U, Pu, Fe, and Ta shown in black, blue, red, and green respectively.

Results

We found that all but the XRS3 vs. XRS4 Golden x-ray sources showed promise for accurate material identification as manifest with each target material taking on different nominal flux ratios. The lack of easily identifiable materials with the XRS3 vs. XRS4 is likely due to the similarity of their spectra when compared to that of the XR-150 Golden source.

Conclusion

We find that further exploration into using single-sided radiography for the Future Development of a Compact Manned-Portable Radiographic Device is warranted, especially for the case where the radiographic sources are neutron beams. Future work will consider more realistic cone beam configurations, apertures for the detection of back-scattered particles, and target shielding/container configurations to determine the spatial resolution and required beam-time cadence for the real-world viability of this technique.

User-Centered Remote Testing and Operations

UCRTO Projects

Fundamental Experiments for Detonation Signature Modeling

Clare Kimblin[a]
24-007
Year 2 of 3
Co-Authors: Roy Abott[a], Manuel Manard[a], Thomas Myers[a], Ian McKenna[a], Tristan Richmond[a], Clif Watkins[a], Mary O'Neill[b], Josef Dufek[c], Joshua Mendez Harper[d], and Michelle Zimmerman[e]
[a]Special Technologies Laboratory, [b]Keystone International, [c]University of Oregon, [d]Portland State University, [e]University of California, Santa Barbara

Abstract

Our goal is to perform low technical readiness level (TRL) experiments that lead to improvements in understanding signatures produced by particulates in over-pressurized, supersonic flows. To achieve this we are taking a multipronged approach, employing a variety of experimental platforms and simulations. This year we used the Special Technologies Laboratory (STL) particulate shock tube to explore differences in electrical discharge production, detected as optical and prompt radio frequency (RF) emissions, as a function of carbon allotrope, size, and quantity. We focused on insulating diamond discharge production as a function of particle size, and on electrically conductive graphite (typically RF-silent relative to diamond) discharge production as a function of quantity. Diamond particle size was seen to have a significant effect on discharge type (glow to streamer/filamentary discharge) and on the detectability of RF emissions. Increasing graphite particle quantity was associated with increased electrical discharge production. We also performed the first multiphase discrete element fluid dynamic simulations of individual particles released from the shock tube. These simulations indicate that gas-particle mixing in the zone where gas is injected perpendicularly into the shock tube accounts for the peak number of collisions and peak collisional energies. Additionally, we made progress in demonstrating a first-of-its-kind measurement capability, namely quantifying the mass to charge ratio (m/z) of carbonaceous particles produced directly by a detonation. After dampening shock-induced mechanical noise, associated with pairing a high explosive (HE) detonation chamber (DC) with a time-of-flight mass spectrometer (ToF MS), we detected particle time-of-flight signals less than a millisecond post-detonation. Preliminary results (at only one reflectron voltage) indicate detection of particles with mass to charge ratio in the 3000-4000 amu range.

Background

Detonation particles (DPs) are responsible for prompt RF emissions and optical effects, and residual particles can be used forensically. To enable effective use of these signatures, better correlation between signatures and supersonic flow conditions, particle type, and particle quantity is required. Using small-scale, low TRL, controlled experiments involving a particulate shock tube, mass spectrometry, and small-scale detonations with a liquid explosive (the latter soot/no-soot experiments were performed in FY23), we are providing fundamental tools and data to inform RF, optical, and particulate evolution models.

With the shock tube, we aim to better understand the fundamental behavior of particles as a function of known quantities that regulate their ability to become charged and discharged by performing both experiments and simulations. In FY23 we performed experiments using 15 particle types with a range of properties that are expected to influence particle charging and RF emissions via triboelectric and fracto-charging. These particles ranged in electrical conductivity, polarizability, hardness, tensile strength, and surface area. Among the monodisperse particles studied thus far, a proposed hierarchy for increased particle charging and subsequent discharge is as follows: 1) triboelectric charging – increased surface area, 2) triboelectric charging – increased collisional energy (vs. deformability), and 3) fracto-charging – increased fracture resulting in increased charging and RF. In FY24 we have extended these studies to consider more nuanced behavior by exploring particle size and flow density for diamond particles which readily charge, and produce discharges, and particle quantity for graphite, with less propensity to hold charge (as determined by prior fluidized bed studies). Based on the fluidized bed studies it was predicted that sufficiently large particle clouds of graphite might generate sufficient charge, such that observable electrical discharges could be generated [1].

Steady state supersonic gas modeling capabilities were stood up in FY23, providing 2D vorticity and momentum magnitude simulations. These demonstrated the role that the 90-degree gas inlet has on producing supersonic KH instabilities and turbulent mixing - due to regions of strong vertical shear, and distinct regions of high-pressure gradients. FY24 models progressed to incorporate particles in discrete element multiphase shock tube simulations aimed at predicting particle-particle charging. They will ultimately be used to simulate electric fields such that discharge behavior can be predicted.

As a means to explore mass and charge (m/z) of detonation particles produced milliseconds post-detonation we are pairing an HE detonation chamber with a mass spectrometer. Knowledge of m/z is critical for explosive models but not yet incorporated because such values are not available.

Technical Approach

We are using the STL shock tube [2] (developed under STL-024-17 [3] and STL-008-20 [1]) to explore the impact that fundamental particle characteristics have on electrical discharge production. Particles chosen in FY23 ranged broadly in hardness, fracture toughness, permittivity, and conductivity. Flake versus powder morphology was also explored. This year the focus has been on RF emissions as a function of particles size, using insulating natural diamond ranging in size from 5 to 500 microns, and particle quantity, using electrically conductive graphite (~1.5 to 20 g). RF (kHz to GHz) and optical (high speed camera and photodiode) measurements were again used to capture the propensity of the ejected particles to produce electrical discharges. As a step toward being able to predict particle charging as a function of collisional charge transfer, discrete element multiphase fluid dynamic simulations of the STL shock tube were performed at the University of Oregon. Particle-to-particle collisions were modeled following release of the initially pressurized gas vessel. For simulation development, diamond particle properties were used (500-micron, 3500 kg/m^3).

To address gaps in charging and particulate evolution, we have paired a DC to a ToF MS [4] (built under STL-17-11 [5]). A typical mass spectrometer where ions are generated by laser ablation or other traditional means requires an ion funnel to maximize transmission of ions through the system, and an accelerating electric field. We instead use a ~27 mg pentaerythritol tetranitrate (PETN) detonator as the source of clustered carbon ions. These high kinetic energy species do not require additional guidance and acceleration to travel from the source to the detector. In the ToF MS paired with the DC, a reflectron/ion mirror provides a repulsive electric field that reduces the spread in KE for identical m/z ions. This permits detection of particles with higher time resolution. From the particle times of arrival at the Channeltron detector, the known pathlength traveled, and the reflectron electric field, it is possible to calculate m/z of the particles generated. SIMION® [6] was used for this purpose. In FY23 we recognized that high detonation pressures supported electrical breakdown at the high voltage power supplies. We remedied this by increasing the volume of the DC and actively pumped on it. Ringing signals of unknown origin were then observed in scope traces. In FY24 we performed a series of control experiments using blanks to prevent particle flow to the detector and were able to determine the source of the ringing signal and implement a means to prevent it.

Results

Shock tube experiments were performed comparing electrical discharge production as a function of diamond particle size and graphite quantity. With 3 grams of diamond the number of RF pulses detected in the 2-1000 MHz range was significantly impacted by particle size (and quantity), with close to 1000 RF pulses detected for 5-micron diamond particles and progressively fewer detected for 50 micron (<100 counts), 150 micron, and 500 micron particles (~6 counts). High-speed camera imagery reveals what the RF does not reveal. With

500-micron diamond numerous individual particles glow discharges are observed. However, each one is produced asynchronously and is not sufficiently capable of producing a detectable RF signal. As particle size decreases to 150 microns, glow discharges, appearing only below the Mach disc, are still the predominant discharge type. Shock-constrained streamer-like discharges are also observed periodically, apparently when close-proximity corona discharges are active simultaneously. With 50-micron diamond particles, shock constrained streamer discharges are more prevalent than with 150-micron particles, and glow discharges are only observed above the rarefaction region (see figure RHS). It is possible that this behavior is dictated by Paschen's law discharge or "gap" length can be correlated to a predicted "glow duration". Namely for the smaller, 50 micron particles, the electric field diverges [7] too quickly in the rarefaction region such that the effective "gap" length (l) x pressure (P) product is low, and the voltage required to produce gas breakdown lies on the asymptotically increasing left side of Paschen's curve, whereas for the 150 micron particles, the electric field diverges more slowly, such that there is sufficient time to ionize the gas in the rarefaction region, and effectively 'l' is large enough such that breakdown is favored. These results point to the important roles that particle size, flow density, and particle position relative to the shock front have in the production of detectable RF signals. We also compared discharge production when 20 g of graphite vs. ~2 g of graphite was released from the shock tube. As predicted by prior fluidized bed charging studies [1], a significant increase in observable discharges and RF emissions were recorded with increased graphite content. One mechanism for particle charging is fracture. Particle sizing post test using laser diffraction (Malvern 2000) indicated that significant fracture had occurred (mean particle size dropped from ~40 to ~8 micron). FY24 fluid dynamic simulations incorporated particles and predicted particle location and velocity and numbers of particle-particle collisions. These simulations indicate that gas-particle mixing in the zone where gas is injected perpendicularly into the shock tube accounts for the peak number of collisions and peak collisional energies (LHS of figure).

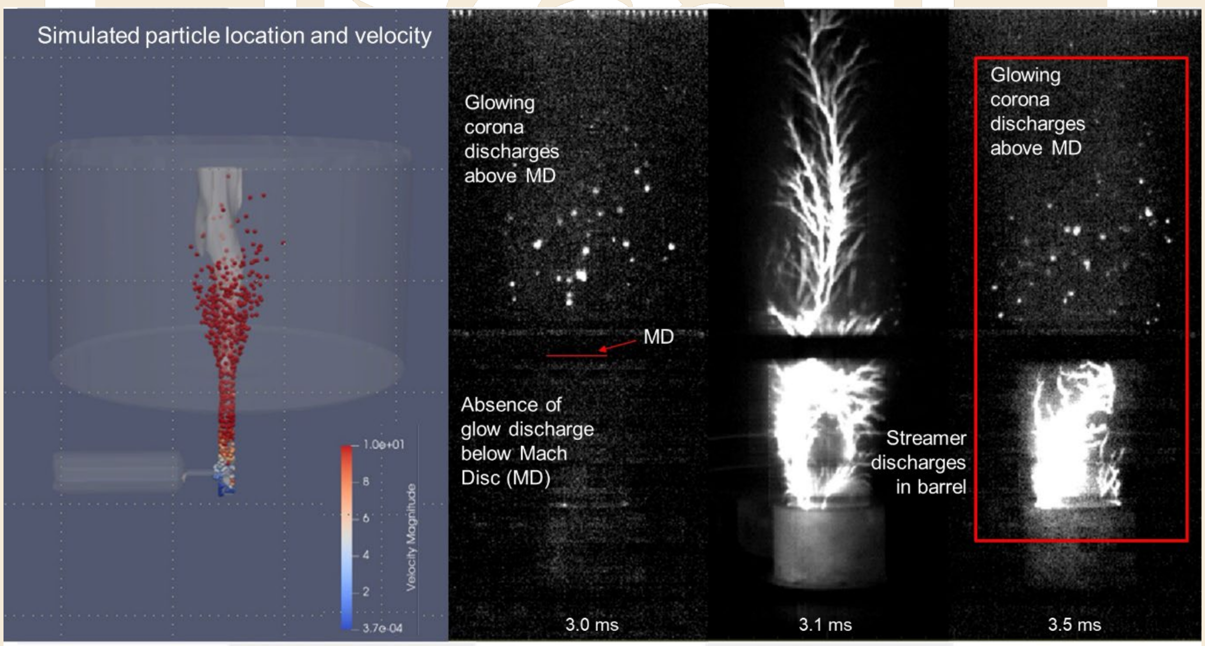

LHS - Simulated particle location and velocity. For clarity only 1% of particles are shown and particles are shown 50x larger. Individual particle velocities are indicated by particle color. RHS - Discharges produced by 50-micron diamond to 3.5 ms. Glow discharges are not observed in the rarefaction region below the Mach disc (MD) with 50-micron diamond; in contrast, with 150-micron diamond, glow discharges are favored below the Mach disc, but not above it. Simulations will be performed in FY25 to better understand this behavior.

In FY24 we removed a significant noise source associated with detonating a 27 mg PETN detonator into the chamber housing the ToF MS. Once high pressures which were leading to breakdown at the high voltage power supplies were reduced, ringing signals appeared in voltage traces in the 2 to 7-ms range. In FY24 we determined these were attributable to mechanical vibrations associated with shock and we were successful in suppressing the ringing by incorporating a bellows. With this source of noise removed it was possible to discern weaker and broader negative signals associated with charged particles in the 100-microsecond range. SIMION® simulations of the experiments indicate that flight times in the 100 ms range would correspond to 3000-4000 amu particles if they are just singly charged.

Conclusion

In FY24 we studied electrical discharge production and RF just as a function of particle size (diamond) and particle quantity (graphite). Our results further demonstrate that RF signals provide information about the structure of flows and particle content, with some caveats. While breakdown criteria are typically relaxed within the low pressure barrel shock region of the jet where spatially constrained leaderless discharge production is favored, large overpressure is not sufficient to guarantee production of detectable discharges in supersonic jets. Flows comprised of larger, insulating diamond particles (500/150 µm; in less particle-dense flow) tend to produce individual glow discharges that are too weak to be detected in the RF, whereas flows comprised of smaller particles (5/50 µm) generate readily detectable discharges. With these smaller particles, early time "continuous" RF is detected from streamers constrained to the barrel shock region, whereas sparse and more intense plume discharges are detected at later times.

In FY24 we moved beyond gas-only shock tube fluid dynamic simulations to those which incorporate particles, predicting particle location and velocity and counting particle-particle collisions. In FY25 we will additionally incorporate particle-to-wall interactions, calculate collisional energies, and charge transfer. We will also examine two models which explore glow to transient filamentary discharges and determine how well they fit the diamond experimental results. The goal of these simulations is to provide a model or models which capture and predict the electrical discharge behavior observed experimentally when particles of known size, density, conductivity, and breakability are exposed to shock in supersonic flow.
Using the detonation chamber paired with the ToF MS, we determined that when shock-associated mechanical vibration was dampened using a bellows, ringing signals in the 2–7 ms time range were greatly diminished. These signals concealed those produced by detonation particles predicted to be in the 3000–4000 mass to charge ratio range. If the particles we are detecting are singly charged, this would correspond to particles on the order of just 300 C atoms. Core detonation nanodiamond particles produced in the sub-microsecond post-detonation regime are predicted to be in the ~5 nm size range (~10,000 C) and these core-detonation particles are expected to aggregate in the sub-microsecond time regime [8]; thus, our results suggest that the particles we are detecting are highly charged. In FY25 we will perform experiments using a broader span of reflectron voltages to bracket particle mass to charge ratios.

References

[1] C. Kimblin et al., 2022. "“Dynamic Sub-Micron Particulate Behavior in Turbulent Media”." *In FY 2022 Site-Directed Research and Development Annual Report. Las Vegas, Nevada: Mission Support and Test Services, LLC.*

[2] J. von der Linden et al., 2021. "Standing Shock Prevents Propagation of Sparks in Supersonic Explosive Flows." *Commun Earth & Environ.* 2, 195. 10.1038/s43247-021-00263-y

[3] Kimblin, C., I. McKenna, B. La Lone, M. Manard, J. Mance, J. Madajian, M. O'Neill, M. Staska, G. Stevens, R. Valencia, 2019. "Transient RF and Optical Signatures." *FY 2018 Site-Directed Research and Development Annual Report, Las Vegas, Nevada: Mission Support and Test Services, LLC.* 108-120.

[4] M. J. Manard, 2012. "A Design for a Compact Time-of-Flight Mass Spectrometer." *Review of Scientific Instruments.* 83 105111-1–10511-7., https://doi.org/10.1063/1.4757864

[5] M. J. Manard, 2011. "Miniaturizing Time-of-Flight Mass Spectrometers." *In FY2011 Site-Directed Research and Development Annual Report, Las Vegas, Nevada: National Security Technologies, LLC.* 139-150.

[6] D. A. Dahl, 2000. "SIMION for the personal computer in reflection." *Int. J. Mass Spectrom.* 200, 3-25.

[7] N. Hamamoto, Y. Nakajima, 1992. "Experimental discussion on maximum surface charge density of fine particles sustainable in normal atmosphere." *J. Electrostatics.* 28, 161-173., https://doi.org/10.1016/0304-3886(92)90068-5

[8] J. A. Hammons et al., 2021. "Submicrosecond Aggregation during Detonation Synthesis of Nanodiamond." *J. Phys. Chem. Lett.* 12, 5286-5293., https://doi.org/10.1021/acs.jpclett.1c01209

Publications

Presentation, Clare Kimblin, Joshua Mendez Harper, Josef Dufek, Ian McKenna, "Spark and glow discharges in supersonic granular flows." https://meetings.aps.org/Meeting/MAR24/Session/Z29.5, 2024. *2024 APS March Meeting.*

Presentation, T. Myers, C. Kimblin, I. McKenna, M. D. O'Neill, "Research at the Special Technologies Laboratory: Highlights from the High Explosive Signatures and UAV Detection." https://wowza.nps.edu/nps_vod/GEAC/DES_Myers_10292024.mp4, 2024. *Naval Postgraduate School Defense Energy Seminar Series.*

Presentation, J. Mendez Harper, C. Kimblin, J. Dufek, I. Mckenna, "Spark and glow discharges in supersonic granular flows." https://agu.confex.com/agu/fm23/meetingapp.cgi/Paper/1437976, 2023. *American Geophysical Union Fall Meeting, Dec. 2023.*

Modernization and Scalability Enhancements for Sub-Nanosecond Accuracy Diagnostic Cross Timing for Use at Current and Future NNSS Testbeds

Dan Champion[a]
24-049
Year 2 of 2
Co-Authors: Jesse Adams[a], Caleb Dahlke[a], Nick Eisenberg[a], Madeline Gorman[a], Andrew Robinson[b], and Ajanaé Williams[a]
[a]Nevada National Security Sites, [b]Lawrence Livermore National Laboratory

Abstract

NNSS stockpile stewardship experiments are amongst the highest complexity scientific experiments conducted within the NNSA and DOE (e.g., subcritical experiments [SCEs] fielded at PULSE). Despite the high complexity, the methods currently used for configuration management and diagnostic cross-timing are holdovers from decades-old practices that struggle to scale to current diagnostic postures and the demands of modern analytics and machine-accessibility. Specifically, there is a real and present risk of data-loss, data-corrupting, or data-insufficiency in the currently configuration management practices because they depend on limited-scalability tools, exhibit a lack or absence of machine-accessible documents and reference data, exhibit an absence of version control, and do not allow for machine access and automation. In this project, we develop a graph database along with associated interfaces and analytics that demonstrate a modernization of the approach to NNSS testbed configuration management and apply to the specific case of diagnostic cross-timing on an active subcritical experiment.

Background

NNSS testbeds field a large quantity of diagnostic systems on dynamic experiments that are timed to nanosecond precision. On experiments conducted at facilities like NNSS's PULSE facility, configuration management must timely track the months-long evolution of the experiment apparatus.
Current methods used for diagnostic configuration management and diagnostic cross-timing involve legacy/hold-over methods from decades past and have evolved as diagnostic postures at testbeds have grown over time. Present configuration management is conducted using non-machine readable/accessible apparatus diagrams (e.g., Visio diagrams), Microsoft Excel spreadsheets, handwritten notes, and generally heavily rely on experimenter awareness and human-in-the-loop for all data access/retrieval.

Data entry and data ingest from measurement through to representation within the configuration management documentation has also become a bottleneck. It is common for measurements of apparatus components, such as component signal delays, to propagate from measuring device to hand-written note, to data entry personnel, and then proceed via email to a source document that eventually becomes part of the configuration management documentation. There can be as many as three human data-entry/re-entry stages as critical apparatus measurements proceed from creation to usage in experiment result analysis.

A modern approach to configuration management would allow for end-to-end machine access, real-time and distributed updating by experimenters, and demonstrate experiment relevant analytics that replication manual or subject matter expert (SME) driven workflows currently undertake with the legacy approach. Such a modern approach would need to scale to at least hundreds if not thousands of diagnostic systems/points and allow for the representation of an experiment apparatus with components beyond the complexity of current SCEs fielded at the PULSE facility.

Technical Approach

Diagnostic cross-timing for a PULSE experiment was selected as a focus application to demonstrate the new approach (stress test of accurate, timely, and comprehensive configuration management).

A Neo4j graph database was used to house the configuration management data. For diagnostic cross-timing, the discrete components that make up the apparatus constitute the nodes/entities. The connective information regarding those entities (i.e., how those discrete components are assembled into the final apparatus) determines the relationships/edges. The graph ontology for the database is shown in the figure below.

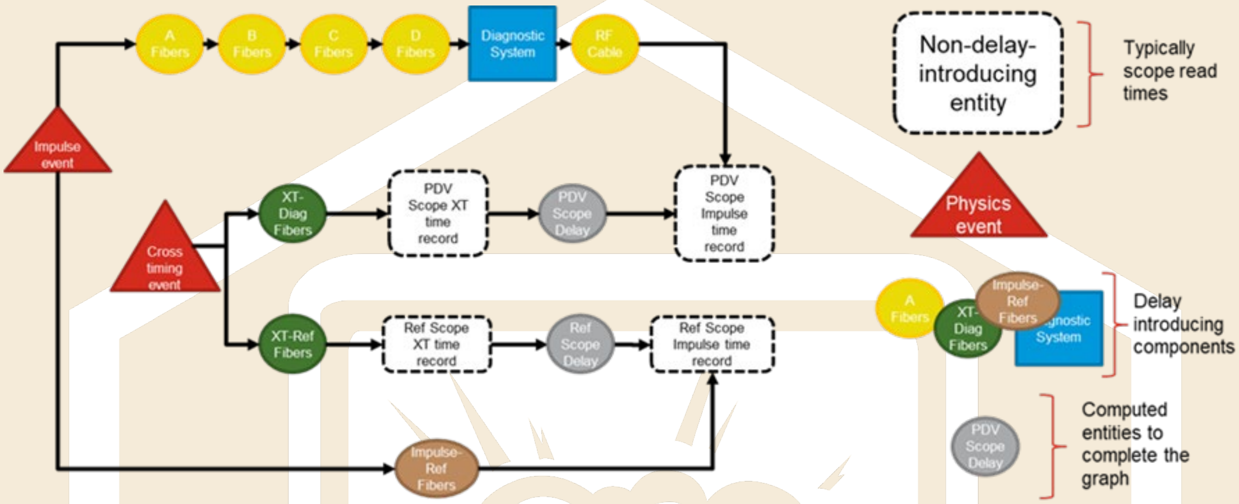

Graph model/ontology used for diagnostic cross timing.

To populate the database, the project developed a 1D barcode scanning process and labeling software and implemented the approach at the PULSE testbed. The figure illustrated below describes how the workflow allows for apparatus connective and topological information to be read directly into a machine-readable format.

Connection	Component A	Component B
1	MPDV_Gen1_S1_Cha3_Cha Ch2_ITU29	SR5_B20891_R3_P06
2	SR5_B20891_R3_P06	Crossover_024
3		
4		

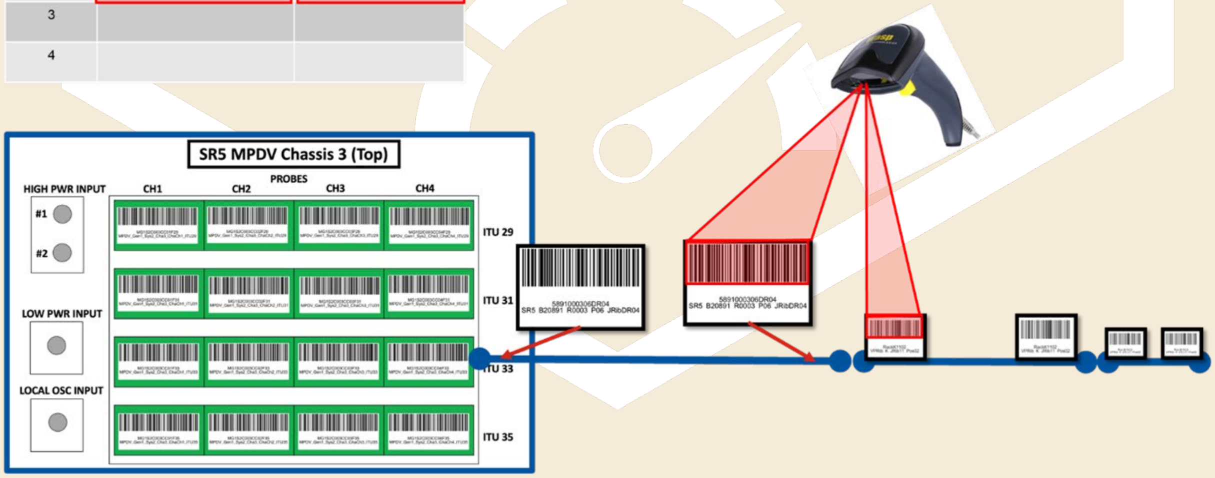

Illustration of the automatic data entry workflow that can result in connective/topology information that documents the apparatus configuration.

The Neo4j graph database allows for efficient data import/export and graph-based queries via the Cypher database query language. A Cypher script was developed to ingest all required signal path and cross-timing path entities and relationships (edges). The figure below shows a small number of fiber components of the signal paths for 5 Photon Doppler Velocimetry (PDV) systems within the Neo4j browser.

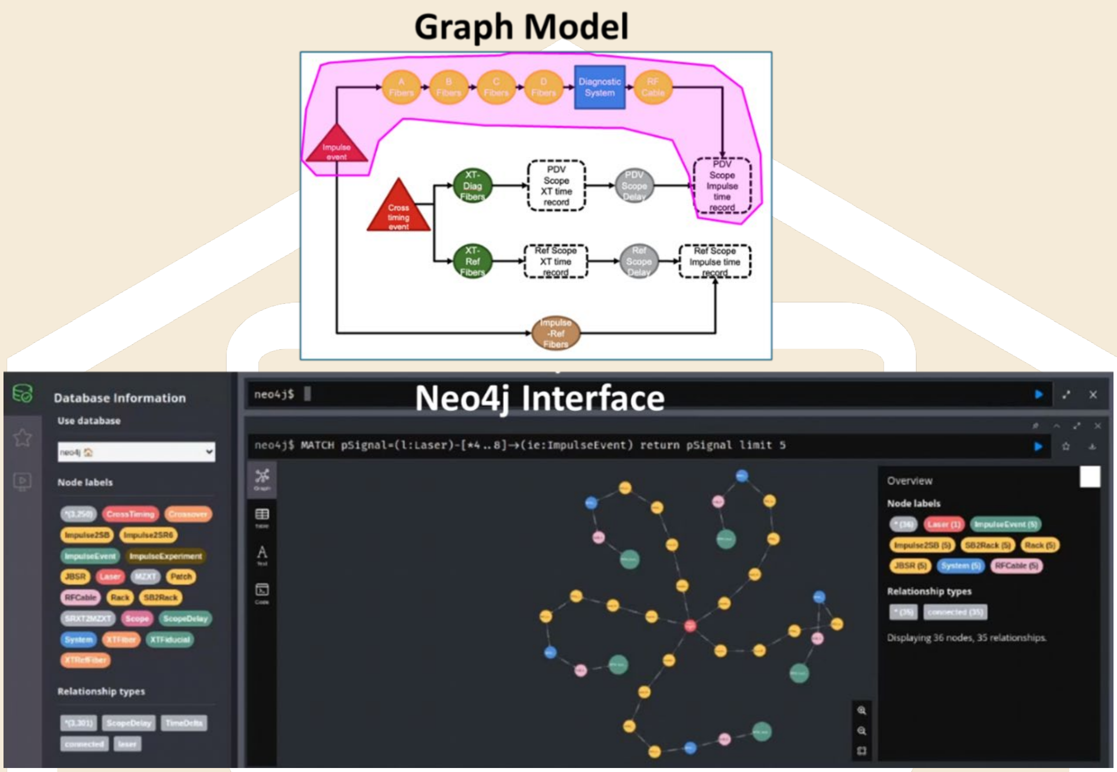

In the bottom figure, the Neo4j database interface illustrated a graph query that returns 5 examples of the signal path nodes + relationships that are present in the database for a single test. The corresponding portion of the graph model is outlined in magenta in the top figure. Colors were configured in Neo4j to approximately match the graph model

Timing loops that appear in the configuration management database are the primary structures of interest that allow for the verification of signal and cross-timing path delay measurements and configuration accuracy. The graph database allows for easy and efficient queries to locate and process timing loops. Cypher queries can specify pre-defined structures for these timing loops so that only those that are of interest are returned (it is also possible to return all possible timing loops). The figure below shows a full timing loop, arranged to resemble the graph model diagram.

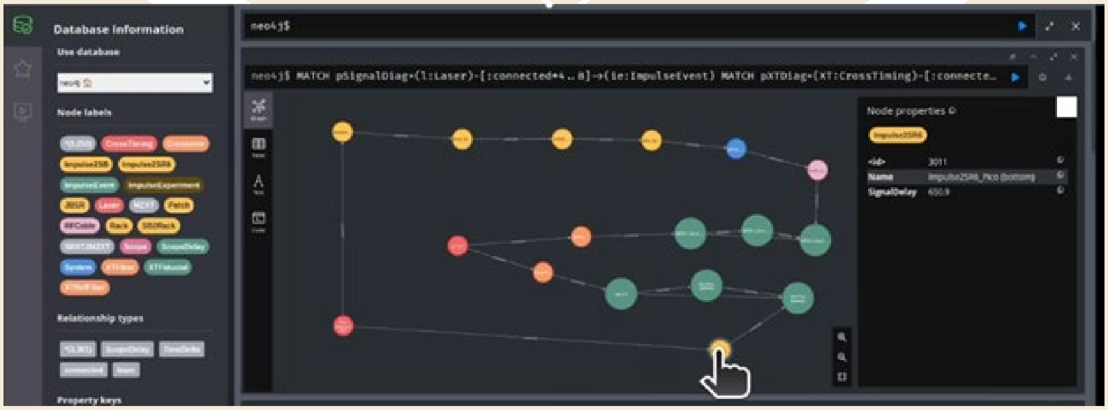

A timing loop is returned using a Cypher query. In this case, the query specifies specific loops of interest (those that involve a specific type of fiber component) and returns an example of such a loop in the database. Any property or feature of the diagnostic systems or components can be used to filter and down-select for specific evaluation.

In year two of the project, a no-code/no-syntax web-browser based interface was developed and demonstrated. The no-syntax interface was run locally on a system that connects to the Neo4j database running in the background and allows for any user to upload, delete, and perform simple/recurring analysis operations. The no-syntax interface allowed for the following operations:

- Add components (add nodes)
- Connect components (add relationships)
- Delete components (remove nodes)
- Disconnect components (remove relationships)
- Run timing loop queries and standardized timing loop analysis
- Update component properties

A sample of the functionality of the no-syntax interface is shown in below.

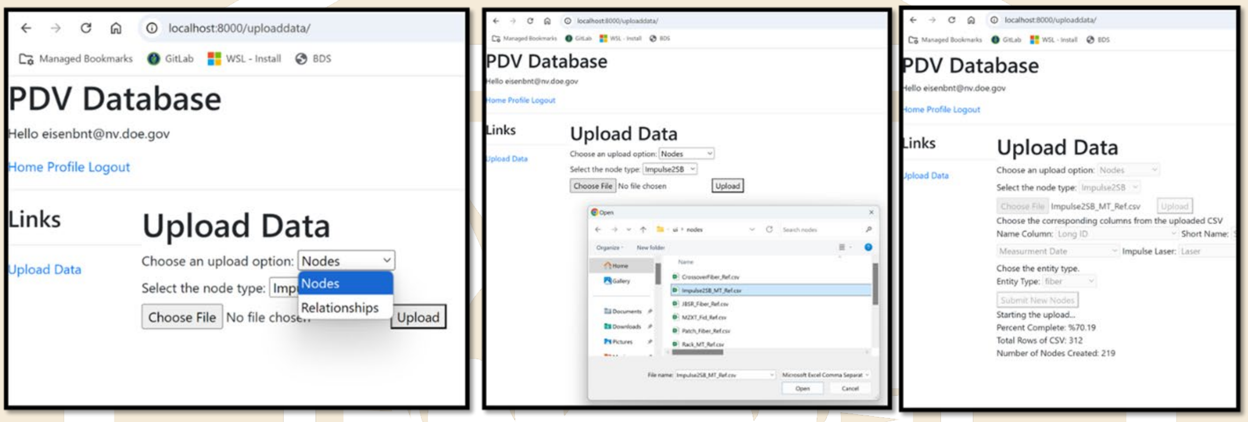

The no-syntax web browser interface allows for easy modifications to the database using menus/buttons (*left*), file dialogs (*middle*), and provides the user with status/progress feedback and change summaries (*right*) when completed.

The graph database approach allows for the efficient identification and retrieval of timing loops following each diagnostic cross-timing test. In the figure "TimingLoopQuerySyntax.png," the syntax for an automated timing loop identification query is shown that performs loop closure analysis. These queries were used to compare the new approach to legacy methods (spreadsheet analysis) and were shown to be equivalent.

```
MATCH p = (a:Laser)--(b:Impulse2SB)-[*3..6]-(c:System)-[*3..9]-(d:MZXT)-[*4..10]-(e:CrossTiming)-[*3..5]-(f:Impulse2SR6)--(a)

WHERE a.Name = "Pilas 1 (middle) 304"

WITH p, c,
REDUCE(
    D0 = 0.0,
    i IN range (1, length(nodes(p)) - 1) |
    D0 +
    CASE
        WHEN startNode(relationships(p)[i-1]) = nodes(p)[i-1] THEN 1
        WHEN startNode(relationships(p)[i-1]) = nodes(p)[i] THEN -1
        ELSE 0
    END * nodes(p)[i].SignalDelay
) AS DeltaTotalSignalPath

RETURN p, DeltaTotalSignalPath, c.Name AS System_Name LIMIT 1
```

The intelligent timing loop query for automatic arithmetic combination determination.

The new approach allows for additional analysis that can be used to find errors in the database by considering all possible timing loops that the database can locate rather than hand/SME selected loops (simulated error is shown below).

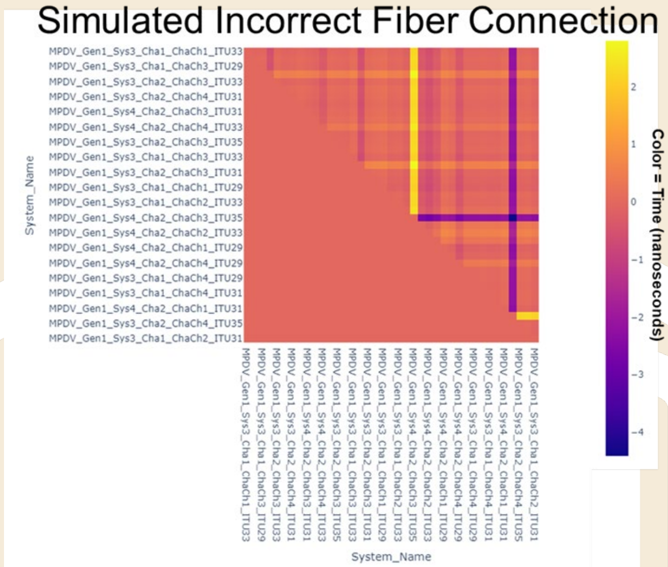

A pair of swapped fibers at a feed-through panel in the apparatus results in a pairing of outlier timing loop residual row/column behavior in the 2D plot. Note that this structure exhibits a pair of outlier columns (one elevated, one deficient), and a pair of outlier rows (one elevated, one deficient).

Results

The primary technical advancement pioneered in this project was the adaptation of a graph database and supporting analytics/queries to accomplish persistent mission needs related to configuration management and diagnostic cross timing. The graph database adaptation to these mission problems was successful and validated on real NNSS testbed SCE data (Lawrence Livermore National Laboratory's Nimble series of experiments). The graph-ontology, analytics, and database queries that replicate and enhance previously SME-driven diagnostic cross-timing analysis work are the tangible products that demonstrate the technical accomplishments of this work.

Supporting and supplementary technical accomplishments include:

1. Development and implementation of an automatic data entry workflow and system to assist in documentation of testbed apparatus configuration.
2. Barcode labeling of PULSE testbed optical diagnostic equipment to facilitate (1).
3. Demonstration of automatic cross-timing error detection signatures.
4. Development of a no-syntax user access interface for the database and common experimenter interactions.

Conclusion

This SDRD project demonstrates the feasibility of modernizing NNSS experimental configuration management to include database, analytic, and automation capabilities on contemporary NNSS datasets and use-cases (subcritical experiment configuration management). The benefits and significance are broad and impactful to experimental cadence, apparatus accuracy, and documentation efficiency/best-practices, as well as technical acceleration for future capabilities. Furthermore, the machine-accessible solution developed for this project demonstrates the possibility of a database solution for a “single-source of truth” for configuration management data. Such a solution would provide improved data access, version control, and data provenance for experimenters and data analysts. The path forward for this project is implementation into NNSS testbeds and training of fielding personnel.

Incorporation of Geologic Data into Centralized Database

Devon Smith
24-062
Year 2 of 2
Co-Authors: Matthew Dietel, Marc Llanes, Jacob Gochenour, Jennifer Larotonda, Maggie Townsend, Hali Montano, Andrew Miller, Garrett Datlof, and Morgan Aittama
Nevada National Security Sites

Abstract

Seismic wave propagation and gas migration are critical factors for monitoring underground nuclear explosions (UNEs). Because these factors are influenced by the geologic media with which they interact, geologic data and 3D subsurface geologic modeling play a critical role in nuclear treaty monitoring. The NNSS has accrued an exceptional suite of subsurface data through over 60 years of drilling in support of many projects. Historically, drilling data has been managed as part of individual projects, which did not focus on long term management of geologic data. The data currently exists fragmented across several low-tech platforms. Through our work, we have developed a long-term geologic data management solution. A centralized database has been established on an enterprise server managed by NNSS. The data interface is Datamine Fusion X software, developed specifically for managing drillhole data. Although this software is standard in the mineral resource industry, adapting it for use at NNSS had several unforeseen challenges and many delays in the project. After working through these challenges, the database was established, and data from 2,856 holes was imported into the database.

Background

The NNSS has drilled thousands of drillholes in support of many projects including nuclear testing, environmental restoration, and defense nuclear nonproliferation (DNN). These projects prioritized short-term data management specific to the needs of the project and did not plan for a centralized solution where all geologic data could be compiled and preserved. Drillhole data produced by these programs includes parameters such as drilling logistics (hole location, orientation, diameter, depth, etc.) and geologic data (lithology, alteration, rock quality, physical properties, etc.). Coupling these two types of information in a 3D application, helps geologists construct 3D models of the subsurface geology, which provide the geologic context for numerical modeling of parameters such as seismic wave propagation and gas migration. Drillhole datasets of this magnitude are typically found in the mineral resource industry where the uncertainty of the 3D geologic model drives the spatial density of the drilling campaigns. For many types of resources (i.e., gold, copper), the depositional nature of the commodity demands a dense grid of drilling resulting in a large set of drillhole data. These datasets are housed on a server, managed using software developed specifically for the industry, and supported by generous industry funding.

Technical Approach

Modern servers are capable of housing massive amounts of data in a centralized location. Modern database management software builds a relational data model which creates links to data fields, eliminating the need for duplicate storage of field data. This provides a more compressed dataset that the user can either rapidly query through the database software or manually using SQL.

Additionally, modern 3D geologic modeling software is designed to query a database and display geospatial data in 3D. This type of database technology, coupled with 3D geologic modeling, is common in the resource industries (oil and gas, mining, and exploration) and this project harnesses and adapts this same technology for use at the NNSS.

Data is imported into the NNSS server hosted database using Datamine Fusion X [1] data management software, Service Pack 4.0.1. Because several members of our group have experience working with datasets and centralized databases in the resource industry, we realized the value of incorporating a systematic approach into these large data compilation and preservation projects. This massive data undertaking was highly organized and shared among several members of our technical staff, including student interns. A catalog was used to track which datasets have been located and their current formats.

Following the initial locating and cataloging, the datasets must be vetted to ensure data quality and identify the original source of the information. Once vetted, datasets are reconciled against each other to better understand differences and identify any potential discrepancies between them. Then the dataset must be filtered to include only the data being targeted for import.

The final step involves configuring the database and formatting the data for successful data import. It is critical to ensure continuity between columns in the data and fields in the database. The data itself is carefully compared with the database tables, fields, and picklists, and any necessary modifications are made to the database configuration or within the datasets themselves. Many of the fields are controlled by a picklist or lookup table. This restricts the data values for that field to a predefined list of values. This is necessary in order to maintain consistent input data free from redundant data caused by typos. The process of creating the picklists is meticulous but the result constrains the import values, allowing for accurate queries. Once continuity between the data and the database is reached, a batch importer is built which maps the database fields with columns in the data being imported.

Results

We applied for IT support from the Enterprise Project Customer Counsel in June 2022 and received approval. Shortly thereafter, the project overcame several delays caused by technical setbacks. Cyber and IT finalized the technical requirements for the project in March 2023. Geologists worked with Datamine support personnel to configure the initial Fusion X database before it went live May 30, 2023.

After a year of efforts and development, NNSS IT established a license server to host the Fusion X software licenses which was a key step toward having widespread access to the database. NNSS IT also completed Fusion X installs and server connections on an additional 8 Geoscience group devices in August 2024, bringing the total to 11 devices.

Several datasets were targeted for import in FY24. Initial database efforts focused on forty-five (Area 12) drillholes which were initiated in the database using Excel files. An access database known as the RedBook was previously compiled and maintained by Geosciences until the sole user retired. Information from the dataset was filtered, formatted, and imported into the Fusion X database initiating an additional 2,793 drillholes (Figure 1) in August 2024.

An additional dataset the project planned to tackle was an unknown amount of paper information for underground holes drilled at the NNSS. The paper log information was discovered in an additional dataset that was previously compiled by the United States Geological Survey [2]. The dataset was reconciled against RedBook and filtered using Python. Through the reconciliation process, discrepancies were identified in subsets of data which was removed from the import until these discrepancies can be resolved. To date, we have imported lithological information for over 1,000 drillholes (see figure on next page) which were previously initiated by the RedBook logistical data.

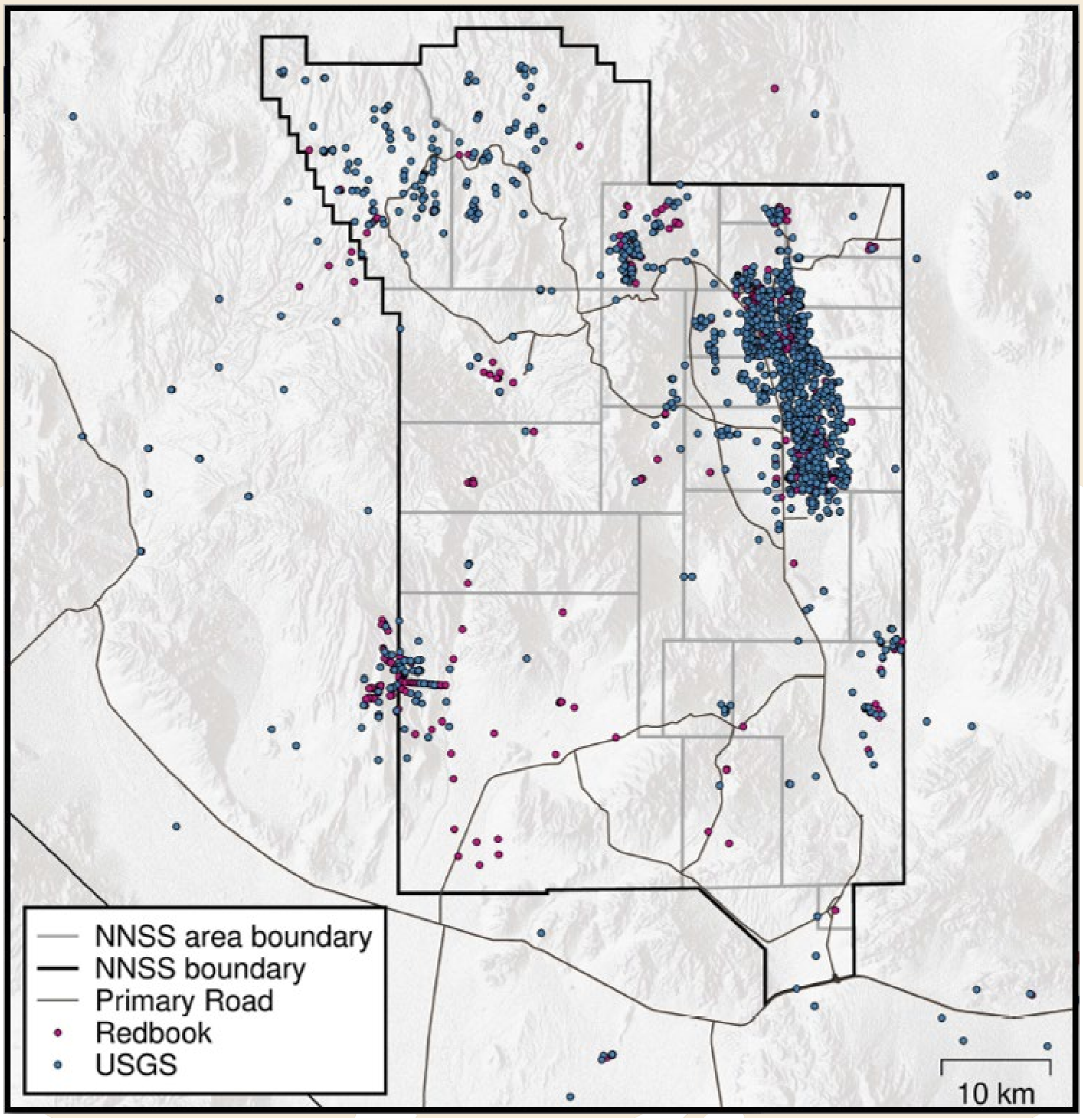

Locations of NNSS drillholes from the RedBook and USGS datasets. Shown on a shaded relief map. Modified from figure by J.Gochenour.

Conclusion

Although the software is an industry standard, adapting the software for use in the NNSA Enterprise proved to be an unprecedented accomplishment. Ongoing efforts include resolving the many discrepancies we discovered in data that was excluded from import, importing additional USGS data (i.e. rock physical properties), and completion of the .las file importer.

Although still in its infancy, this newly established centralized geologic database will preserve our valuable legacy and modern data for the long term. It will also allow geologists to leverage the compiled data in its entirety. This is something we have never been able to accomplish before. Modern geologic modeling software is designed to query and display borehole data from a centralized relational database. Completion of this project will allow us to rapidly display large datasets and to model larger areas across the NNSS. This capability will also allow us to spatially analyze complex geologic trends in 3D. This will benefit programmatic efforts by more quickly providing detailed characterization of active testbeds and areas of interest for future testbed development.

The database will also add value for current and future programs by modernizing our workflow. Historically, geologists captured data on paper logs and then later entered the data into spreadsheets. The database will allow us to enter new information directly into the database, whether collection occurs at the NNSS Core Library or in the field. This will be an additional cost saver for our ongoing projects. Additionally, the Report Builder tool in Fusion X will allow us to build a queried report template that meets our customer's needs, reducing the time to deliver data to programs. Recent updates to the Datamine Fusion X software have added drill core photo management, which will allow geologists to attach images to the logs and annotate and comment directly onto the image. This can be done in the field during drilling and logging. There's also a drillhole visualizer that allows geologists to view the log data in 3D, directly from the logging application. As the software technology develops, we will advance our own capabilities, and the database will continue to develop its contributions to NNSS programs.

References

[1] 2023. "Datamine Product Documentation." Fuxion X Documentation., https://docs.dataminesoftware.com/Fusion/index.htm

[2] D.B. Wood, 2007. "Digitally Available Interval-Specific Rock-Sample Data Compiled from Historical Records, Nevada National Security Site and Vicinity, Nye County, Nevada." *U.S. Geological Survey Data Series 297.* https://doi.org/10.3133/ds297

Optical Remote Sensing for Facility Monitoring: An Integrated Approach to Modeling, Simulation, and Sensors

Chris Burt[a]
24-076
Year 1 of 3
Co-Authors: Saketh Ayyalasomayajula[a], Michael Howard[b], Milton Smith[c], Ian Bortins[a], Luke Borders[a], and Avalon Everett[a]
[a]Special Technologies Laboratory, [b]Remote Sensing Laboratory, Nellis, [c]Chrysalis Systems LLC

Abstract

Optical remote sensing (ORS) is a core Nevada National Security Sites (NNSS) capability with Principal Investigators (PIs) at the Remote Sensing Laboratory-Nellis (RSL-N), and the Special Technologies Laboratory (STL). Our organizations have worked closely to build new sensors, field airborne and ground-based systems, and create a test environment used by national labs and other government agencies. However, due to staff attrition and advancement, much of our current technical staff has had limited experience in MASINT [Measurement and Signature Intelligence] analysis, specifically in facility characterization. Recently developed analysis techniques (computational fluid dynamics [CFD] and ray trace visualization) allow for ORS integration of sensor and facility simulations through physical collections and analysis. First, ground-based and airborne hyperspectral sensors will be reconfigured as primary data sources in Year 1. From interior and limited exterior facility CFD simulations, DIRSIG [Digital Imaging and Remote Sensing Image Generation] plume models will be created to simulate sensor performance in Year 2. Finally, a combined airborne/ground-based data collection will occur at an NNSS testbed in Year 3.

Background

This project brings together previously disconnected teams and skillsets from within the NNSS complex. The topics of interest require expertise from remote sensing scientists, mechanical engineers, computational mathematicians, and technicians. Several topics that are integral to the project are described below.

Hyperspectral imaging (HSI) is an integral piece, and it refers to an imaging technique that obtains the spectrum for each pixel in the image of a scene. Since it collects hundreds of more images at different wavelengths for the same spatial area, it is extremely useful for material classification, object detection, etc. Long wave infrared [LWIR] HSI, specifically is being utilized as the primary source of data for this project. Due to the nature of this region in the electro-magnetic spectrum, LWIR data is inherently noisy during collections, making data analysis/target library matching challenging.

Neural networks are an emerging and revolutionary method to process datasets, similar to how humans will problem solve using machine learning. Specifically, autoencoders are utilized in this project, and they are a subset of neural networks which use encoders/decoders to compress input data and reconstruct the input data. Over many iterations, the difference between the reconstructed output and the input or "ground-truth" is minimized, creating increased pattern recognition. Research in this area has shown great benefit in improving signal-to noise-ratio [SNR] for LWIR data and thus improving data classification.

Technical Approach

Our goal is to integrate sensor and simulation capabilities and create a remote sensing capability for facility monitoring. Facility monitoring is a major Defense Nuclear Nonproliferation (DNN) thrust area and there are testbeds emerging at NNSS, across the DOE enterprise, and at commercial production facilities. Remote sensing of production surrogates is most often driven by sensor availability, production schedules, and ground truth knowledge. If the desired facility knowledge is not sufficiently modeled from a sensing perspective, the data acquisition of complex sensors, such as HSIs, is often driven by sensor availability, not information requirements. At a production facility, there are numerous points of interest. Aperture releases represent heat and effluents due to vents, windows, HVAC [heating, ventilation, and air conditioning] systems and effluent releases are fugitives from stacks. Heat generated in processes and interior turbulence impact what is observed externally as exterior forces will likewise impact internal air flow.

This project involves remote sensing expertise from RSL-N & STL subject matter experts with support from Lawrence Livermore National Laboratory (LLNL) (sensor reconfiguration) and Rochester Institute of Technology (RIT) (for DIRSIG scene building). Chrysalis Systems LLC will assist with autoencoder algorithm development for processing hyperspectral data cubes.

Two $8M US Department of Defense (DOD) airborne hyperspectral sensors were acquired: BG13XR and BG8X for STL and Remote Sensing Laboratory-Nellis (RSL-N), respectively. BG13XR was modified to be a ground-based HSI system, which required a new mounting scheme, optical mirror adjustments, and a new panning tilt configuration for scanning. BG8X is being reconfigured for aircraft and is being appropriately configured by RSL staff. Additionally, facility scenes were created in Blender for use in DIRSIG, a radiometric ray-tracing software, with the assistance of several interns. These simulations of HSI data products will be created in collaboration with RIT and will be complementary to the hyperspectral sensors.

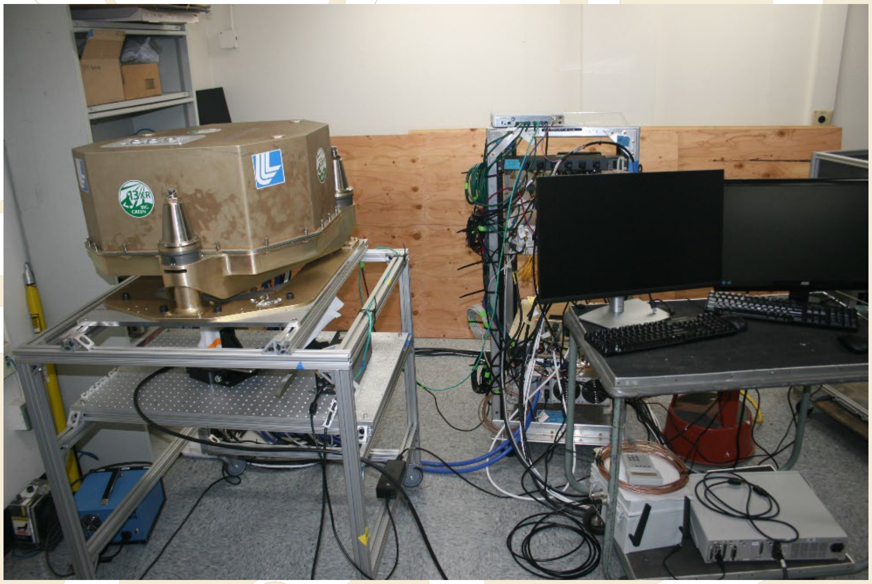

BG13xr Ground Based HSI Setup at 226

Year 2 and 3 will introduce collaboration/consultations with Dr. Milton Smith of Chrysalis Systems LLC, who will provide the architecture for creating autoencoder neural networks in MATLAB and Python. These networks will improve the efficiency of calibration, better process data cubes, and create training sets for future sensors to utilize. The importance of autoencoders can be described as follows: the use of the GETBAGS [Gas Effluent Target Bags] target arrays to generate scenarios with varied gas concentrations act as a set of reference inputs. With more diverse inputs, these neural networks can better recognize patterns and distinguish objects at a faster rate than traditional data analytics.

In Year 3, simulation and physical experiments come together (starting late-FY25) with combined efforts to simulate, calibrate, acquire, and train combined airborne and ground-based imagery products. Combined experiments will occur at an NNSS surrogate testbed such as the Signals Exploration Testbed (SET) or the Solids Array (NPTEC) with surrogate plume releases. It is our intention that this will produce a complete picture of sensing, with possible collections at an off-site production facility.

Results

The STL team built a ground-based configuration apparatus for BG13XR, using an 80-20 stand for ease of mobility. Two optical mirror mounts were designed and machined in order to accommodate the two gold mirrors that will reflect light coming from the nadir. One mirror is mounted on a Newport Rotation Stage and is an adjustable "turn" mirror while the latter is angled but is fixed. This allows us to scan images in front the sensor (scanning left to right) depending on the angular change of the stage. Additionally, STL interns also developed a Blender model of the 226 facilities at STL, allowing for a realistic facility characterization for the simulated spectrometers in DIRSIG to train against.

B13XR is mostly operational with a slight software bug in the Aerotech Stage Controller which controls the line-of-sight (LOS) mirror internal to the sensor bulkhead. This functionality allows the user to control the mirror positioning, angling, etc. and is a key parameter for other calibrations including the internal blackbody sources. With this error, BG13XR can be run with data cubes collected on a particular scene though without proper calibration.

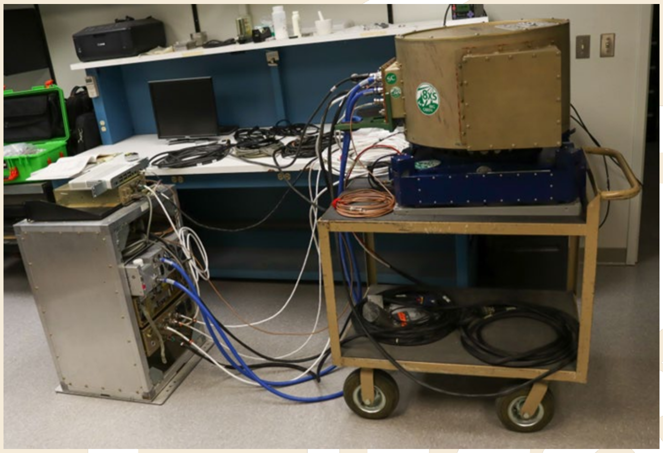

BG8sx Airborne HSI Bench Test Setup At RSL

For the airborne HSI system, RSL developed a plan to design, engineer, and fabricate the hardware mounting provisions required to install the optical payload on an RSL-N B350. A subcontract was in place with AVCON to perform the Designated Engineering Representative services and it was concluded that legacy electronic component racks must be replaced. A flight electrical load analysis was conducted and an initial BG8SX bench test setup was completed, with a DAC [digital-to-analog] motherboard issue identified. This system configuration issue prevents the bootup of the graphical user interface and the software to operate the sensor, with alternatives being tested in early FY25.

On the autoencoder/software development aspect, Chrysalis Systems has created numerous MATLAB scripts to process hyperspectral data and remove noise/ease calibrations. Automated control of the Newport rotation stage for BG13XR for ease of access for changing rotation angle, etc. These autoencoder algorithms are completed and tested on sample hyperspectral data from other facilities. In FY25, generated data cubes from BG13XR and BG8SX will provide sufficient datasets for better classification for different types of gases, solids, etc.

Conclusion

In Q1 of FY25 for the ground-based HSI, we plan on repairing the Aerotech stage controller with LLNL assistance and reconfiguring the log files for controlling the LOS mirrors and blackbody sources. After several dry runs, the ground-based HSI will be fully operational by the end of the calendar year and will begin to collect data at the STL Laser Range. For the airborne system, by middle/end of Q2 of FY25, the sensor payload will be fully integrated, including cabling, electrical loads, and computers.

Additionally, Blender scenes of facilities of interest will be fully constructed and holistically integrated with a simulated LWIR [longwave infrared] spectrometer in DIRSIG. Comparisons can be made with the real sensor systems and provide feedback/insight on how the hyperspectral data might appear before real-life collection.

The first test collect is tentatively planned at the Signals Exploratory Testbed (SET) with flights coordinated by RSL-N for the airborne HSI collection and ground-truth provided by BG13XR. The ideal programmatic customer to pitch this combined capability to would be NA-20 for remote sensing applications in DNN. This can also be utilized at other NNSS testbeds (Nonproliferation Test and Evaluation Complex [NPTEC]) and non-NNSS sites for facility characterization.

Spatial Spectral Observations from Near and Far

Michael Howard
24-095
Year 2 of 3
Co-Authors: Heather Howard
Remote Sensing Laboratory, Nellis

Abstract

We will identify spatial and spectral signatures of surface materials that characterize the experimental design and proliferation intention of underground weapons testing in vertical emplacement shafts. Early detection and characterization of an underground weapons testing program is critical intelligence for the formation of national nuclear proliferation policy but is subject to denied access and intentional concealment to conventional detection methods, making optical remote sensing an ideal tool in remote detection and surveillance capabilities of underground construction activities. There are many surficial signatures surrounding the construction and use of subsurface testing grounds that will be investigated from a spatial-spectral perspective. We will coordinate airborne imaging and ground-based spectral measurements of the Rock Valley Direct Comparison (RVDC) site during its construction, testing, and shutdown and analyze the data using spatial-spectral convolution techniques to simulate current and in-development satellite-based and high-altitude aircraft-based surveillance optical imaging systems.

Background

Early detection and characterization of an underground weapons testing program is critical intelligence for the formation of national nuclear proliferation policy. This ability is subject to denied access, requiring remote detection. Optical remote sensing is the primary method that can overcome access limitations and provide long-distance detection and characterization. This research will fill the knowledge gaps that exist which limit the ability to identify and characterize vertical drilling related to underground nuclear weapons testing. Since the 1960s, nuclear weapons testing has largely been conducted underground in accordance with the terms of the Limited Test Ban Treaty. The primary consideration for nuclear test operations involves the complete containment of the test effects from the environment. Various methods are used for the emplacement of nuclear test devices to ensure containment, the most common of which is at the bottom of a vertical shaft which also effectively conceals the nuclear weapons testing activity [1,2]. This has created a technical challenge in verifying undeclared testing intentions. This project will research optical signals that can verify undeclared nuclear testing and characterize the operational use of the device.

A key non-optical signal used today to detect and characterize nuclear testing events is from global seismic arrays monitoring earthquake activity. For example, in 2016, North Korea claimed they successfully tested a hydrogen device, a claim that was never substantiated, and exactly what was detonated is still unclear. Most of the evidence came from seismic data which was inconclusive due to its reliance on a good depth-of-burial or estimate of the device [3]. To improve well-vetted seismic capabilities and add new evidence of proliferate state nuclear testing intentions, this project investigates optical signals generated by anthropogenic activities of the drill site and exploits surrounding surface geologic and geomorphological features to improve seismic estimates.

Technical Approach

Using the RVDC testbed and cores from other boreholes in the vicinity, key observables will be examined to test optical dependencies from multiple data collection modalities offering varying spectral resolution, ranges, and ground sample distances. The data collections will be used to analyze the strengths and weaknesses of each modality. An airborne hyperspectral instrument will be used to collect high resolution image data.

Spectral convolution techniques will be used to simulate satellite-based sensor spectral responses, allowing different modalities to be equitably compared as they are collected in near time of each other.

The primary observables at these testbeds will be centered on drilling activities. Drilling will provide both anthropogenic and geologic signatures. A common geological research topic with both adversarial mining and drilling operations is to assess to what degree the drill cuttings or muck piles explain the site activities. A central objective for the geologic portion of this research is to interpret the spectral content of the cuttings with respect to rock properties. The first two years of this project focused on this objective using both remote sensing and in situ data of the RDVC site and in situ measurements of Test Well F (TWF) cores. To ensure an accurate account of this relationship, spectral measurements of cores from TWF, a nearby borehole with similar geologic content, were used to map the change in spectral content and associated mineralogy with depth. A synthetic image of the high-resolution single pixel long-wave infrared (LWIR) spectra was constructed from which LWIR endmembers were extracted that corresponded to geologic descriptions in core logs of TWF. In year two, machine learning models were also applied to associate spectra of TWF with coincidental x-ray diffraction (XRD) and x-ray fluorescence (XRF) measurements. These results provide a baseline for the airborne measurements of the cuttings from the upcoming drilling operations at RVDC in the third year.

Anthropogenic activity creates signatures that indicate drilling intent. Actions that greatly dictate design and intent include containment of radionuclides, treaty compliance, safety guidelines, and concealment for undeclared testing. A general framework for anthropogenic activity for vertical hole drilling can be broken into two categories: smaller-yield devices emplaced in relatively shallow holes that have a small footprint and alteration to the environment, and higher-yield devices in deeper holes that have a larger disturbed area, more on-site equipment, and greater infrastructure needs in terms of power and utilities [1]. Many of the anthropogenic signatures will be observed in the spatial domain. The spatial domain can only be useful if the ground sample distance (GSD) is sufficient to resolve the spatial form of relevant drilling indicators that distinguish testing intent. After key indicators are determined, a suitable GSD will be verified by assessing different collection geometries.

Results

The analysis of the FY24 data collections strongly corroborated the initial hypothesis of this SDRD project. By using the RVDC testbed and cores from other boreholes in the vicinity, key observables of pre-drilling construction were measured and examined for their optical dependencies from two data modalities. Analyzing visible and near-infrared (VNIR)/short-wave infrared (SWIR) airborne hyperspectral image data with in situ spectral measurements identified new construction activity which was the result of site preparation for upcoming drilling operations. The analysis utilized a supervised classification method that clearly delineated surface features of two vintages of drill pad and a large tuff outcrop. A second data modality of ortho-rectified broadband imagery was used to further characterize the new construction drill pad properties using the spatial domain. This analysis involved estimating the terrain displacement caused by construction activity using two temporally different Digital Elevation Models. A cut and fill calculation resulted in a 20 cm relative displacement, which indicated that grading and smoothing the new pad lowered the elevation. Advances were also gained in characterizing the geologic medium from borehole cores that will help constrain estimates of physical parameters such as rock density. Spectral separability of lithologies were assessed using 172 samples from TWF (Figure 1). This data was reduced to 5 endmembers identified as gypsum, tuff, granite, quartz conglomerate, and limestone. In addition, mineral composition was accurately identified indicating the presence of montmorillonite, sepiolite, dolomite, calcite, and feldspars with XRD. Significant progress was made in the development of statistical and machine learning methods to associate rock and mineral spectral features with sample physical properties (XRF and XRD). At the beginning of the FY24, a statistical method was developed to pre-process and sort core spectra using PC loadings. By the third quarter, the pre-processing transitioned to a machine learning effort and the development of an artificial neural network to predict spectra from physical properties.

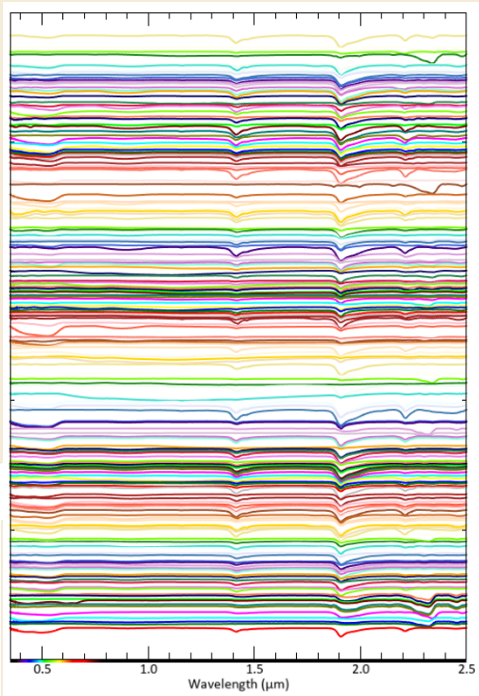

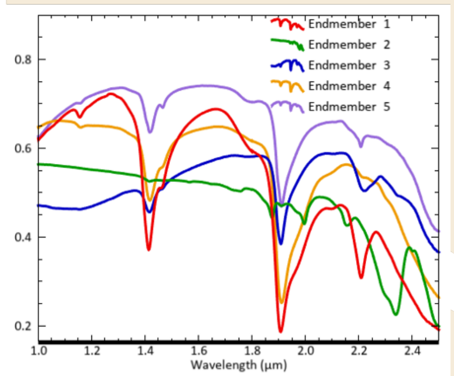

Spectra of 172 samples from TWF were reduced to 5 distinct endmembers consistent with lithologic descriptions in core logs.

Conclusion

The TWF data collection at the U.S. Geological Survey Core Library provided very valuable data. Analysis confirmed the theoretical framework for the project and allowed us to expand the analysis to machine learning. This data added valuable signatures to the ISSL that will be used to exploit future imagery collected over drill operations. The TWF spectral data was also used to initialize a relevant geologic spectral library with rock and mineral classification using matched filters with an industry reference library. In parallel, using a multivariate approach with extensive metadata to develop preprocessing routines allowed a natural transition into a machine learning environment to enhance geologic physical characterization of boreholes that could corroborate results from traditional spectral libraries. Airborne imagery collections established background of the RVDC site and later collections allowed tracking of initial activities. Orthorectified imagery captured the background state of surface material distribution and permitted the extraction of a high geospatial resolution terrain model. A hyperspectral imaging data collection captured the spectral distribution of surface materials and highlighted the recent surface grading and access road construction at RVDC.

The final year of the project and the path forward will continue to analyze data to establish key observables and test the optical dependencies of the spatial-spectral data collection modalities to determine the best utility of remote sensing in supporting this nonproliferation application. FY25 activities will include the collection of additional spectra and metadata of cuttings and core from both drilling operations and legacy boreholes, expansion of the artificial neural network by including additional diverse geologic data from legacy boreholes, and if funding allows, collection of more airborne imagery of drill operations and legacy sites.

References

[1] E. Rollins, 2008. "Nevada Test Site - Site Description." *Vols. ORAUT-TKBS-0008-2.*

[2] V. I. Khalturin, T. G. Rautian, P. G. Richards and W. S. Leith, , 2005. "A Review of Nuclear Testing by the Soviet Union at Novaya Zemlya, 1955-1990." *Science and Global Security.* 13. pp. 1-42

[3] L. Greenemeier, 2016. "Nuclear Confusion: The Data Suggest North Korea's "H-Bomb" Isn't." *Scientific American.*

Feasibility of Reoccupying Historic Testbeds for Future Experiments

Ian Bortins
24-120
Year 2 of 2
Special Technologies Laboratory

Please see CUI summary for more information.

SDRD

SITE-DIRECTED RESEARCH & DEVELOPMENT